Observational Heliophysics II: Radio Waves

T. S. Bastian (NRAO)

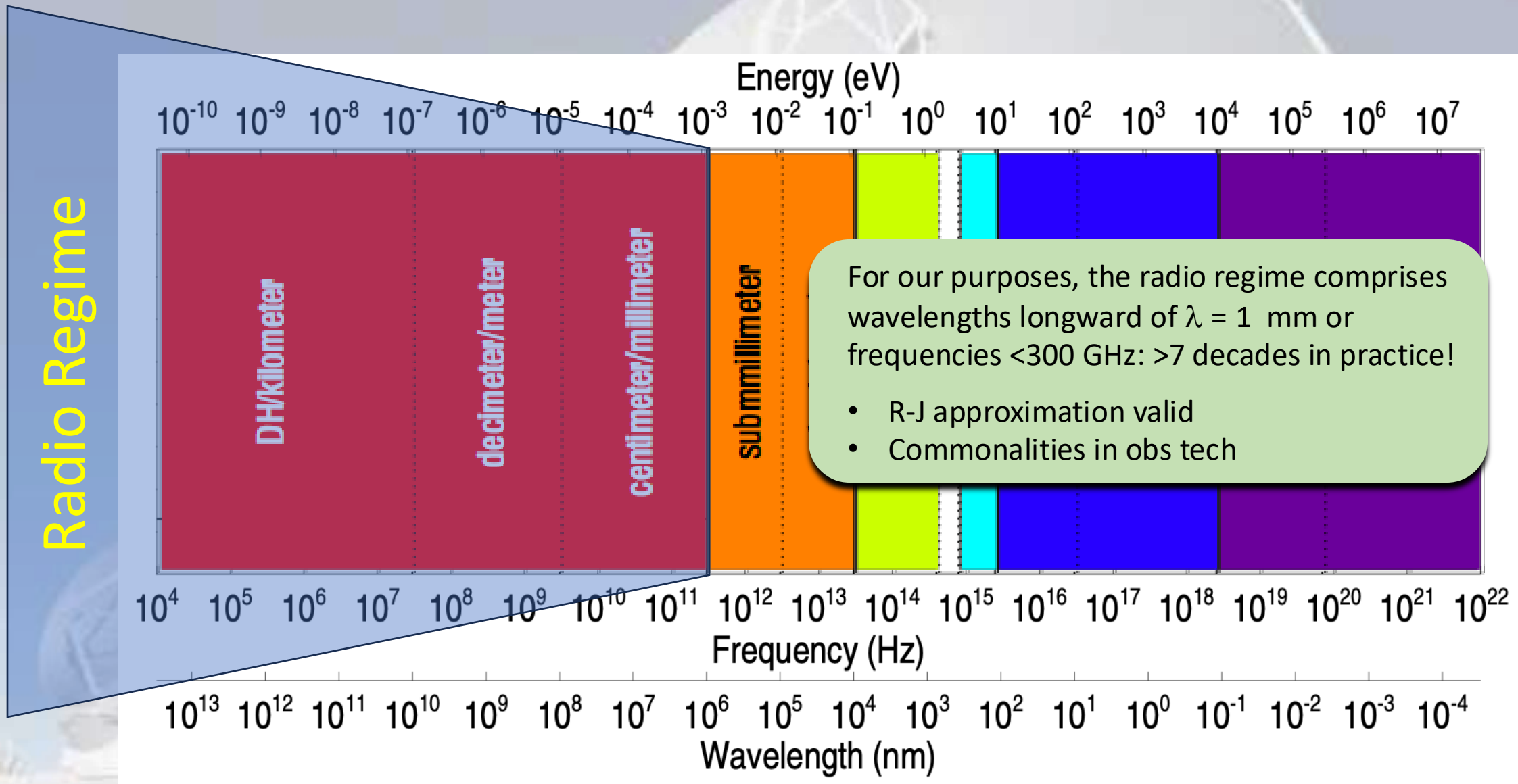
Radio Regime
Energy (eV)
10^{-10} 10^{-9} 10^{-8} 10^{-7} 10^{-6} 10^{-5} 10^{-4} 10^{-3} 10^{-2} 10^{-1} 10^{0} 10^{1} 10^{2} 10^{3} 10^{4} 10^{5} 10^{6} 10^{7}
DH/kilometer
decimeter/meter
centimeter/millimeter
submmillimeter
For our purposes, the radio regime comprises wavelengths longward of λ = 1 mm or frequencies <300 GHz: >7 decades in practice!
• R-J approximation valid
• Commonalities in obs tech
10^{4} 10^{5} 10^{6} 10^{7} 10^{8} 10^{9} 10^{10} 10^{11} 10^{12} 10^{13} 10^{14} 10^{15} 10^{16} 10^{17} 10^{18} 10^{19} 10^{20} 10^{21} 10^{22}
Frequency (Hz)
10^{13} 10^{12} 10^{11} 10^{10} 10^{9} 10^{8} 10^{7} 10^{6} 10^{5} 10^{4} 10^{3} 10^{2} 10^{1} 10^{0} 10^{-1} 10^{-2} 10^{-3} 10^{-4}
Wavelength (nm)

Preliminaries: Concepts & Definitions

For the moment, think of radiation as propagating along rays. Consider differential area dA normal to a given ray **r** and consider all of the rays incident on dA within a solid angle $d\Omega$ centered on **r**. The energy *dE* traversing *dA* in a time *dt* in a frequency range $d\nu$ is defined through

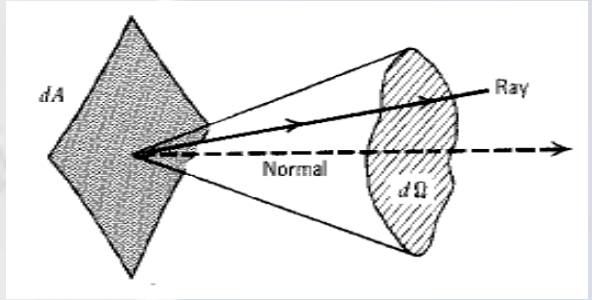

$$dE = I_\nu \, dA \, dt \, d\nu \, d\Omega$$

where I_ν is the **specific intensity** or **brightness,** with units ergs cm^{-2} s^{-1} Hz^{-1} $ster^{-1}$. Integrating over all rays incident on *dA* from all directions the **flux density** (or **spectral flux density**) is

$$F_\nu = \int I_\nu \cos\theta \, d\Omega$$

which has units ergs cm^{-2} s^{-1} Hz^{-1} or W m^{-2} Hz^{-1}. At radio wavelengths the flux density unit is the Jansky (Jy) where

$$1 \text{ Jy} = 10^{-26} \text{ W m}^{-2} \text{ Hz}^{-1} = 10^{-23} \text{ ergs s}^{-1} \text{ cm}^{-2} \text{ Hz}^{-1}$$

While flux densities measured in μJy are routinely observed in astrophysical contexts, radio emission from the Sun and heliosphere is very intense. It is usually the case that **solar flux units** are used where 1 SFU = 10^4 Jy.

Preliminaries: Concepts & Definitions

Rays in free space have constant specific intensity: $dI_\nu/\mathrm{ds} = 0$. It can only be changed by emission, absorption, or scattering along the ray path. We ignore scattering for now.

The **emission coefficient** is defined as the energy emitted per unit time per unit solid angle per unit volume per unit frequency: $dE = j_\nu \, dV \, d\nu \, dt \, d\Omega$. For rays traversing a path length ds they span a volume $\mathrm{d}V = dAds$ and the incremental increase to the specific intensity is $dI_\nu = j_\nu ds$.

The **absorption coefficient** is defined by $dI_\nu = -\alpha_\nu I_\nu ds$ where $\alpha_\nu > 0$ when it results in a decrement in specific intensity. The **radiative transfer equation** can then be written

$$\frac{dI_\nu}{ds} = -\alpha_\nu I_\nu + j_\nu$$

Defining the **optical depth** τ_ν through $d\tau_\nu = \alpha_\nu ds$ and the **source function** $S_\nu = j_\nu / \alpha_\nu$ and we can rewrite the transfer equation as

$$\frac{dI_\nu}{d\tau_\nu} = -I_\nu + S_\nu$$

Preliminaries: Concepts & Definitions

A system of particles and radiation is in **thermodynamic equilibrium** when it is characterized everywhere by a single temperature *T*. The radiation from a system in TE is referred to as **blackbody radiation** and we have $I_\nu = B_\nu(T)$, where

$$B_\nu(T) = \frac{2h\nu^3/c^2}{e^{h\nu/k_BT} - 1} \qquad (Planck\ Law)$$

At radio wavelengths $h\nu \ll k_BT$ and so, to a high degree of accuracy, we have (*Rayleigh-Jeans approximation*)

$$I_\nu = B_\nu(T) \approx \frac{2\nu^2}{c^2} k_BT = \frac{2k_BT}{\lambda^2}$$

It is useful to express the specific intensity at a given frequency in terms of a temperature $T = T_b$ of the black body yielding the same brightness at that frequency. We refer to this temperature as the **brightness temperature**. Defining an **effective temperature** through $S_\nu = 2k_BT_e\nu^2 \,/\, c^2$ the transfer eqution can be rewritten

$$\frac{dT_b}{d\tau_\nu} = -T_b + T_e$$

Preliminaries: Concepts & Definitions

For uniform source, in the absence of background emission, the solution to the transfer equation is just

$$T_b = (1 - e^{-\tau_\nu})T_e$$

When $\tau_\nu \gg 1$ we describe the medium as **optically thick** and $T_b = T_e$; if the material is in TE we have $T_b = T$. If the emitting material is not in TE – that is, it particle distribution function is non-Maxwellian – T_e is the mean energy of the emitting particles.

When $\tau_\nu \ll 1$ it is **optically thin** and we have $T_b \approx \tau_\nu T_e$. All of the microphysics is embodied by τ_ν!

In practice, cosmic radio sources are observed by telescopes characterized by an angular resolution Ω_o, often referred to as the "beam". If the source is resolved then we have a measure of the radiation flux density per resolution element Ω_o. The observed flux density is then $F_o = I_\nu \Omega_o$ and $I_\nu \approx F_o/\Omega_o$ and, hence, the specific intensity or source brightness is often expressed in terms of flux density per beam, or Jy/beam.

Substituting for I_ν:

$$F_o = 2k_B T_b \frac{\nu^2}{c^2} \Omega_o$$

While we have not discussed polarized radiation, this expression is for the combination of two orthogonal senses of polarization (X, Y or R, L). For a single polarization it would be reduced by a factor 2.

Emission Mechanisms

Although spectral line emissions at radio wavelengths – molecular lines, maser emission, radio recombination lines – are important in many astrophysical contexts, they do not play a role (to date) in solar or heliospheric radio emission. We therefore focus on continuum emission mechanisms.

Continuum radiation results from charge acceleration. For a single particle of mass m and charge q undergoing an acceleration $\boldsymbol{a}$ the power (ergs s^{-1}) emitted into solid angle $d\Omega$ is

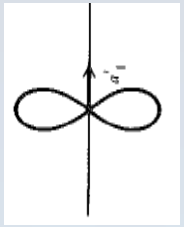

$$\frac{dP}{d\Omega} = \frac{q^2\boldsymbol{a}^2}{4\pi c^3}\sin\theta^2 \qquad (Larmor\ formula\ -dipole\ emission)$$

$$P = \frac{2q^2\boldsymbol{a}^2}{3c^3} \qquad Total\ power$$

Since $a = F/m$, all other things being equal, we see that electrons emit $(m_i\ /\ m_e)^2$ as much power as ions.

Where θ is the angle relative to the acceleration vector. When the particle is relativistic and acceleration is perpendicular to v:

$$\frac{dP}{d\Omega} = \frac{q^2}{4\pi c^2}\frac{a^2 sin^2\theta}{(1-\beta\cos\theta)^4} \qquad \beta = \frac{v}{c}; \qquad \gamma = 1/\sqrt{1-\beta^2}$$

$$P = \frac{2q^2\boldsymbol{a}^2}{3c^3}\ \gamma^4$$

The primary relativistic effects are a boost in power and relativistic beaming.

Emission Mechanisms

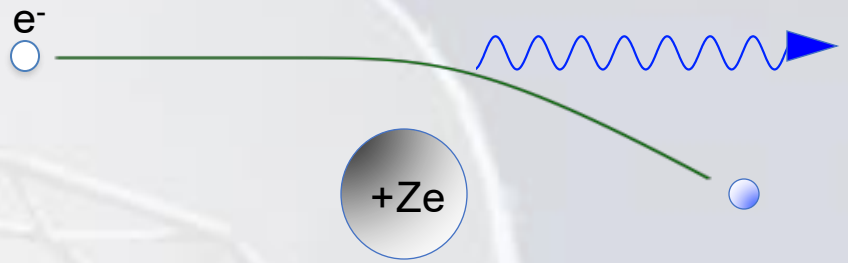

What are sources of electron acceleration?

Coulomb collisions (electrons on ions for radio regime)

AKA "breaking radiation" or brehmsstrahlung. For a plasma in TE (Maxwellian distribution) we refer to **thermal bremsstrahlung** or **thermal free-free** radiation. (Nonthermal e-i/e-e brems relevant to HXR emission.)

In the RJ approximation the absorption coefficient is

$$\alpha_{ff} = \frac{n_e n_i}{\mu_\nu (2\pi\nu)^2}\left[\frac{32\pi^2 Z^2 e^6}{3(2\pi)^{1/2} m^3 c}\right]\left(\frac{m}{k_B T}\right)^{3/2} \ln\Lambda$$

$$\approx \frac{9.786 \times 10^{-3}}{\mu_\nu \nu^2}\frac{n_e n_i}{T^{3/2}} \ln\Lambda$$

$\Lambda \approx 4.954 \times 10^7 (T^{3/2} / Z\nu)$ for $T < 3.16 \times 10^5$ K

$\Lambda \approx 4.7 \times 10^{10} (T / \nu)$ for $T > 3.16 \times 10^5$ K

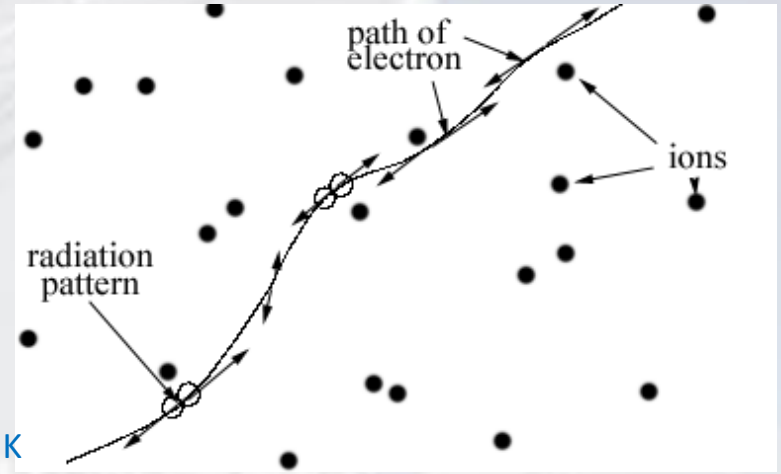

$$\tau_{ff} = \int \alpha_{ff}\, \mathrm{ds} \;\propto\; n_e^2 L \nu^{-2} T^{-3/2}$$

Note: for a uniform, optically thin source $T_b \approx \tau_{ff} T \sim EM / \nu^2 T^{1/2}$

The optical depth due to thermal free-free absorption *increases* with column EM, and *decreases* with increasing frequency and temperature. Optically thin emission depends on EM but is relatively insensitive to T.

Emission Mechan

What are sources of electron accelerat

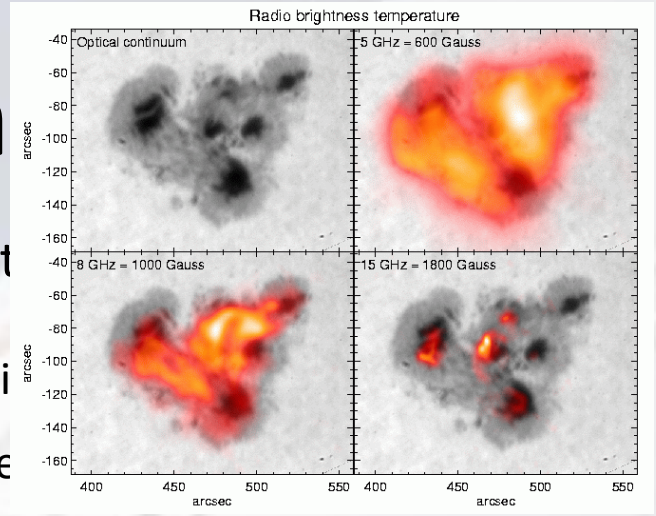

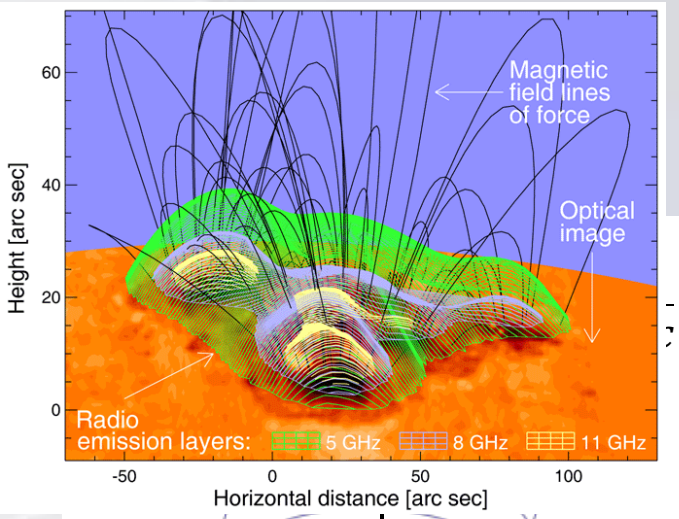

$\boldsymbol{v} \times \boldsymbol{B}$

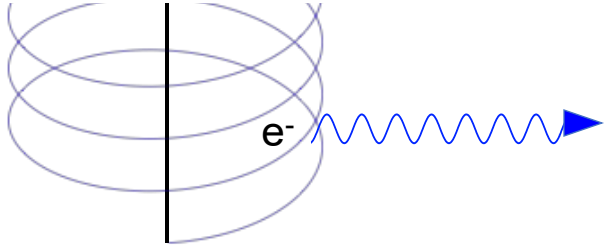

$$\nu_B = \frac{qB}{2\pi mc} = 2.8\ B\ \text{MHz}$$

Electron cyclotron frequency

The **Lorentz force** (when a magnetic field i

"Gyromagnetic radiation", sometimes calle

The terminology used to describe gyromagnetic emission depends on the electron energy.

- If the distribution is in TE and $\gamma = 1$ it is referred to as thermal **gyroresonance emission**.
- If the electrons are mildly relativistic ($\gamma \sim$few) it is referred to as **thermal** or **nonthermal gyrosynchrotron radiation**.
- And if the electrons are fully relativistic ($\gamma \gg 1$) it is referred to as **synchrotron radiation**.

Thermal GR and nonthermal GS emission are strongly to moderately circularly polarized in the sense of the x-mode. Synchrotron emission is linearly polarized.

Thermal bremsstrahlung and the **gyromagnetic radiation** described above are examples of **incoherent** emission mechanisms, where the electrons emit independently and one can sum over a distribution to determine j_ν.

Emission Mechanisms

What are sources of electron acceleration?

The **Lorentz force** (when a magnetic field is present)

"Gyromagnetic radiation", sometimes called "magneto-bremsstrahlung"

The terminology used to describe gyromagnetic emission depends on the electron energy.

- If the distribution is in TE and $\gamma = 1$ it is referred to as thermal **gyroresonance emission**.
- If the electrons are mildly relativistic ($\gamma \sim$few) it is referred to as **thermal** or **nonthermal gyrosynchrotron radiation**.
- And if the electrons are fully relativistic ($\gamma \gg 1$) it is referred to as **synchrotron radiation**.

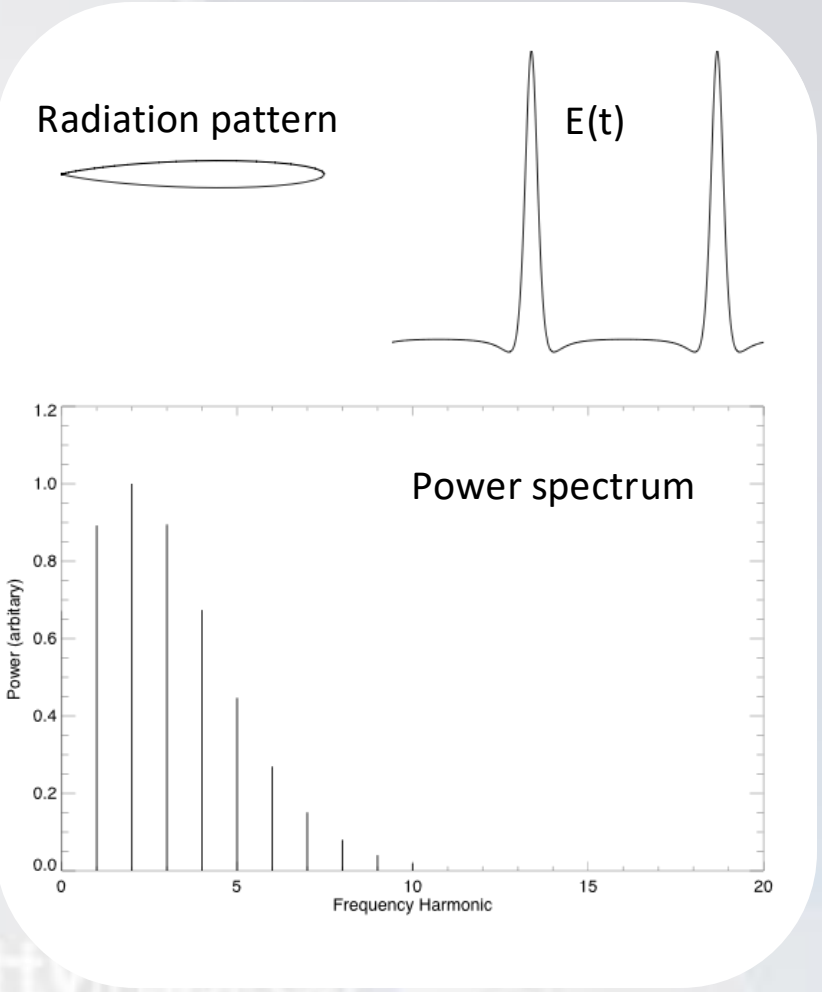

Thermal GR and nonthermal GS emission are strongly to moderately circularly polarized in the sense of the x-mode. Synchrotron emission is linearly polarized.

Thermal bremsstrahlung and the **gyromagnetic radiation** described above are examples of **incoherent** emission mechanisms, where the electrons emit independently and one can sum over a distribution to determine j_ν.

Coherent Emission

Coherent radiation involves collective effects - wave-wave or wave-particle interactions - that can result in very intense emission. They occur at natural frequencies of the plasma or combinations of the same.

One natural frequency is the **electron plasma frequency** $\nu_e = \omega_e/2\pi = (q^2 n_e/\pi m)^{1/2} = 9n_e^{1/2}$ kHz which, for $n_e \sim 10^8 - 10^{10}$ is $\nu_e \sim 100$ MHz to 1 GHz. Plasma waves are a longitudinal oscillation.

Solar radio bursts are attributed to **plasma radiation** at ν_e and/or $2\nu_e$; e.g., type III radio bursts.

The idea goes back to Ginsberg & Zheleznyakov (1958) but there have been many refinements since. Production of plasma radiation is a two-step process:

1. Production of Langmuir waves: two-stream, bump-on-the tail, or gap instability where $\partial f/\partial v > 0$ for some range of *v*
2. Three-wave interactions between L and t and a third wave:
   - $\omega_t = \omega_L + \omega'$ and $k_t = k_L + k'$
   - Fundamental: $\omega_t \approx \omega_L$ and so ω' small and $k' \approx -k_L$
   - Harmonic: $\omega' = \omega_L$ and $k' \approx -k_L$ (need secondary spectrum Langmuir waves)

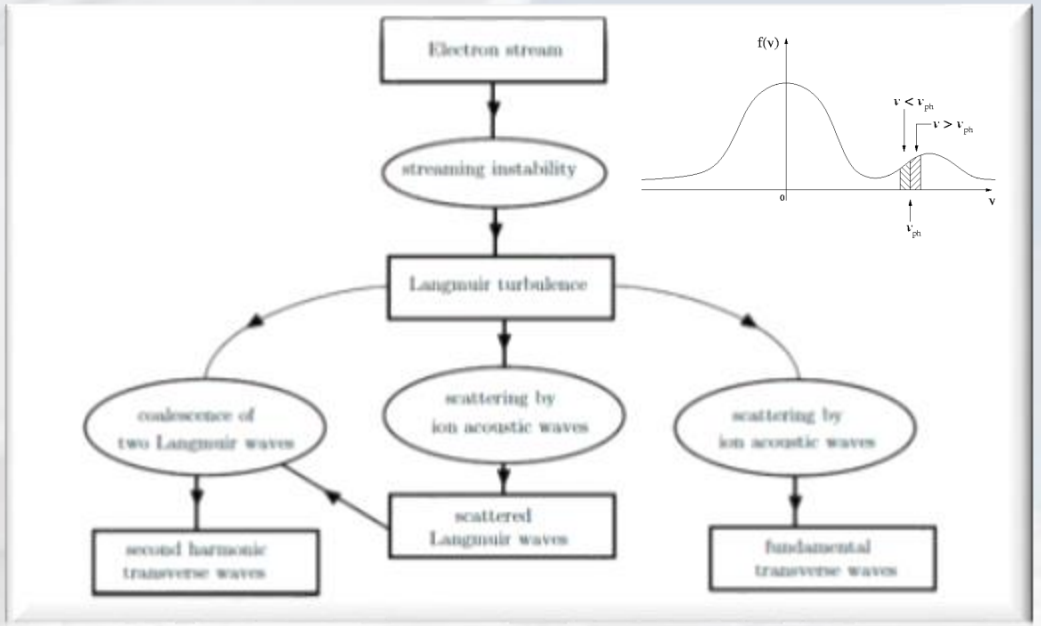

Coherent Emission

We've already discussed a second natural frequency in the Sun's corona, the **electron cyclotron frequency** $\nu_B = 2.8B$ MHz which, for *B = 100-1000* G, is $\nu_B = 280$ MHz to 2.8 GHz.

A loss-cone anisotropy or horseshoe distribution ($\partial f / \partial v_\perp$) provides the free energy to directly amplify EM waves at ν_B (x-mode favored) – so called **electron cyclotron maser emission.** Highly circularly polarized.

The idea goes back to Twiss (1958) but its modern incarnation began with work by Wu & Lee (1979) with Melrose & Dulk (1981) pointing out its possible relevance to the Sun and stars. It is relevant to coherent emission from planets (terrestrial AKR, Jovian DAM) and certain stars (brown dwarfs, dMe, and Ap/Bp stars).

The mechanism is likely relevant to solar "spike bursts" but evidence for its role on the Sun more broadly has been elusive.

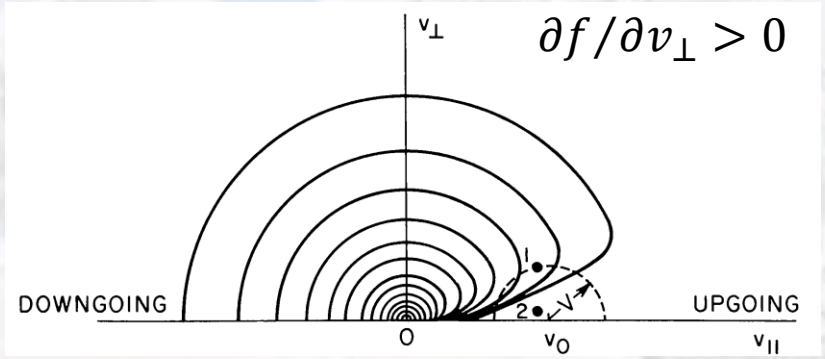

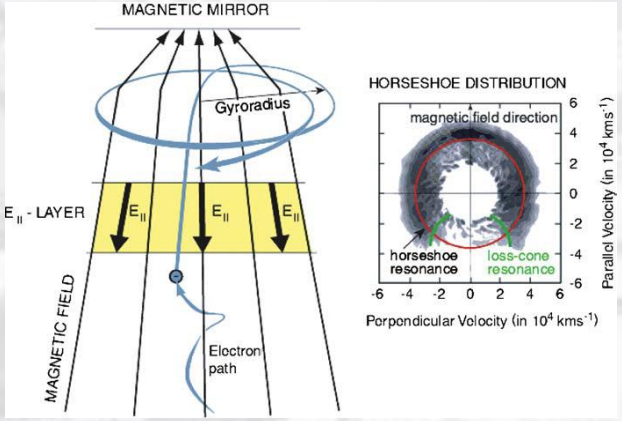

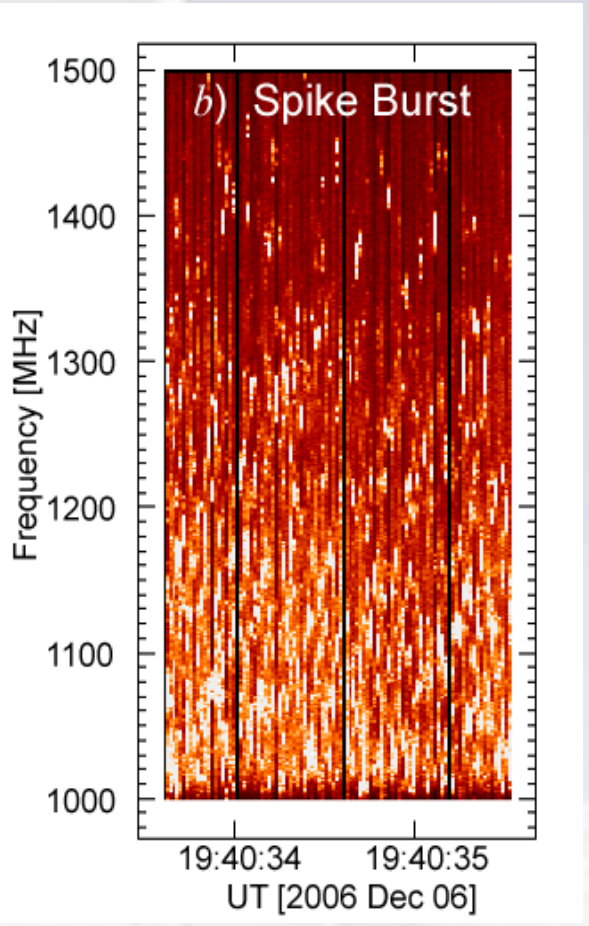

Types of Observations

- The simplest type of measurement at radio wavelengths is a measurement of the flux density of a source at a particular time and frequency. Such **total flux** measurements are taken by, e.g., Penticton F10.7 (EUV Proxy!) or the USAF RSTN network daily at local noon at selected frequencies.
- Also simple is a record of flux density at a particular frequency as a function of time, a **light curve**. RSTN **radiometers** do so at selected frequencies in total intensity. The Nobeyama **polarimeters** do so in both senses of circular polarization (RCP & LCP).

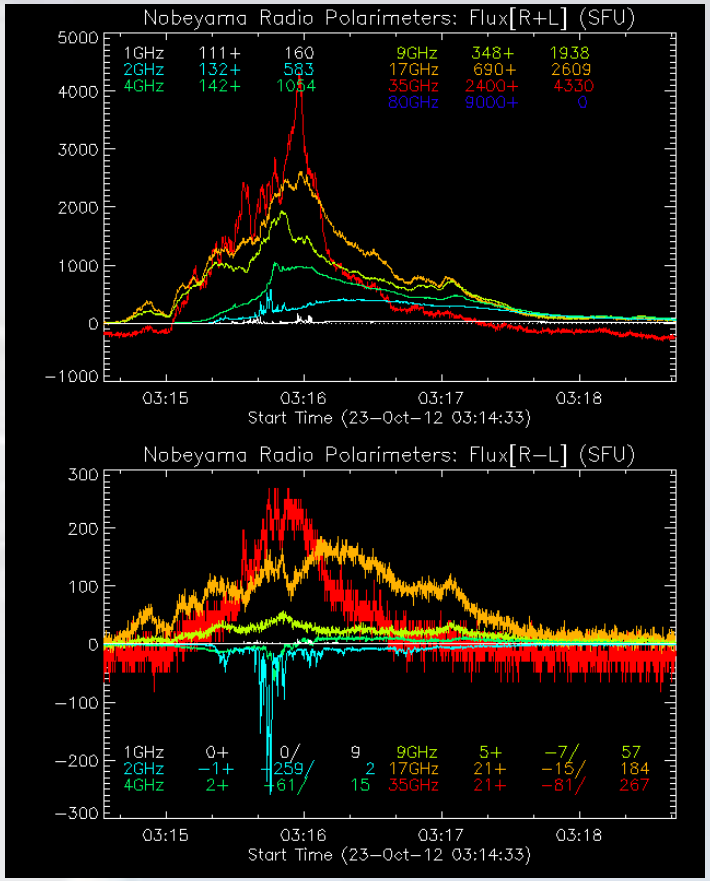

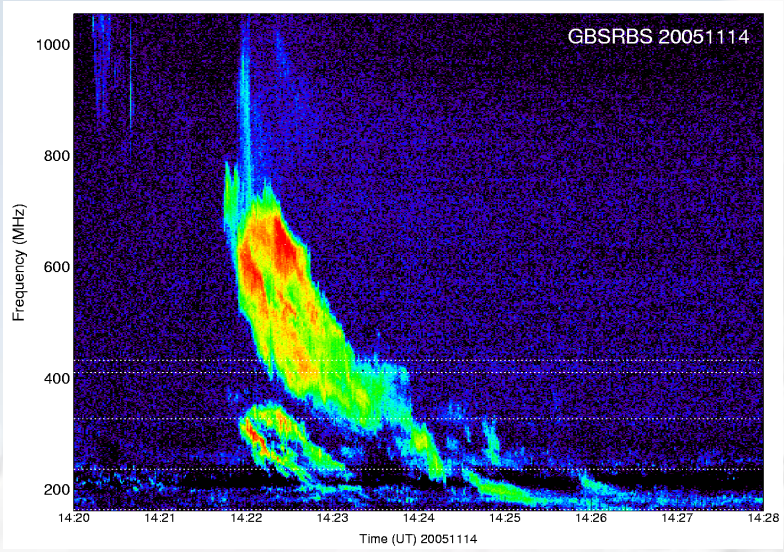

- The flux density as a function of frequency – the spectrum – is an important tool in astrophysics. For the Sun (and, increasingly, stars) **dynamic spectroscopy –** a record of (polarized) flux density as a function of frequency **and** time – has been a mainstay of solar radiophysics since its earliest days. RSTN obtains dynamic spectra, as do many instruments across Europe and Asia (e.g., Tremsdorf, Hiraiso).

Types of Observations

- High resolution (polarized) images of the Sun are of critical importance, too!

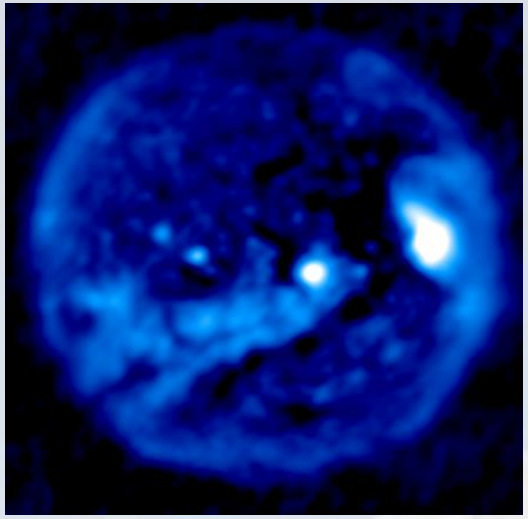

VLA: 1.4 GHz (λ=21 cm)

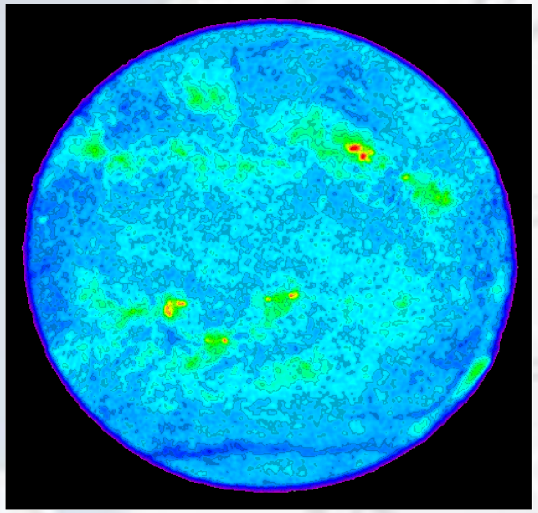

VLA: 4.9 GHz (λ=6.1 cm)

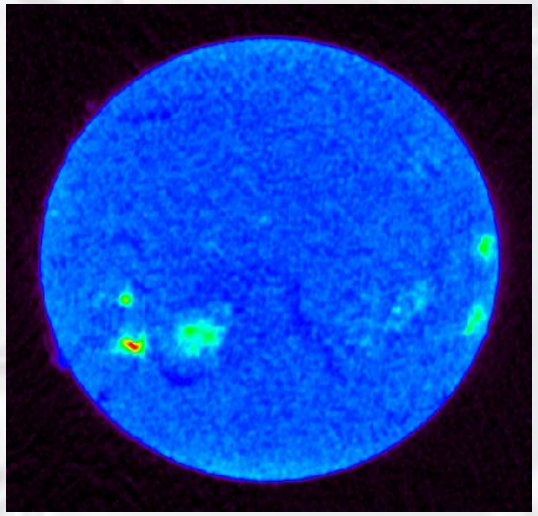

NoRH: 17 GHz (λ=1.76 cm)

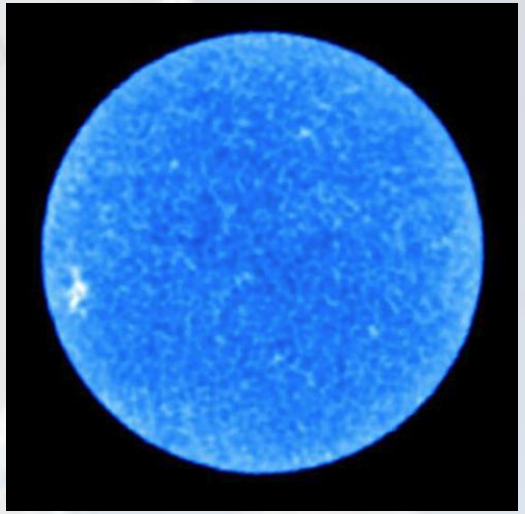

ALMA: 239 GHz (λ=1.25 mm)

Ideally, we'd have the ability to combine **all** of these observables: time-resolved broadband imaging spectropolarimetry!

Radio Instrumentation

Instruments that perform total flux measurements, obtain light curves, or perform dynamic spectroscopy use small antennas that are typically designed to observe the full disk of the Sun. Since the Sun is roughly 0.5° in size and the angular resolution of an antenna is $\theta \sim \lambda / D$ the diameter of the antenna must be $D \lesssim 115\lambda$ (both in cm).

To resolve the Sun at radio wavelengths one needs a very large aperture *D*. However, even the 1000 ft (305 m) telescope at Arecibo only yielded an angular resolution of 3’ at a wavelength of 20 cm – and imaging is cumbersome (raster mapping, focal plane array).

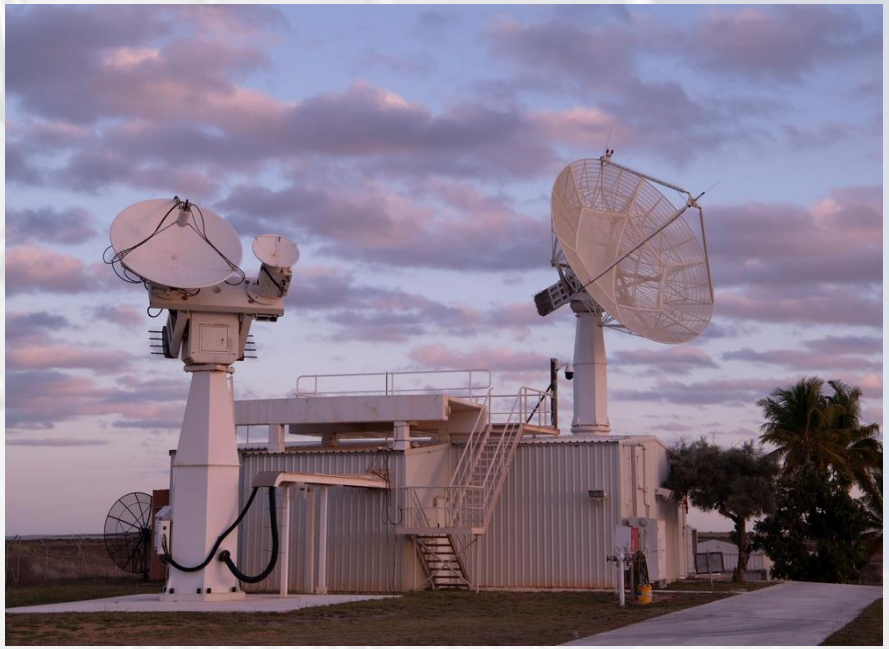

USAF/RSTN station at Learmonth, W Australia

Radio Instrumentation

The answer? Use many small antennas to sample a large effective aperture: **Fourier synthesis**. A Fourier synthesis telescope measures the (discrete) Fourier transform of the sky, with each **antenna pair** (baseline) measuring a Fourier component. The angular resolution of the instrument is therefore determined by the maximum separation between antennas!

The future: synthesis imaging across very large bandwidths to enable broadband imaging spectropolarimetry with high temporal and angular resolution! EOVSA (1-18 GHz) is the pathfinder.

Jansky Very Large Array (VLA)

Nobeyama Radioheliograph (NoRH)

Expanded Owens Valley Solar Array (EOVSA)

Observational Heliophysics II:

Radio Emission from the Sun and Heliosphere

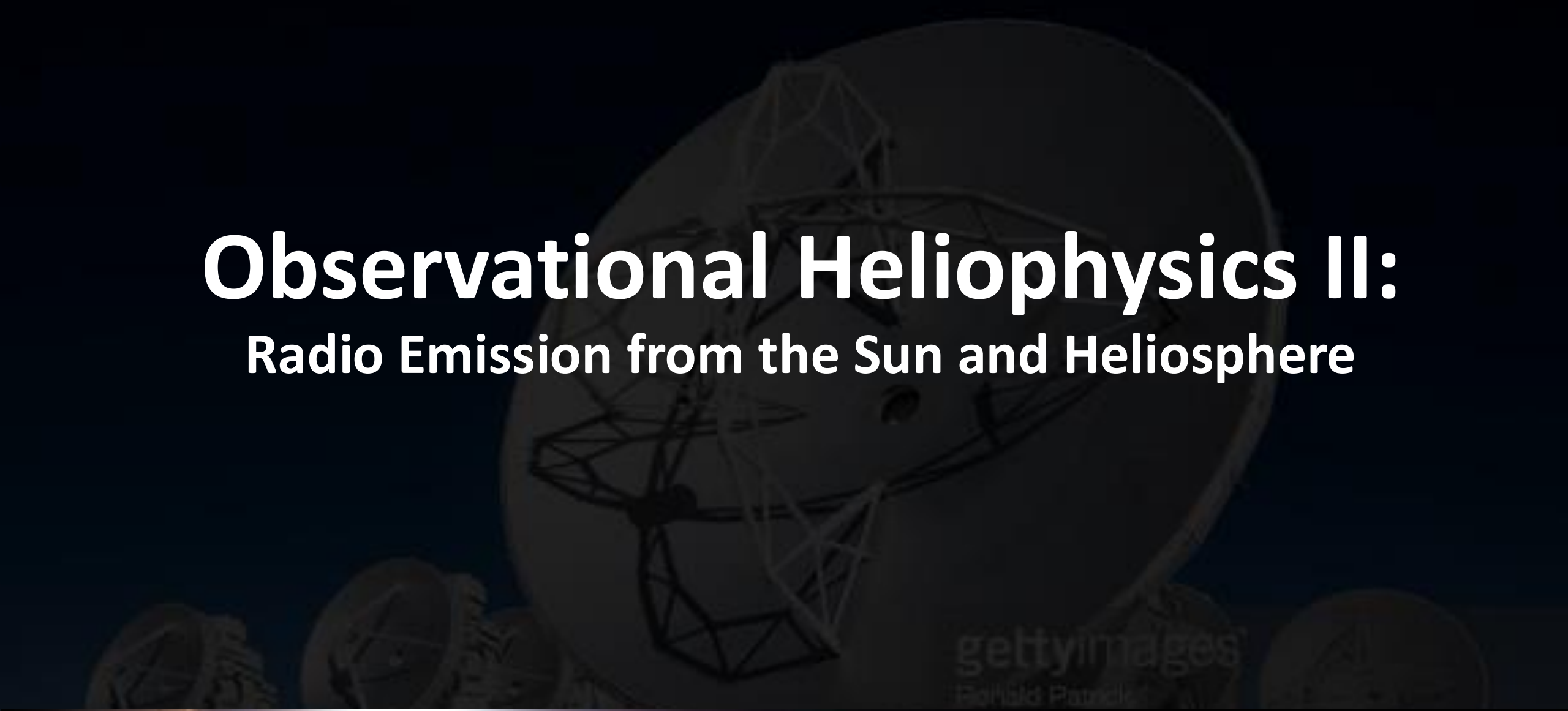

ADVANCING THE SCIENCE OF HELIOPHYSICS

A partnership between NASA UCAR COMMUNITY PROGRAMS | CPAESS

The utility of radio observations: some examples

Radio emission occurs from the low solar chromosphere, out into the corona, in the IPM, to the very boundary of the solar system. It is produced by thermal and nonthermal populations through incoherent (thermal free-free and gyromagnetic emission) and coherent (plasma, ECM) mechanisms. As such, serves as a probe and diagnostic of physical conditions in remote plasmas for an extraordinarily wide range of phenomena.

- Emission from the quiet Sun – chromospheric and coronal heating; active regions
- Flares – spatiotemporal evolution of n(E) and B; electron acceleration and transport
- Coronal mass ejections – nascent stages and the evolving magnetic field
- Radio bursts – coronal electron beams (type III) and shocks (type II)
- The solar system boundary (heliopause)

submm/mm-λ | cm-λ | dm-λ | m/Dm-λ | Hm/km-λ

ALMA* | JVLA*, EOVSA, MUSER, NoRH | JVLA* | LOFAR*, MWA, LWA-OV, NaRH | PSP, WIND, STEREO, SunRISE

thermal
H & H^- ff

thermal ff, GR
NT GS

thermal ff
NT GS
coherent

NT GS
coherent

coherent

chromosphere → upper chromo to low corona → mid- to outer corona → outer corona to 1 AU

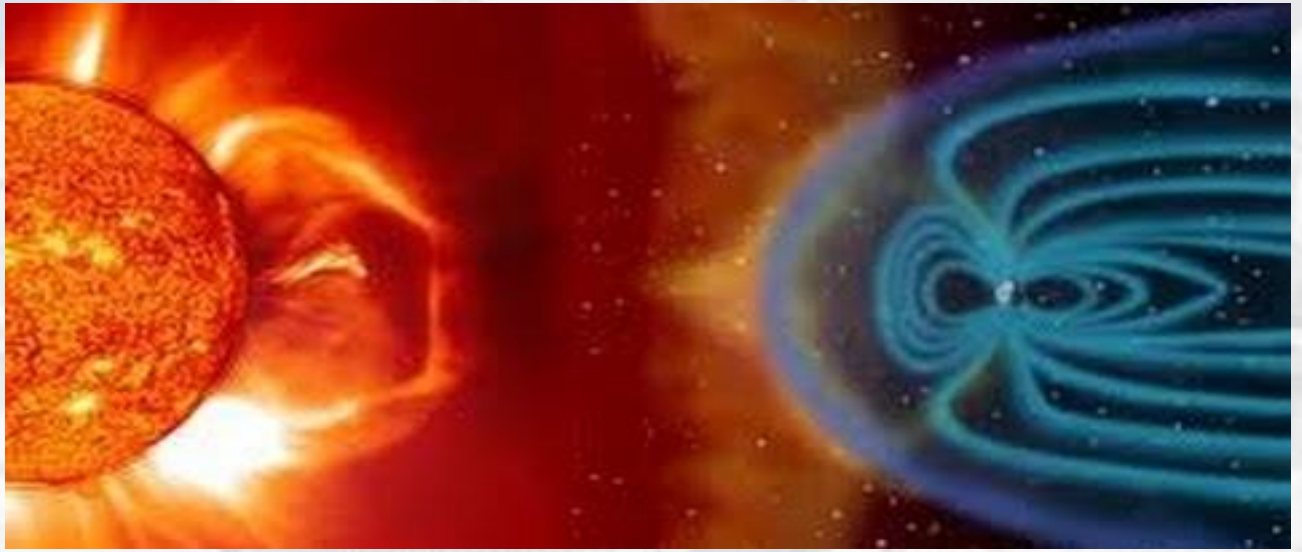

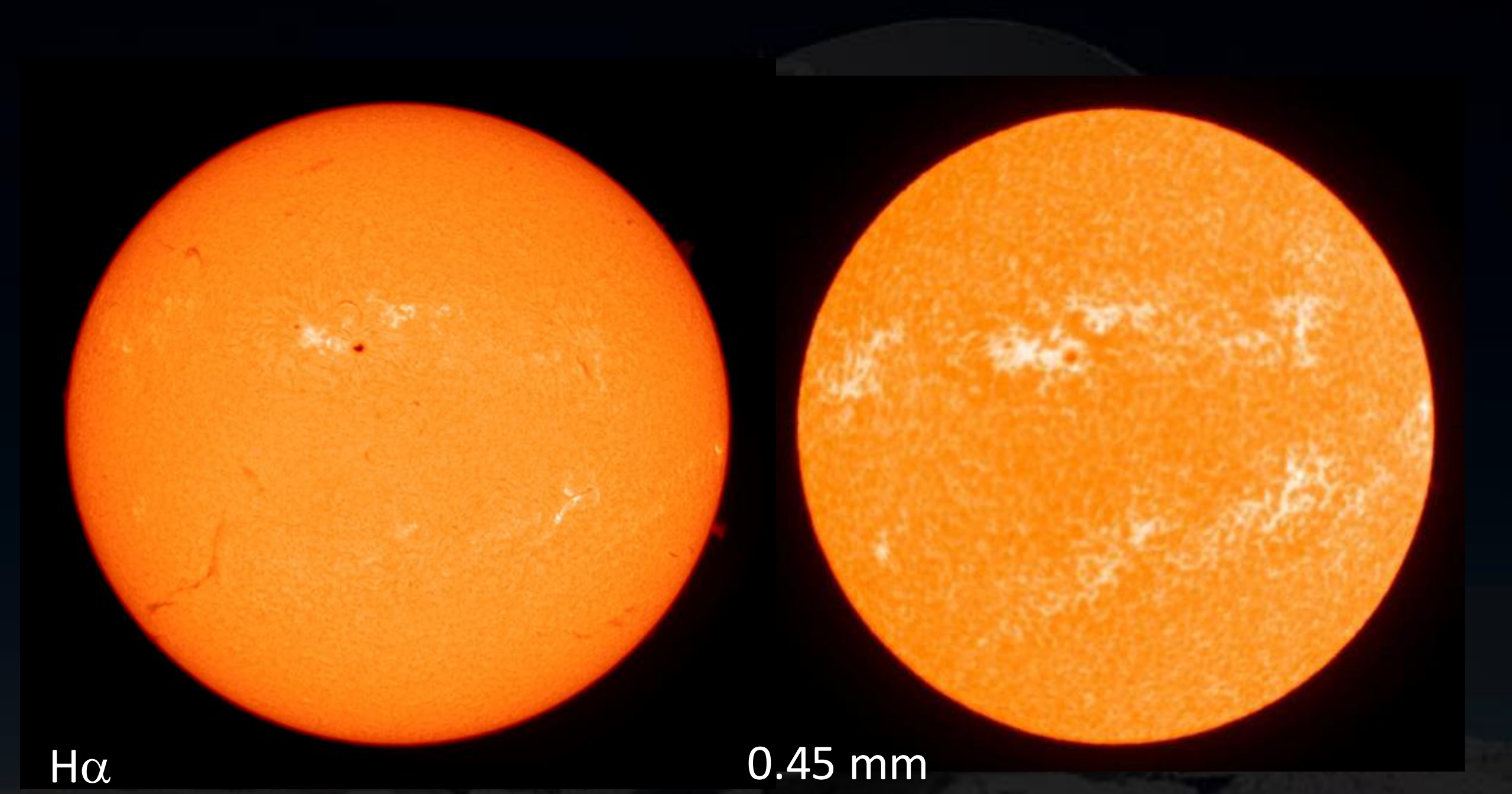
Hα
0.45 mm

Solar Chromosphere

To date, the chromosphere has been studied primarily in optical and UV spectral lines.

- O/UV spectral lines generally form under conditions of non-LTE.
- RT is complex – resonant scattering, partial frequency redistribution, non-equilibrium ionization

ALMA observations offer a powerful complement to O/UV observations.

- mm-λ continuum forms under LTE/RJ
- Sources of opacity are well-understood (thermal free-free and H^-)
- RT is relatively straightforward

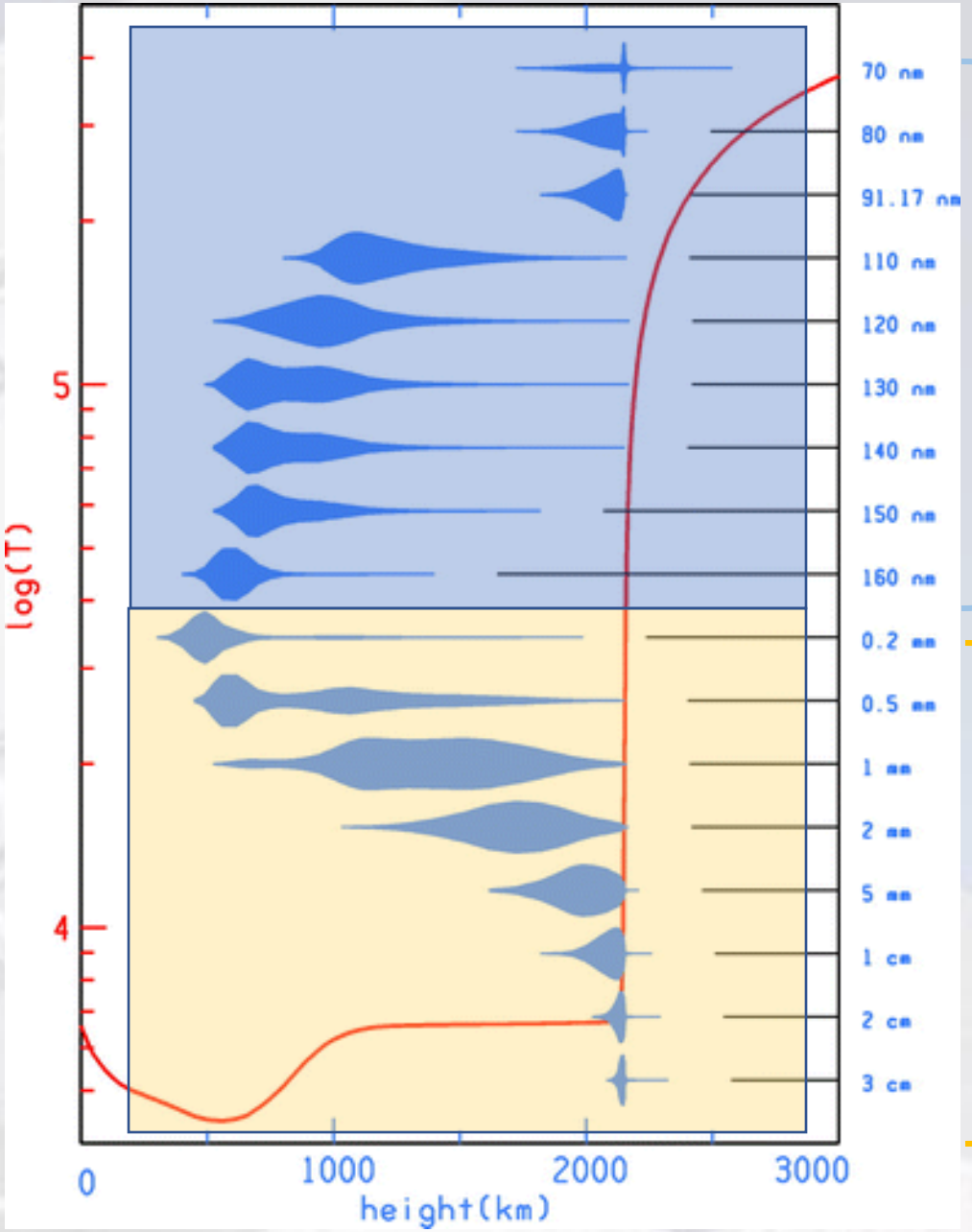

Avrett 2008

Solar Chromosphere

Complex & dynamic

- Onset of non-radiative heating
- Waves, shocks, mass motions
- Transition from dominance of gas pressure to magnetic pressure
- Transition from low ionization to high ionization

Outstanding issues include the structure, dynamics, energy budget, and energy transfer in the chromosphere.

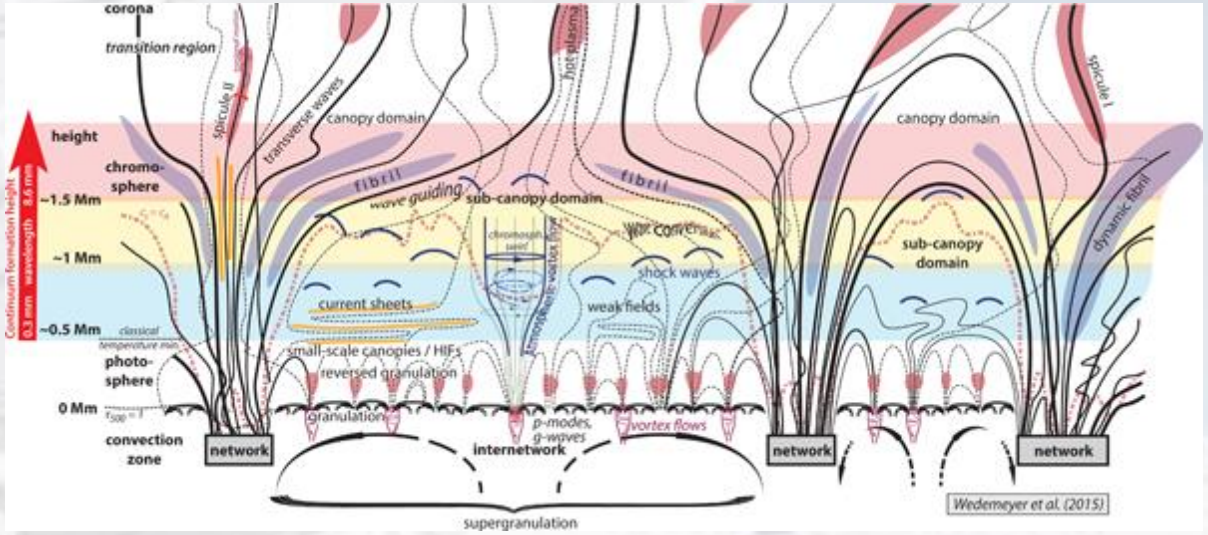

Example: spicules

The idea that spicules are launched and heated, delivering significant mass and energy to the solar corona, revives and builds on ideas from some time ago. Authors have suggested that an **eruptive distribution** that also includes, in addition to spicules (Sterling & Moore 2016, Sterling + 2024), "jetlets" (Raouafi & Steborg 2014) and jets (e.g., Raouafi + 2023).

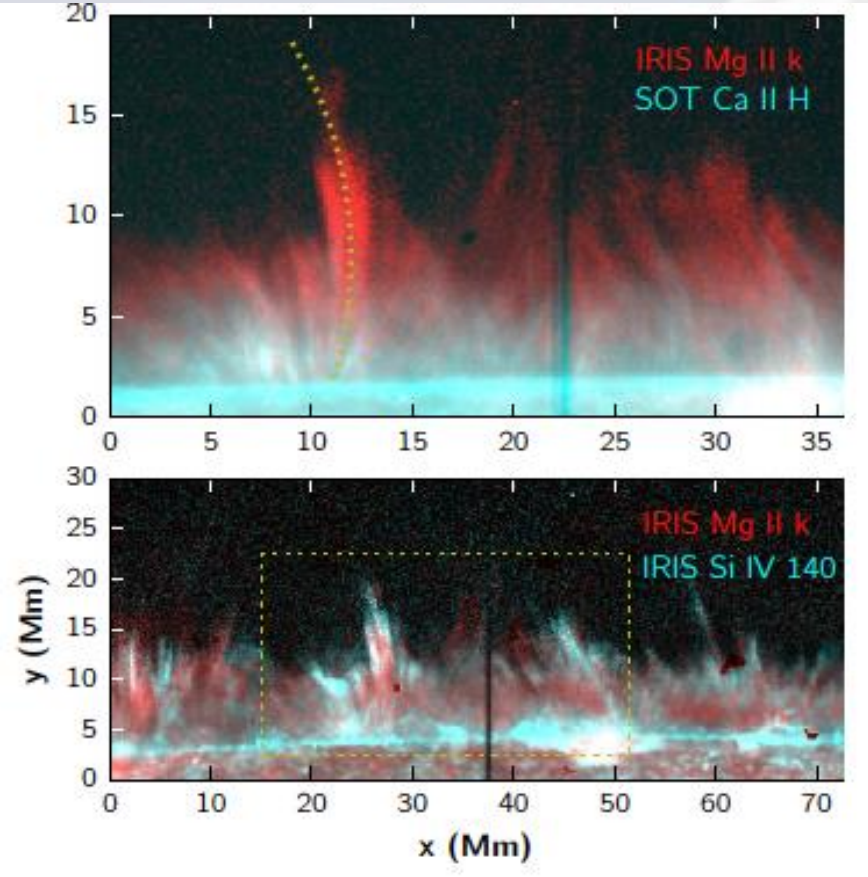

Pereira + 2014

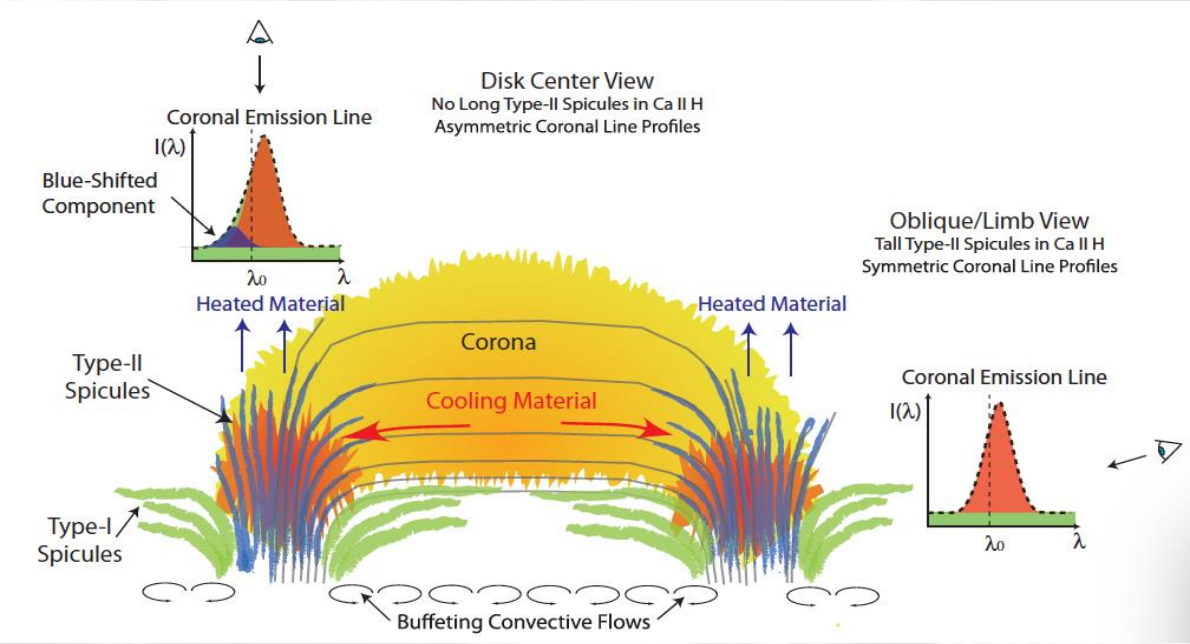

De Pontieu + 2009

ALMA observations challenge these ideas

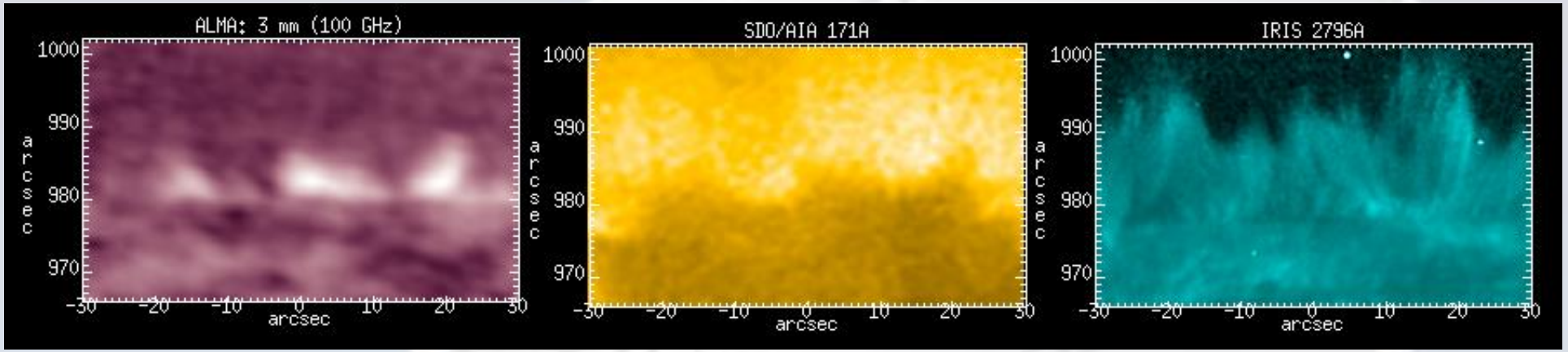

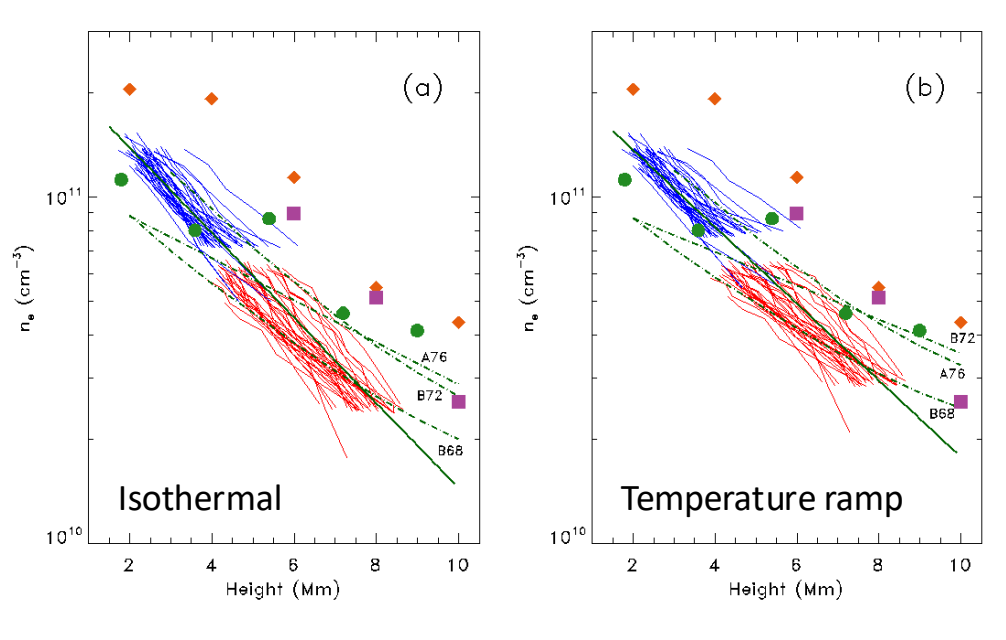

ALMA observations were made of spicules on the solar limb at 1.25 and 3 mm. The emission is optically thin free-free radiation. We have

$$\tau_{ff}(h) = -\log[1 - T_b(h) \,/\, T(h)] \approx T_b(h) \,/\, T(h)$$

$$n_e(h) = \left[\frac{\tau_{ff}(h) T(h)^{3/2} \nu^2}{D_s C \xi(T,\nu)}\right]^{1/2}$$

$$n_e(h) \propto \sqrt{\frac{T_b T^{1/2}}{\xi}} \sim \frac{T^{1/4}}{\xi^{1/2}}$$

submm/mm-λ | cm-λ | dm-λ | m/Dm-λ | Hm/km-λ

ALMA*

JVLA*
EOVSA
MUSER
NoRH

JVLA*
EOVSA

LOFAR*
MWA
LWA-OV
NaRH

PSP
WIND
STEREO
SunRISE

thermal
H & H^- ff

thermal ff, GR
NT GS

thermal ff
NT GS
coherent

NT GS
coherent

coherent

chromosphere → upper chromo to low corona → mid- to outer corona → outer corona to 1 AU

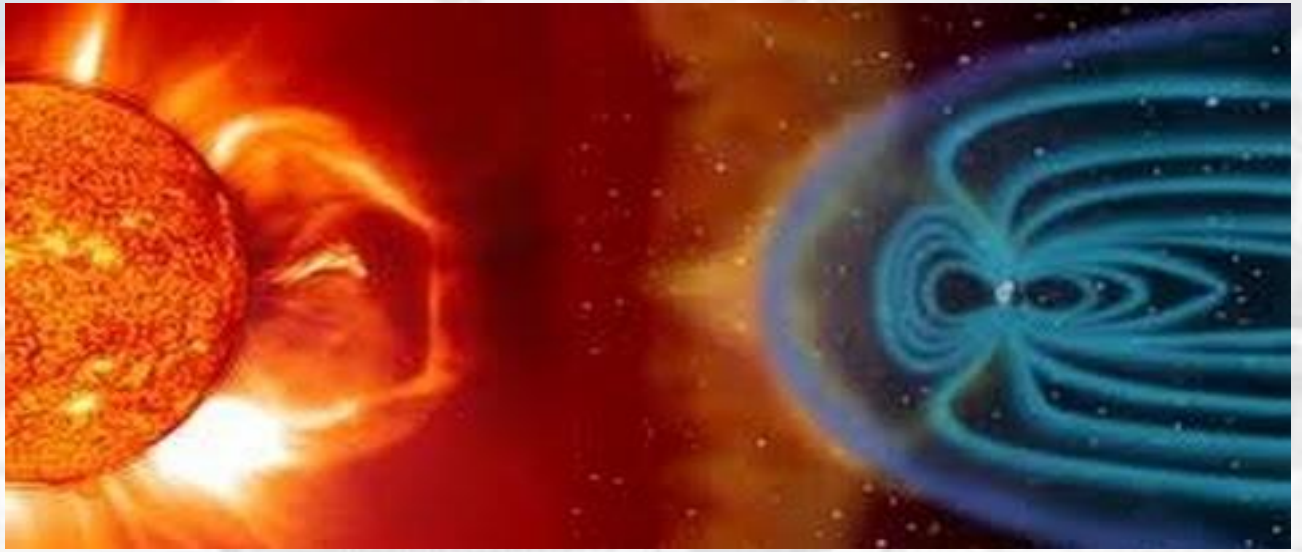

Radio Emission in Microwaves

Radiation at cm-λ is well-suited for exploiting thermal f-f, thermal GR, and nonthermal GS radio emission to study a wide variety of problems, including

- The nature and evolution of coronal magnetic fields
- Particle acceleration and transport
- Eruptive phenomena

as they manifest in the upper chromosphere into the low corona.

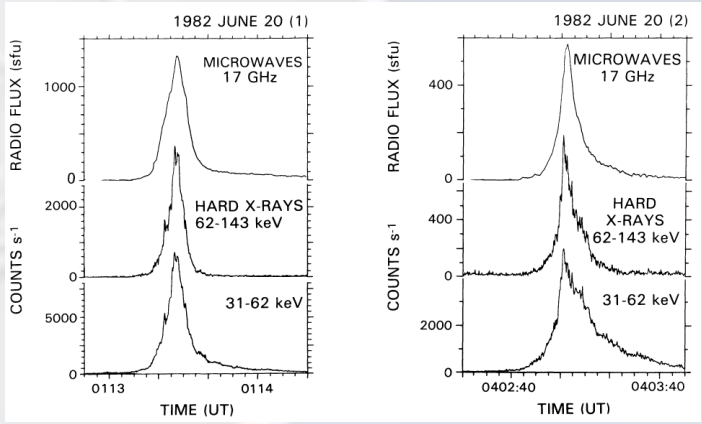

Kosugi, Dennis, & Kai 1988

Particularly interesting is nonthermal gyrosynchrotron radiation from flares involving electrons accelerated to MeV energies.

Gyrosynchrotron emission is highly complementary to HXR/γ-ray emission. While the energies of the emitting population of electrons might be the "same" they have very different dependencies on $n_{th}, T, |B|, \theta,$ and $n_{rl}(E, \phi)$.

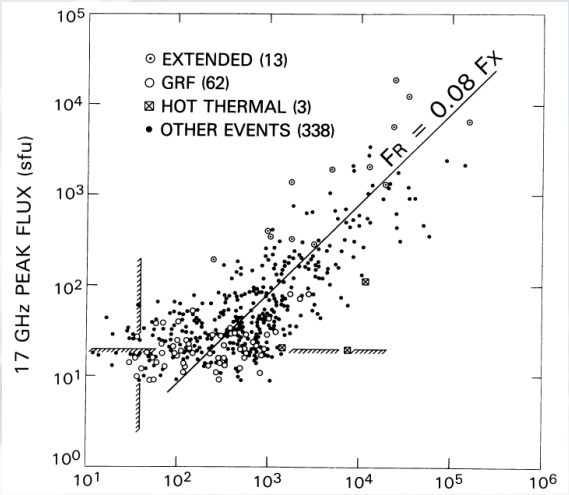

TPP model (Melrose & Brown 1976)

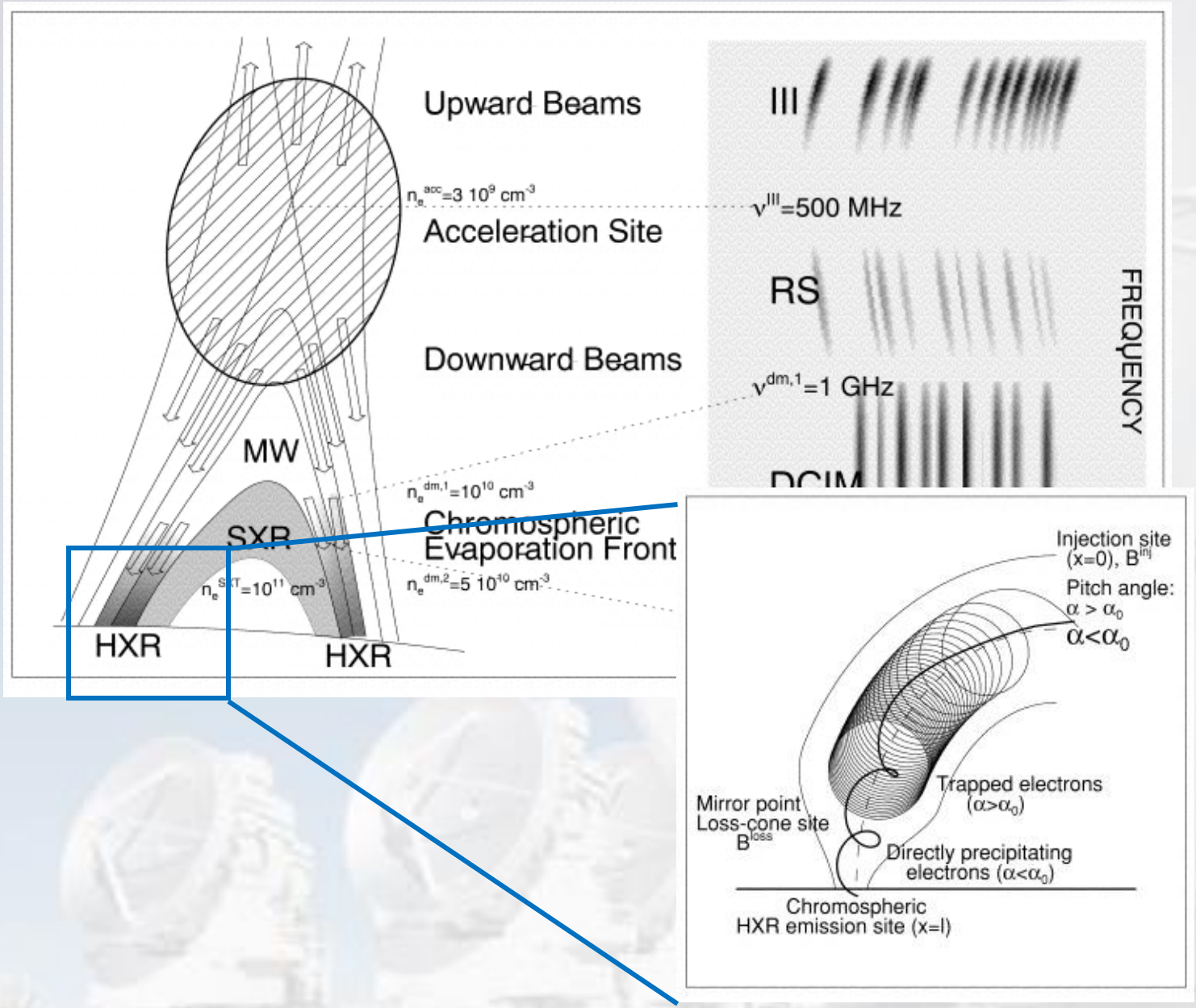

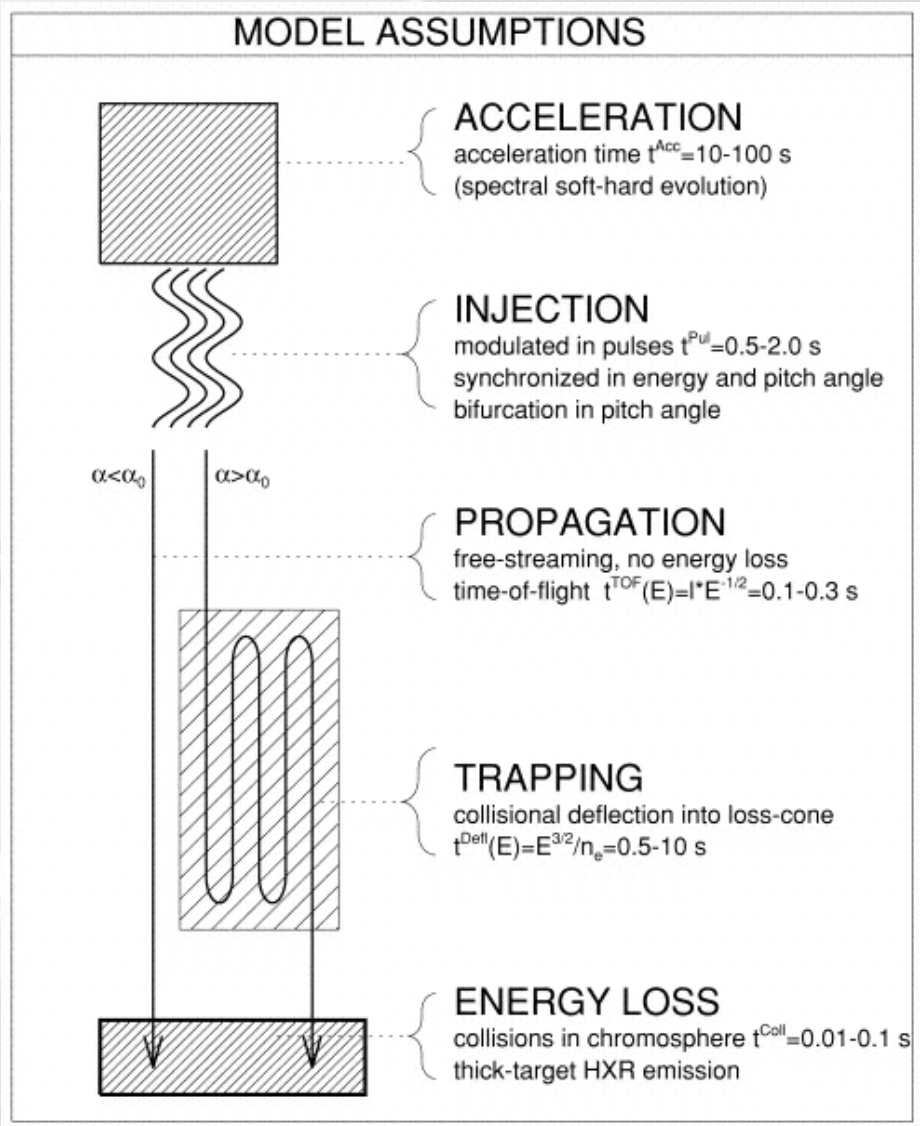

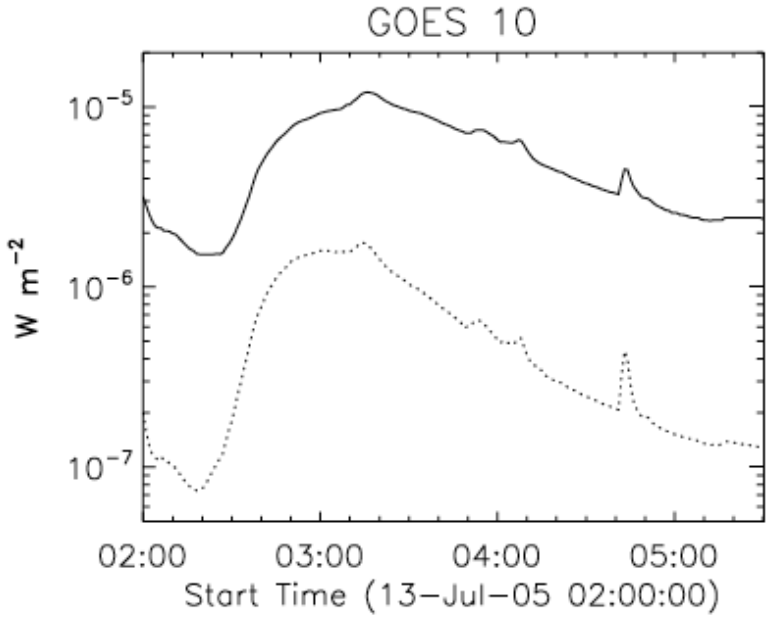

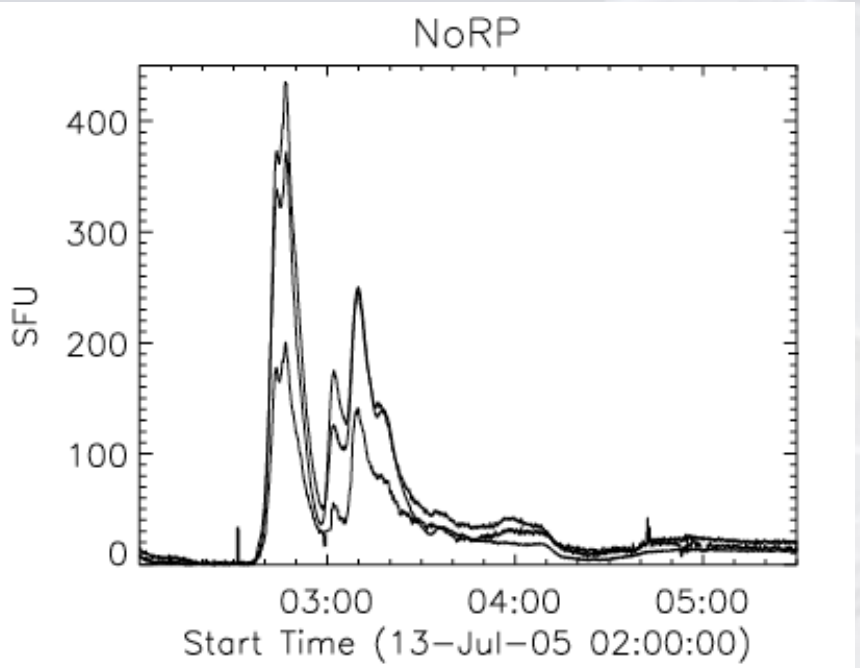

2005 Jul 13 M1.1 flare

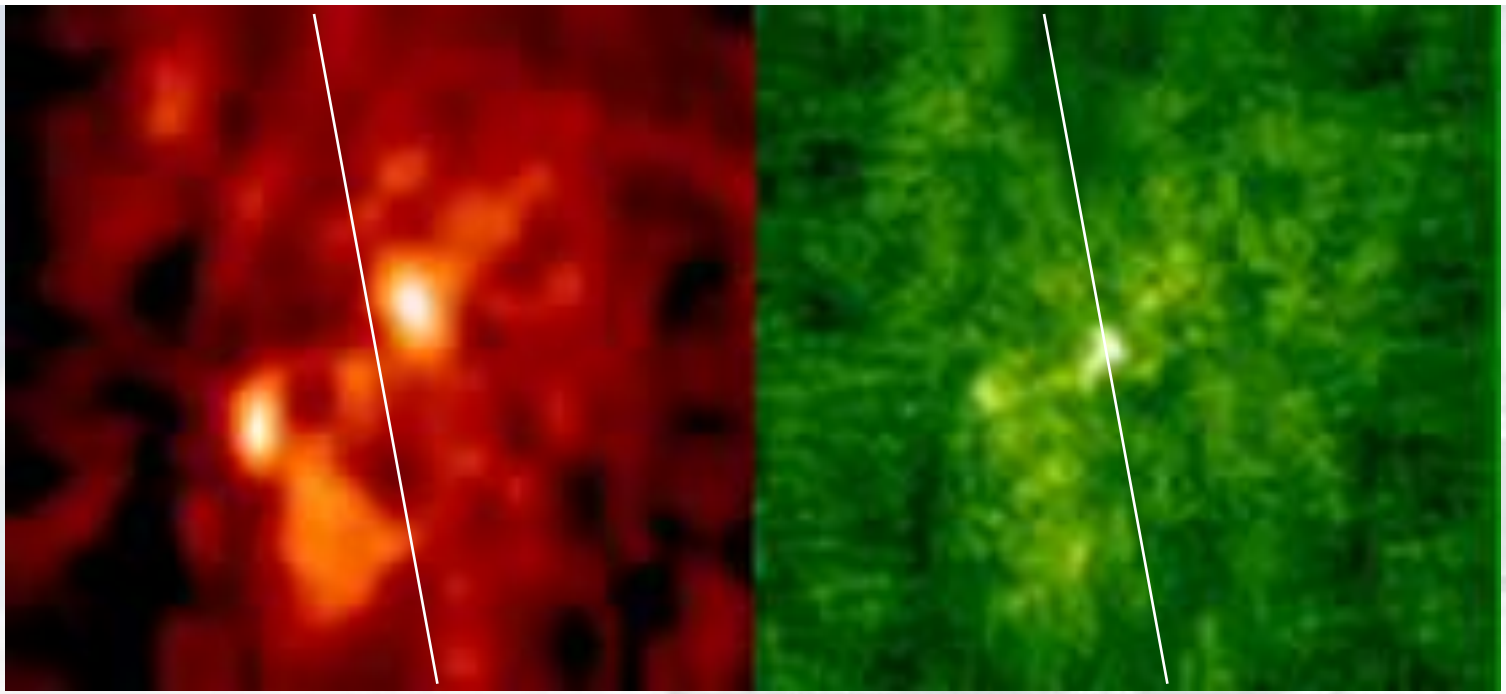

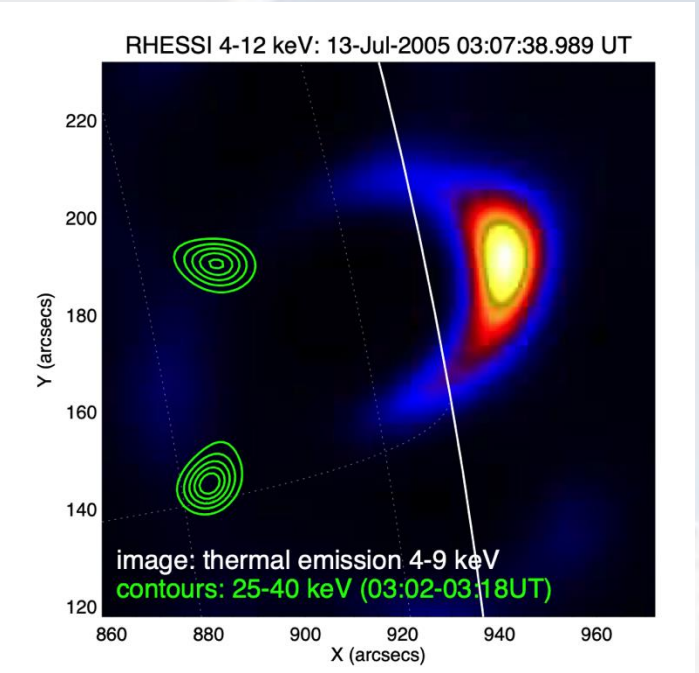

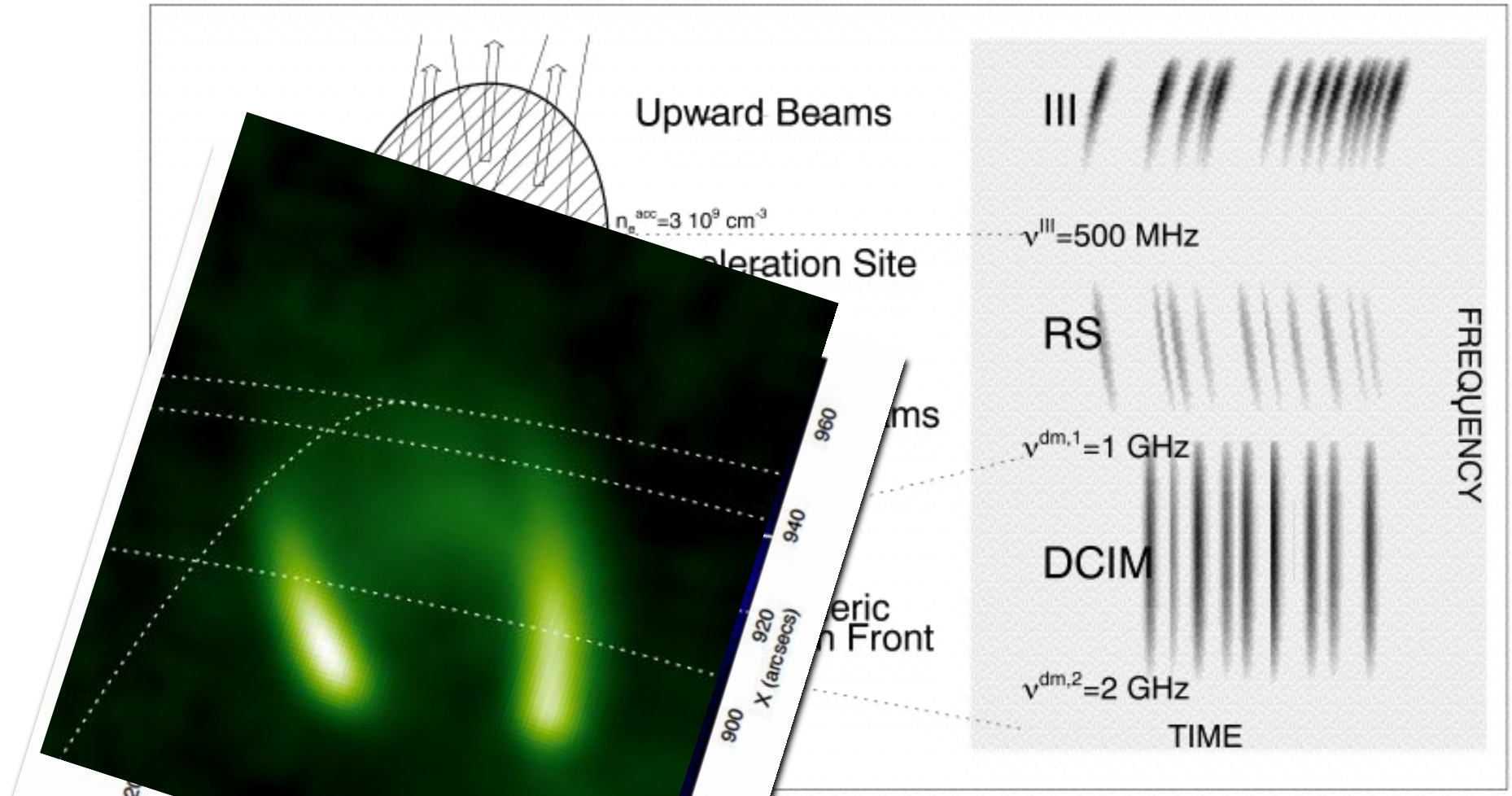

Aschwanden & Benz 1997

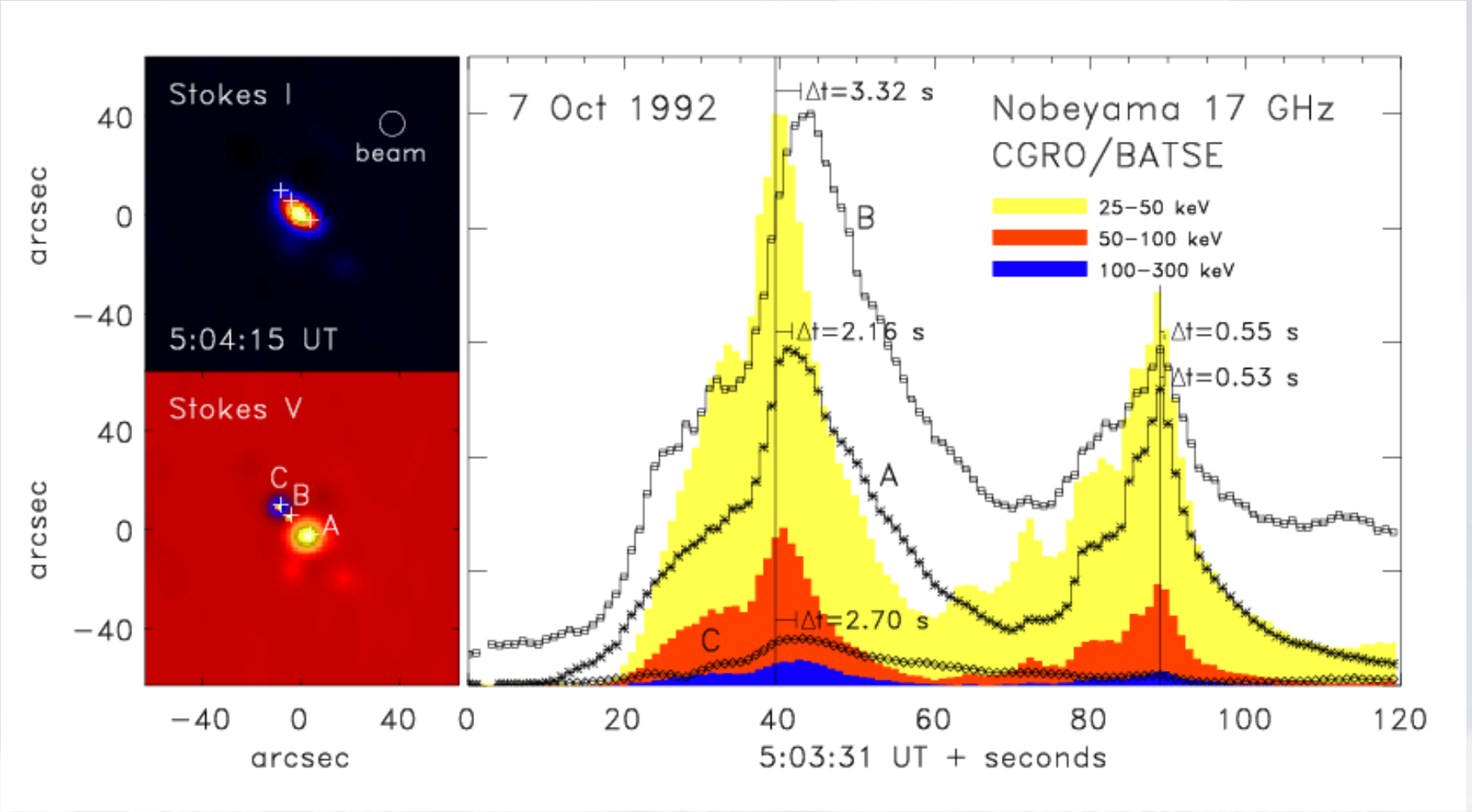

Trapping delays the peak and decay of radio emission relative to HXR emission. The electron deflection time for Coulomb collisions is $t_D \sim 2 \times 10^8 E_{keV}^{3/2}/n_{th}$ sec. Note differences in delay times as a funciton of location within the source.

Variation with B

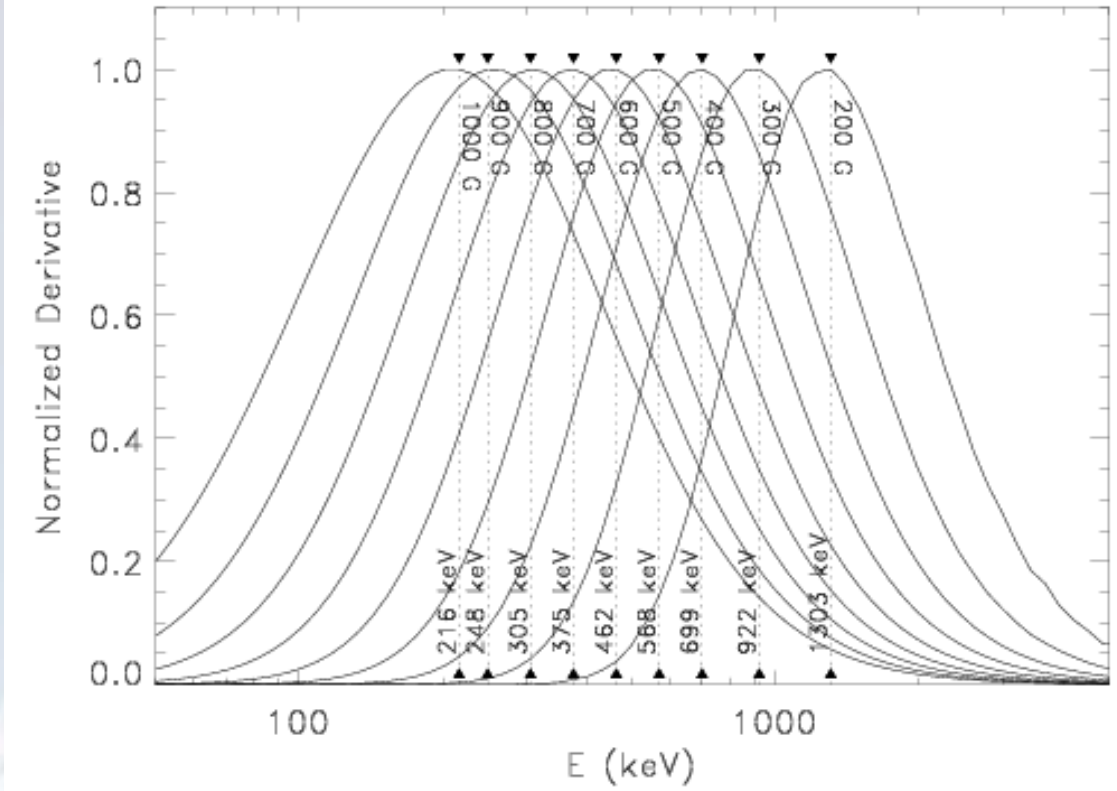

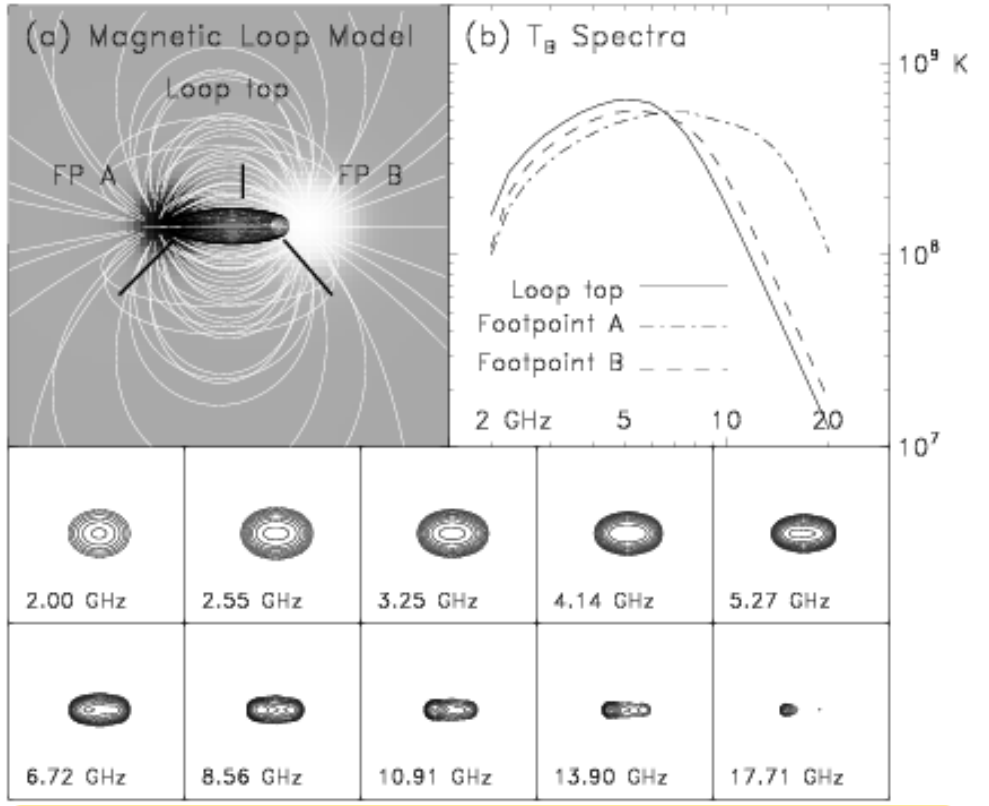

A magnetic loop acts as a dispersive element! Weak magnetic field: higher s, more energetic electrons required.

This dispersive effect is also reflected in the distribution of source brightness.

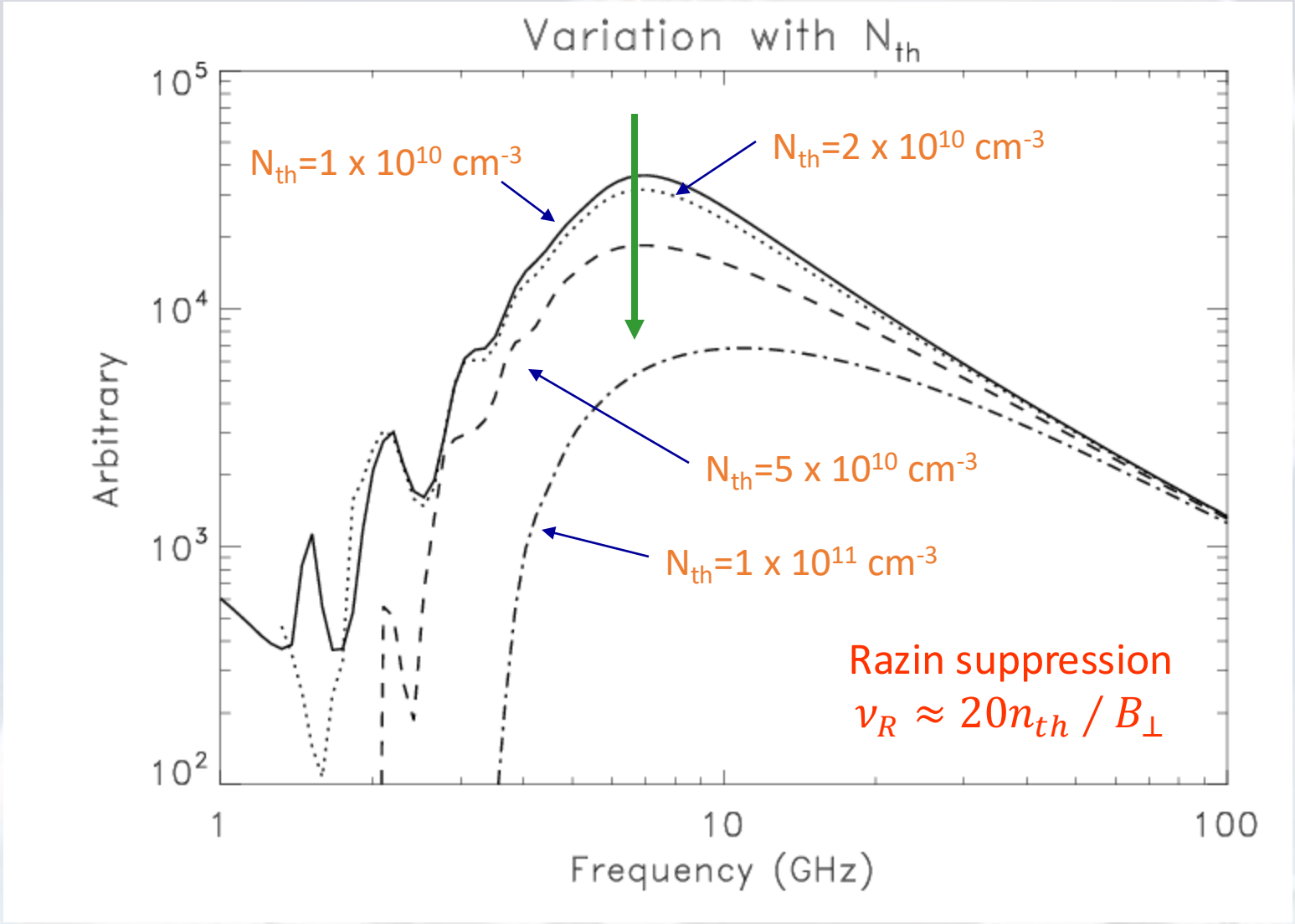
Variation with N_{th}
10^5
10^4
10^3
10^2
Arbitrary
1
10
100
Frequency (GHz)
N_{th}=1 x 10^{10} cm^{-3}
N_{th}=2 x 10^{10} cm^{-3}
N_{th}=5 x 10^{10} cm^{-3}
N_{th}=1 x 10^{11} cm^{-3}
Razin suppression
$\nu_R \approx 20 n_{th} / B_\perp$

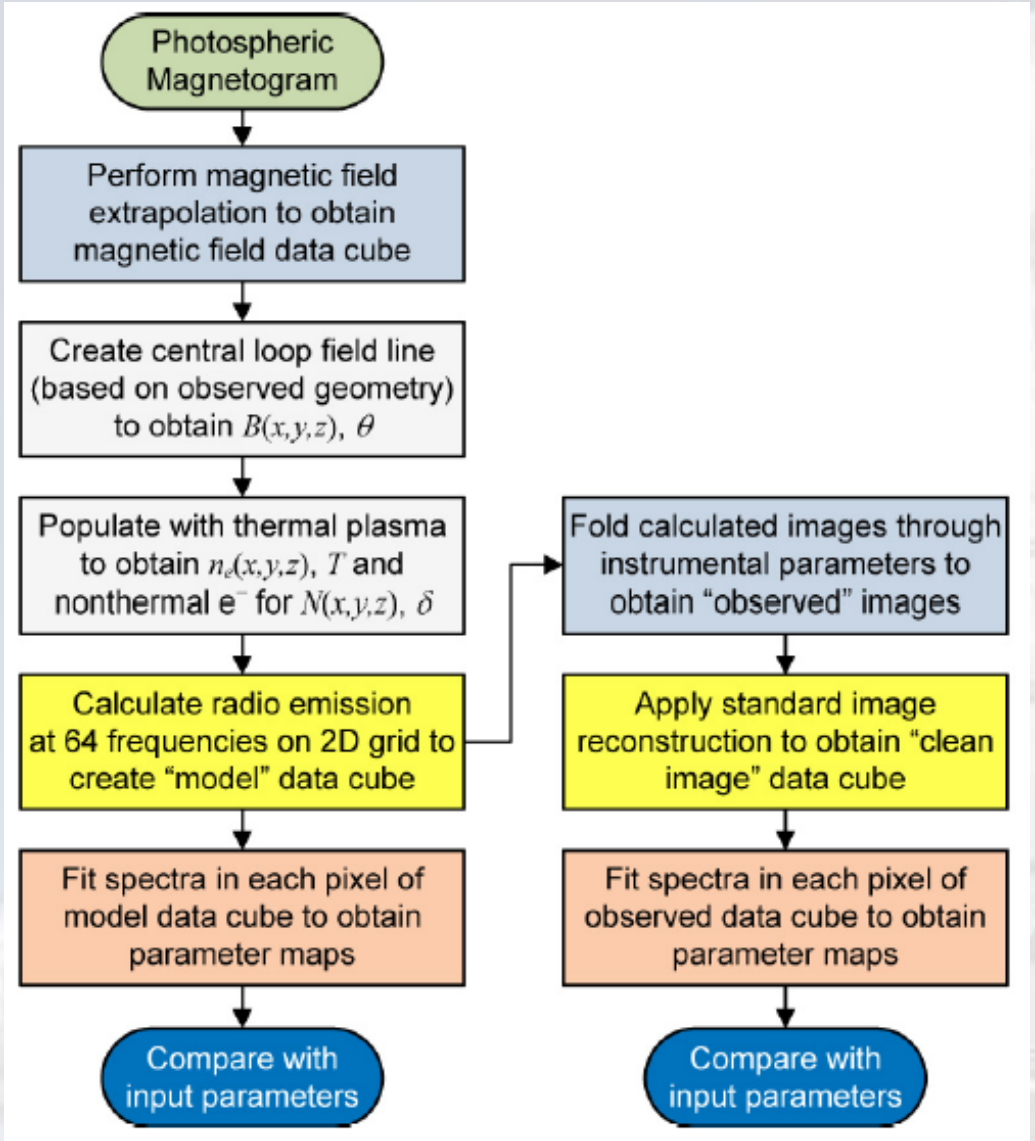
Photospheric Magnetogram
Perform magnetic field extrapolation to obtain magnetic field data cube
Create central loop field line (based on observed geometry) to obtain $B(x,y,z)$, θ
Populate with thermal plasma to obtain $n_e(x,y,z)$, T and nonthermal e⁻ for $N(x,y,z)$, δ
Calculate radio emission at 64 frequencies on 2D grid to create "model" data cube
Fit spectra in each pixel of model data cube to obtain parameter maps
Compare with input parameters
Fold calculated images through instrumental parameters to obtain "observed" images
Apply standard image reconstruction to obtain "clean image" data cube
Fit spectra in each pixel of observed data cube to obtain parameter maps
Compare with input parameters

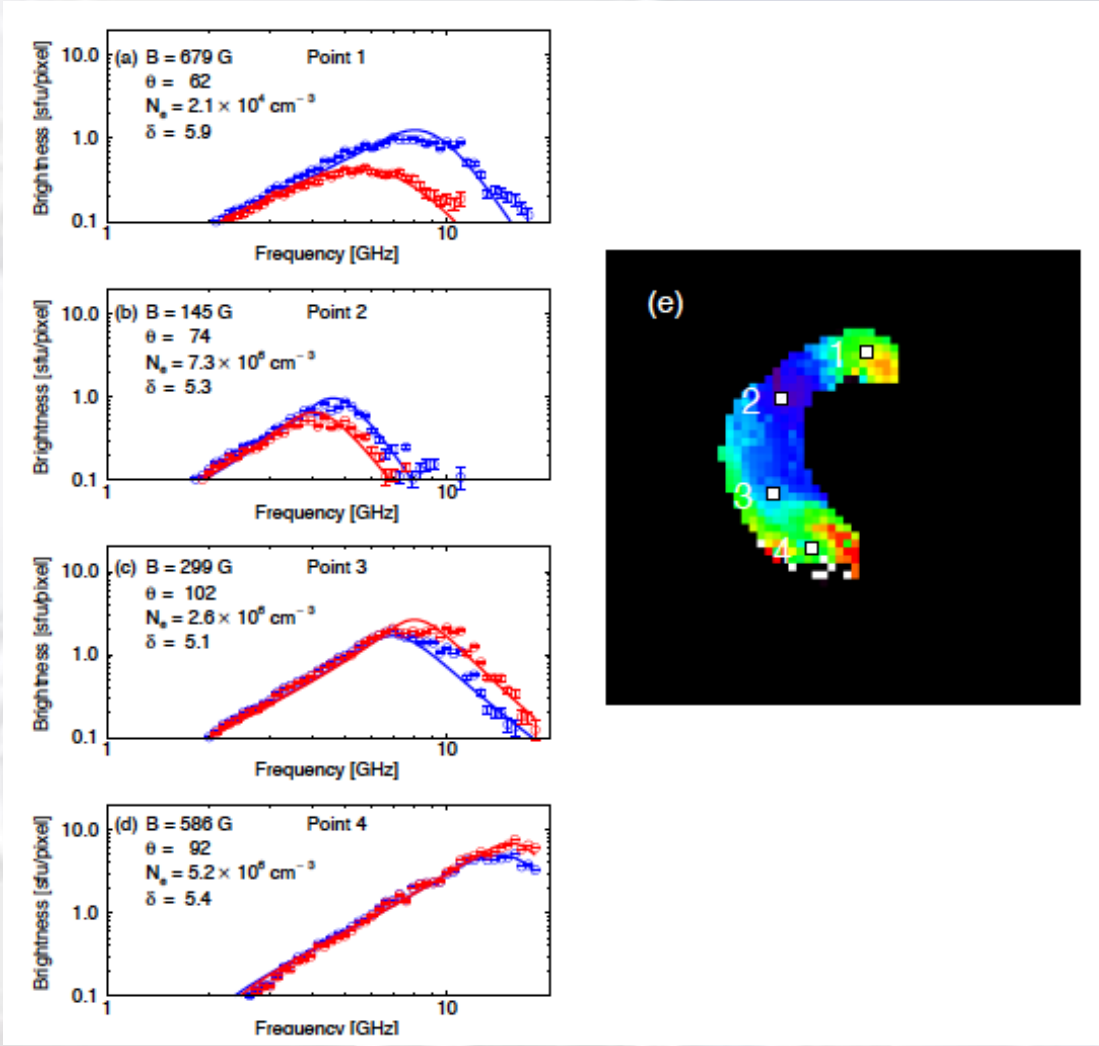
(a) B = 679 G
θ = 62
N_e = 2.1 × 10^4 cm^-3
δ = 5.9
Point 1
(b) B = 145 G
θ = 74
N_e = 7.3 × 10^5 cm^-3
δ = 5.3
Point 2
(c) B = 299 G
θ = 102
N_e = 2.6 × 10^5 cm^-3
δ = 5.1
Point 3
(d) B = 586 G
θ = 92
N_e = 5.2 × 10^5 cm^-3
δ = 5.4
Point 4
Brightness [sfu/pixel]
Frequency [GHz]
10.0
1.0
0.1
1
10
(e)
1
2
3
4

The Celebrated X8.2 Flare of 2017 Sep 10

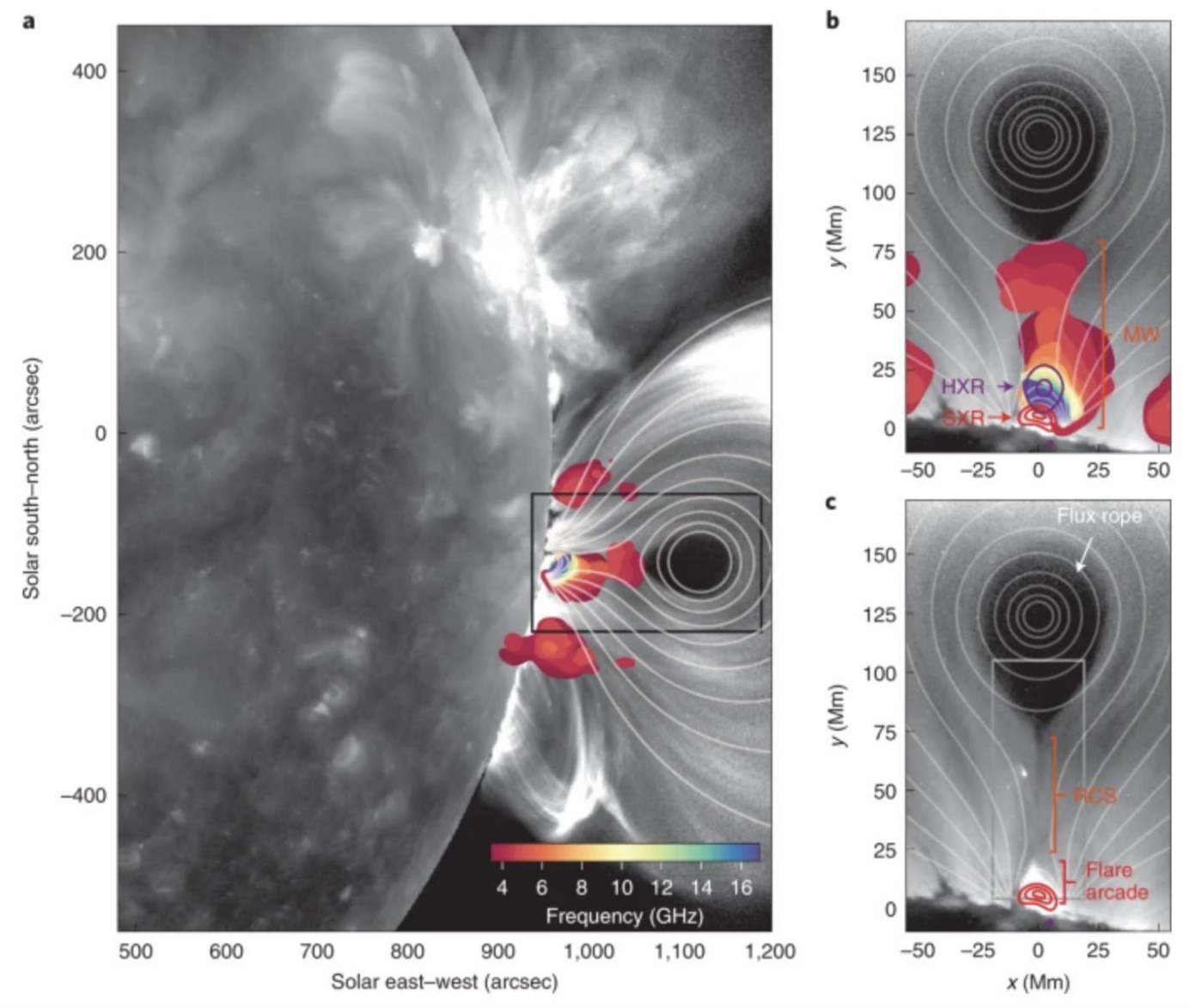

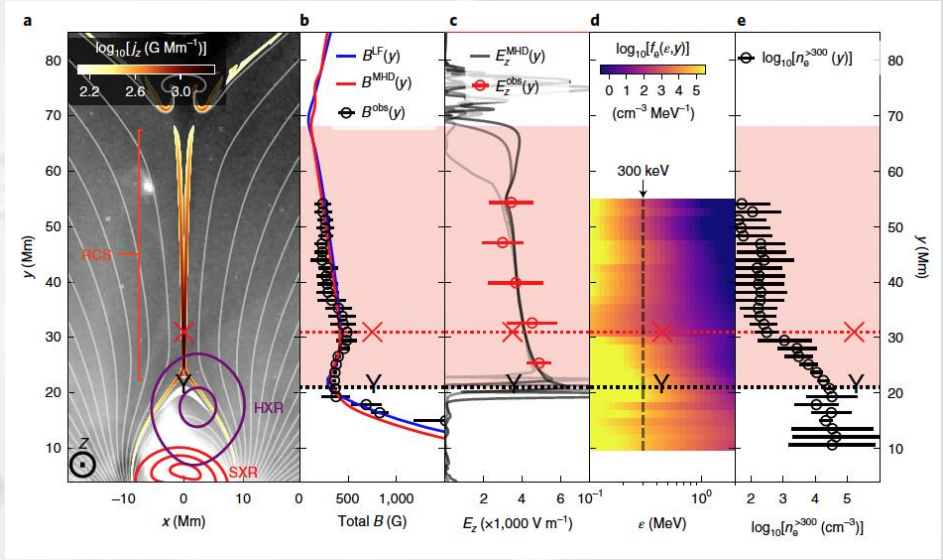

Imaging spectroscopy with EOVSA was used to deduce the magnetic field strength along the RCS as well as the electric field and electron distribution function.

Chen + 2020

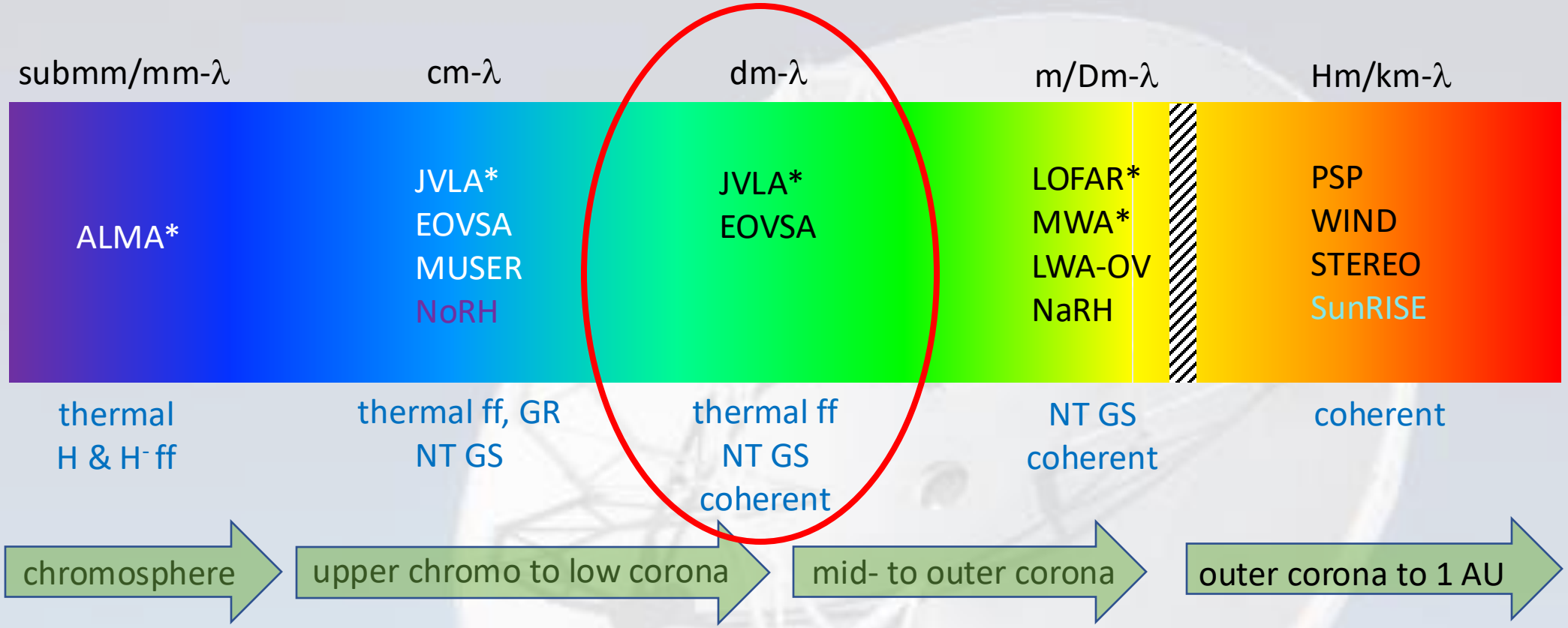
submm/mm-λ
cm-λ
dm-λ
m/Dm-λ
Hm/km-λ
ALMA*
JVLA*
EOVSA
MUSER
NoRH
JVLA*
EOVSA
LOFAR*
MWA*
LWA-OV
NaRH
PSP
WIND
STEREO
SunRISE
thermal
H & H- ff
thermal ff, GR
NT GS
thermal ff
NT GS
coherent
NT GS
coherent
coherent
chromosphere
upper chromo to low corona
mid- to outer corona
outer corona to 1 AU

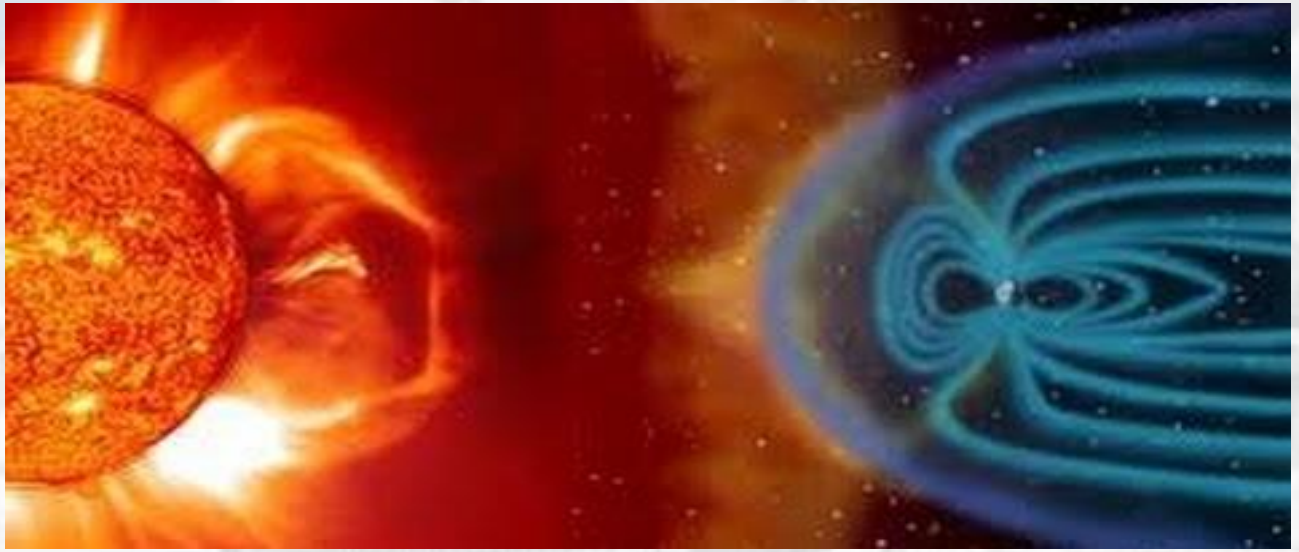

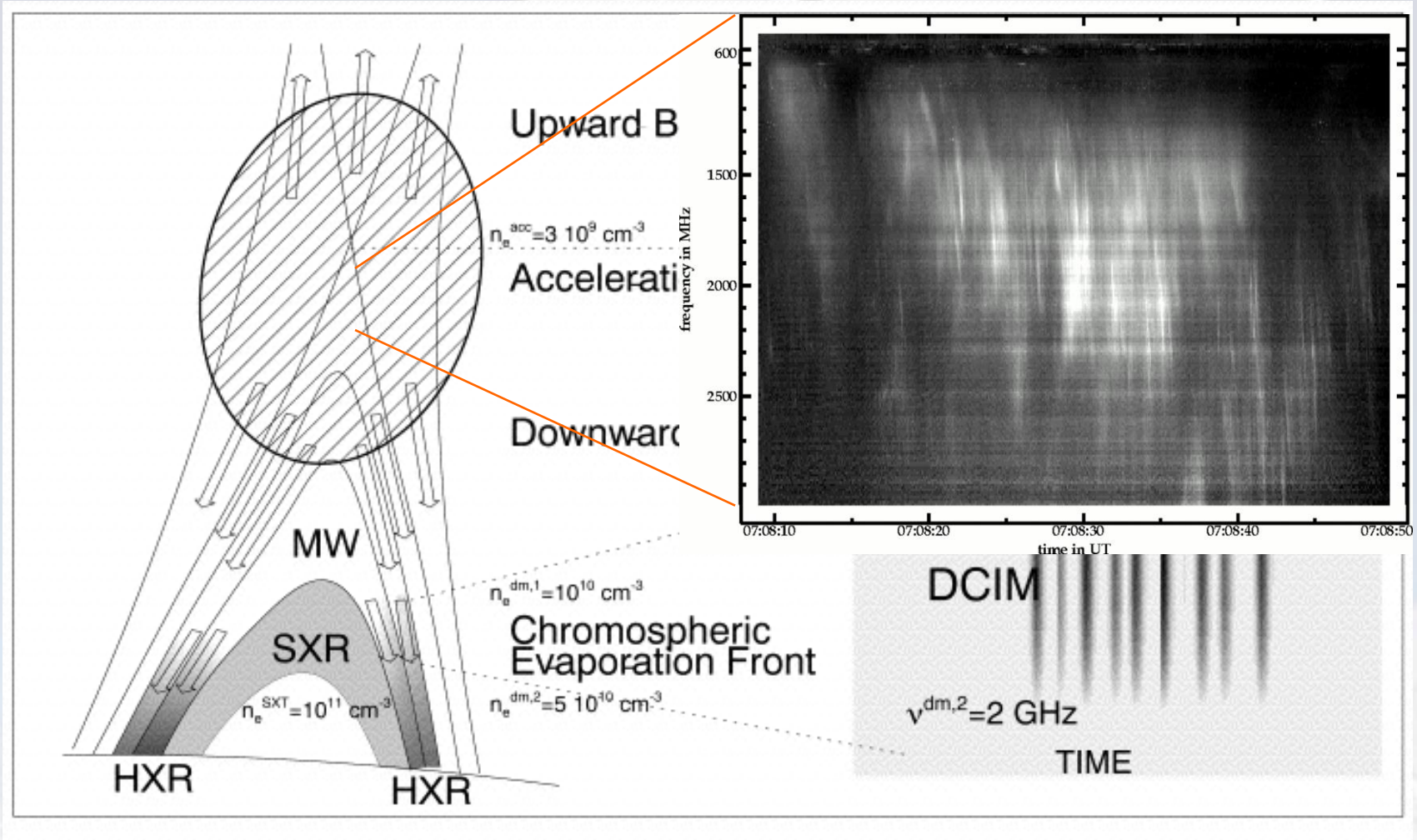

Aschwanden & Benz 1997

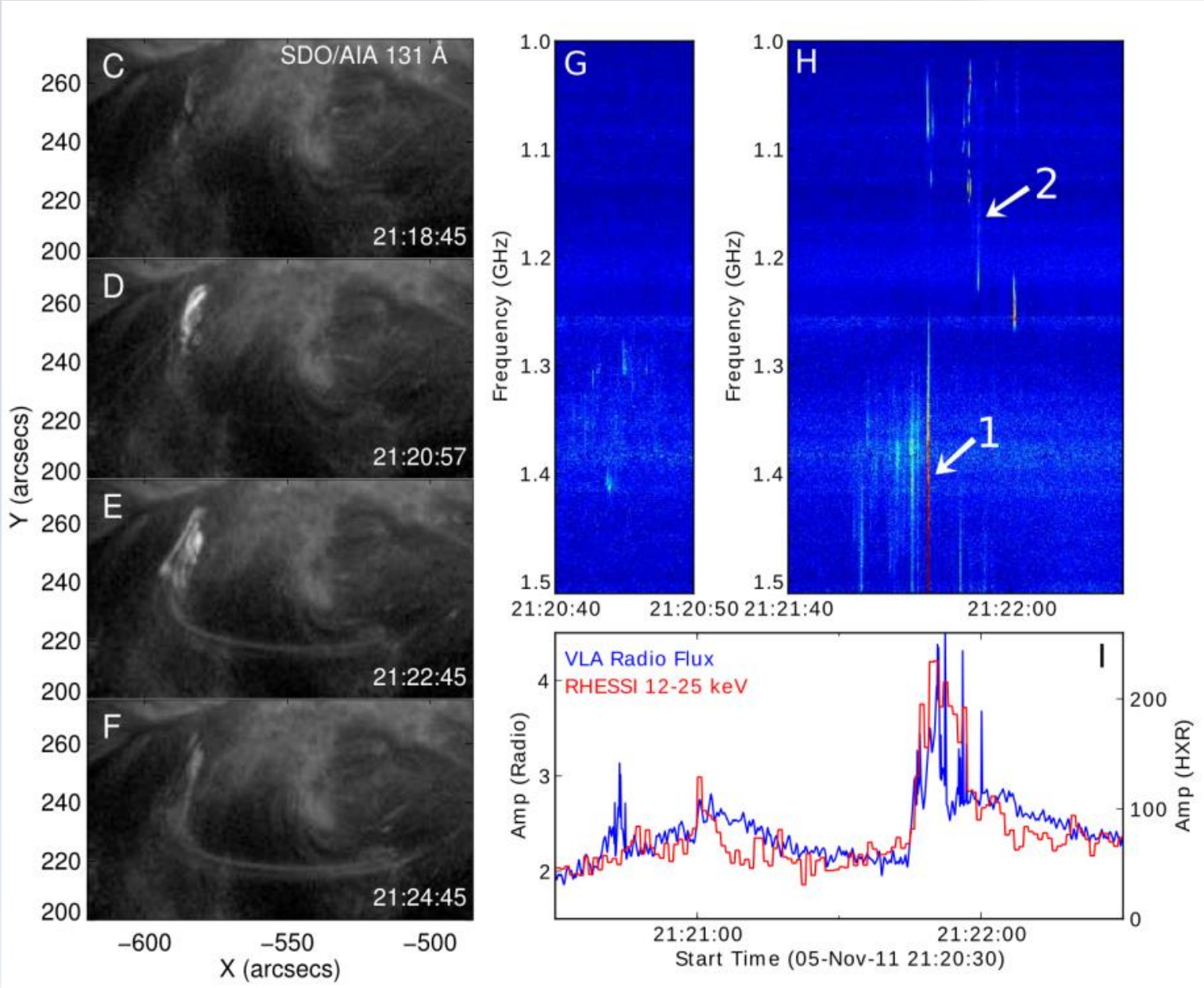

VLA Observations of type III dm bursts associated with an SXR jet eruption (Chen + 2013).

- 50 ms time resolution
- 1-1.5 GHz @ 1 MHz res'ln
- dual polarization

~20000 snapshot images/sec

These observations illuminated the magnetic topology above the jet and demonstrated the highly "fibrous" nature of the corona.

Electron Beam Trajectories

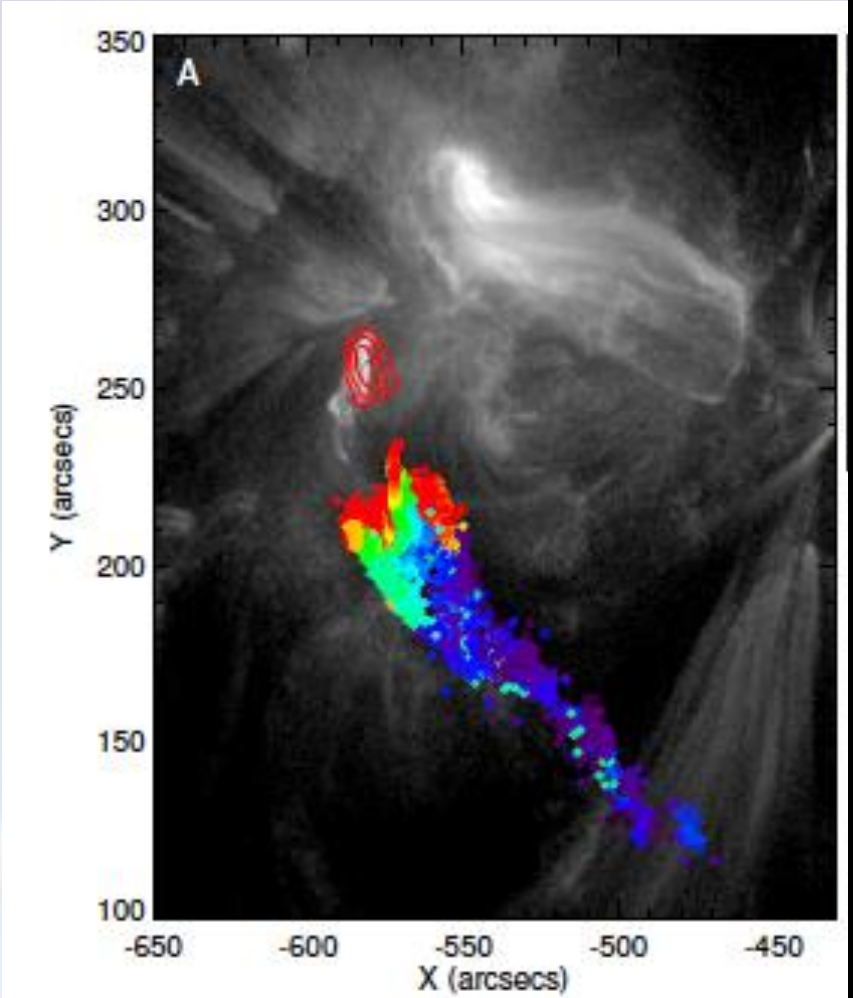

X-Ray jet

Type IIIdm

$\nu \approx 2\nu_e \propto n_e^{1/2}$

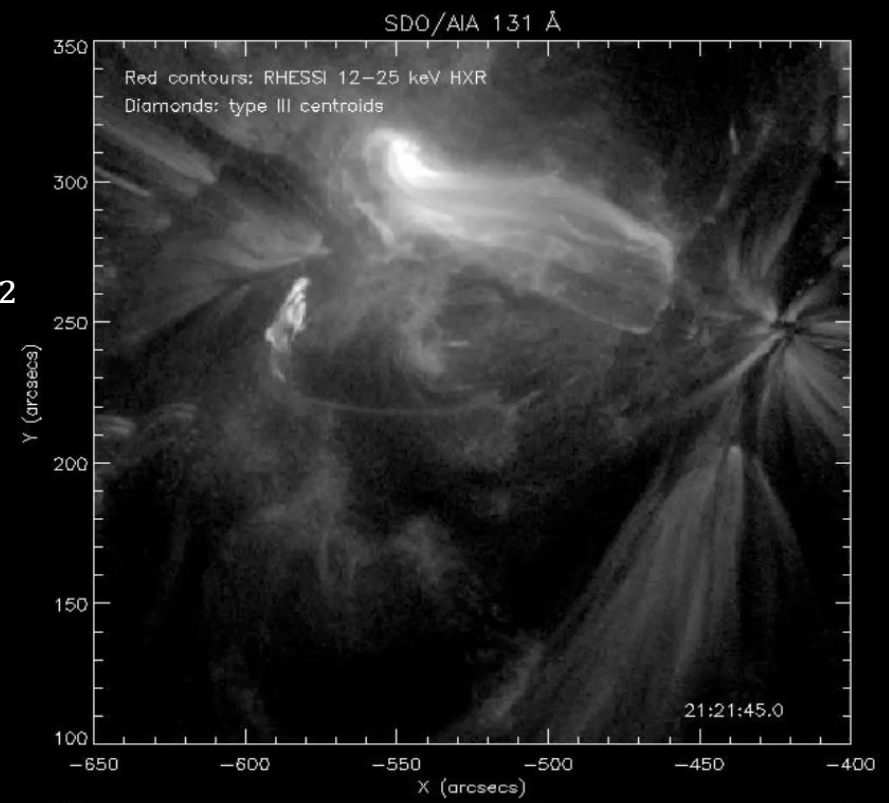

Chen + 2013

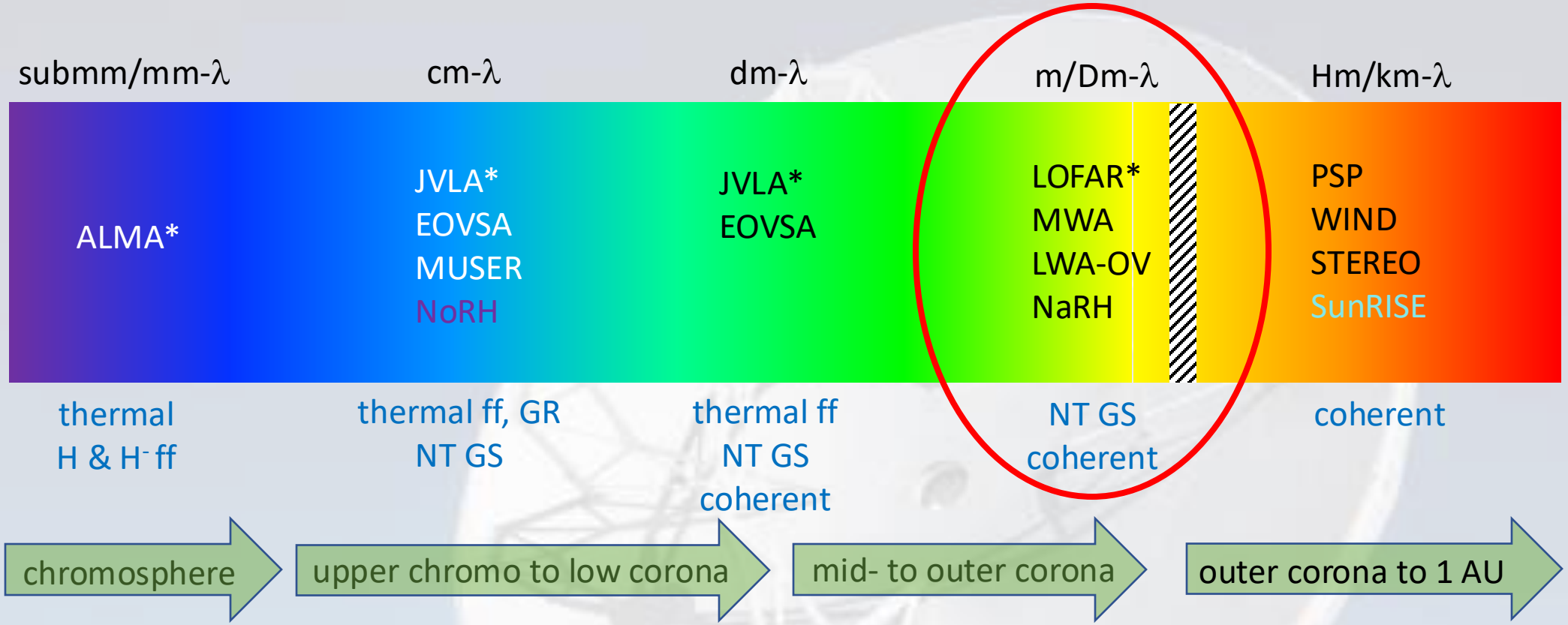
submm/mm-λ
cm-λ
dm-λ
m/Dm-λ
Hm/km-λ
ALMA*
JVLA*
EOVSA
MUSER
NoRH
JVLA*
EOVSA
LOFAR*
MWA
LWA-OV
NaRH
PSP
WIND
STEREO
SunRISE
thermal
H & H- ff
thermal ff, GR
NT GS
thermal ff
NT GS
coherent
NT GS
coherent
coherent
chromosphere
upper chromo to low corona
mid- to outer corona
outer corona to 1 AU

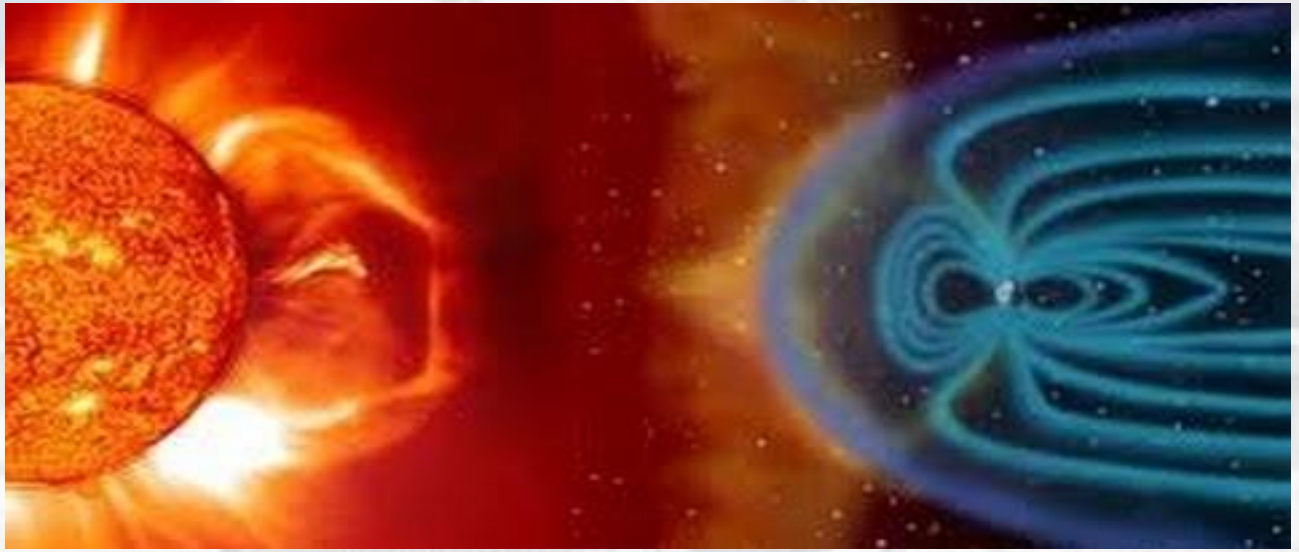

s

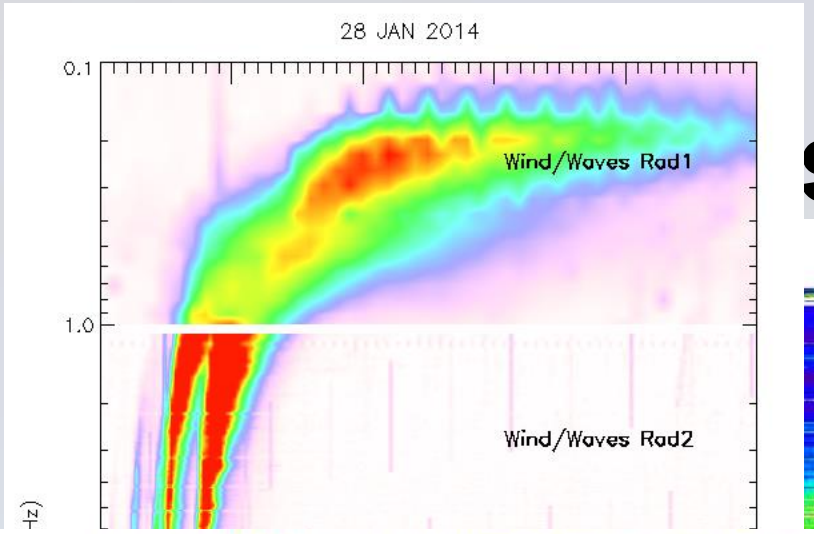

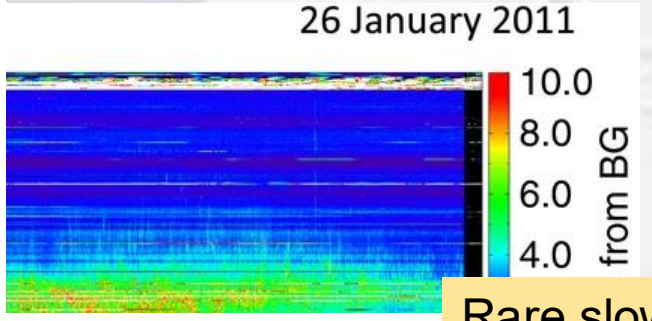

Numerous, short-lived (~1 s), narrow-band (few MHz) bursts occurring over a BW of 10s of MHz in storms lasting hours to days

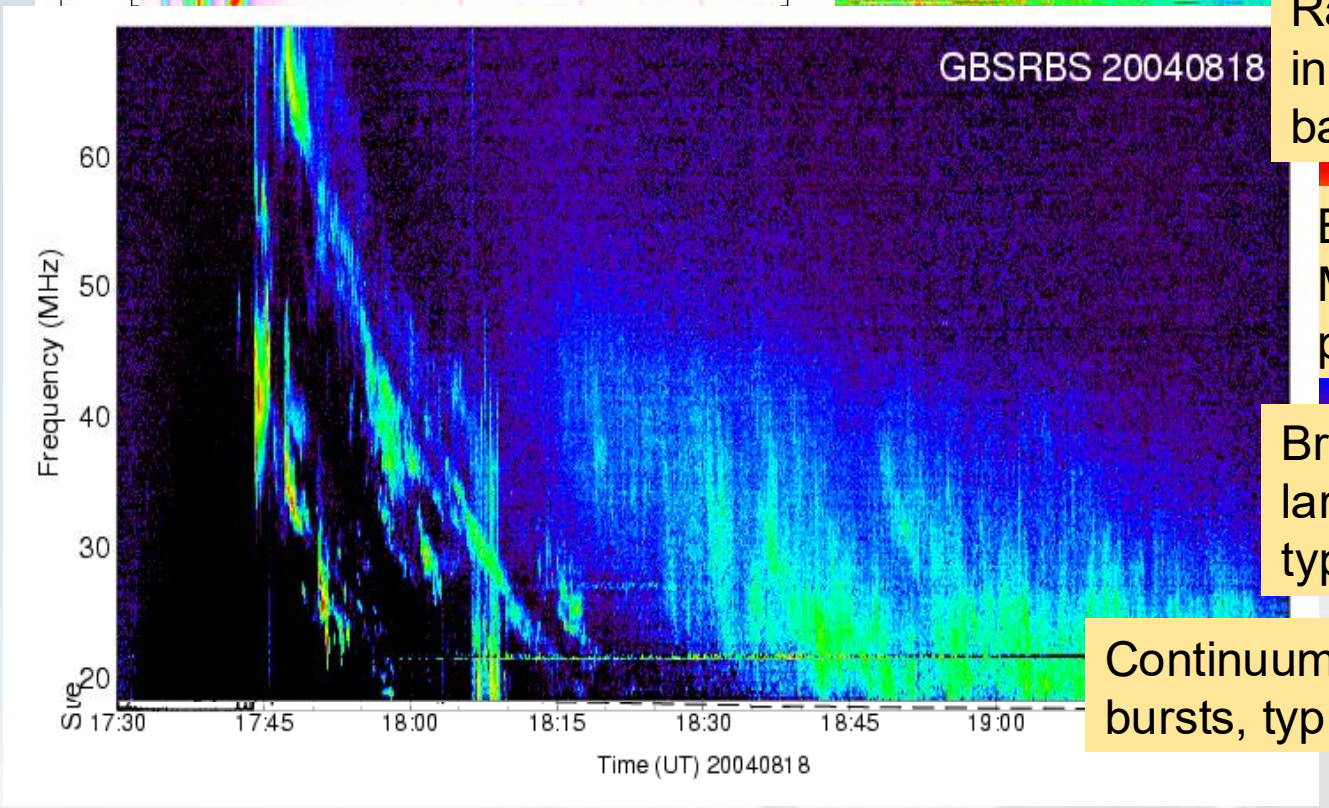

Rare slow-drift bursts (~ -0.25 MHz/s) that occur in association w/ flares, lasting 5-20 min. Narrow-band emission often occurs in harmonic lanes.

Broadband (~100 MHz), fast-drift bursts (~ -20 MHz/s) that occur in association w/ impulsive phase of flares.

Broadband (~10s-100s MHz) continuum following large solar flares, often following an associated type II burst, lasting >10 min.

Continuum emission following groups of type III radio bursts, typically polarized in the opposite sense.

20 April 1998

- M1.4 flare
- partial halo CME ~2000 km/s
- major SEP event

Multi-frequency imaging performed with Nancay RH from 164-410 MHz as radio CME expanded to ~3 solar radii.

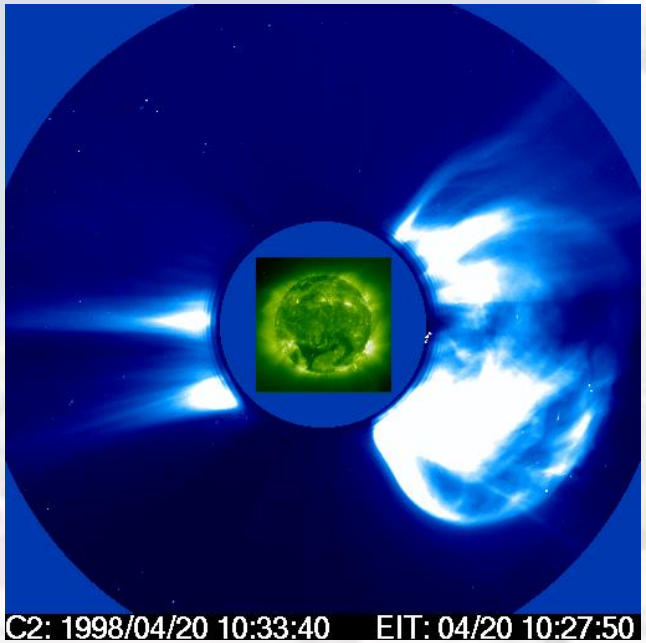

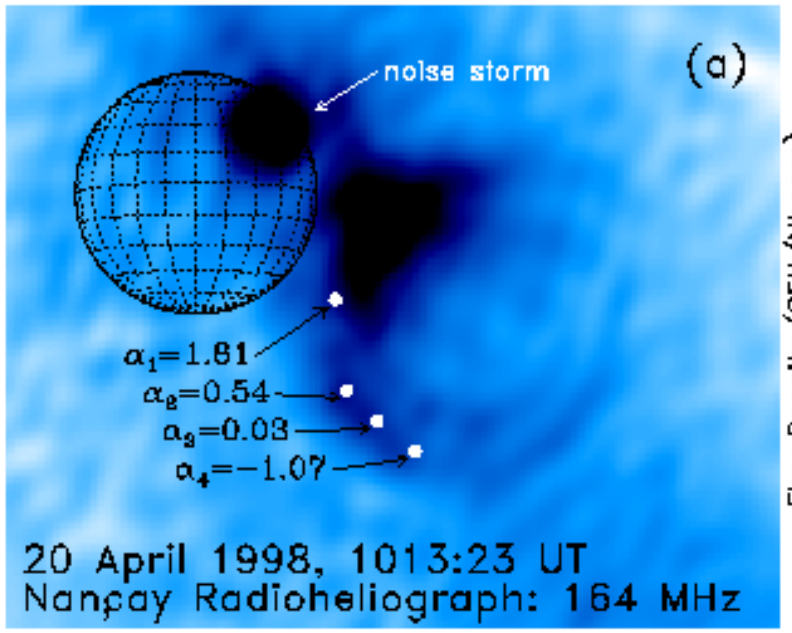

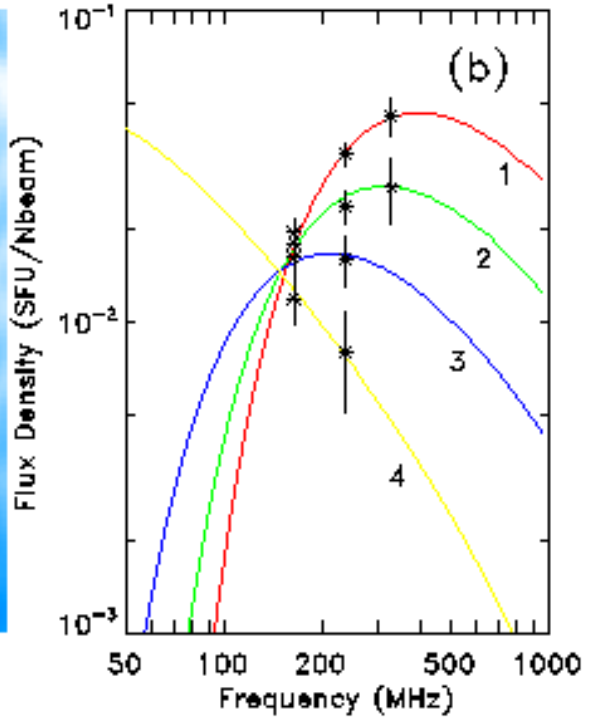

FITTED PARAMETERS AT VARIOUS LOCATIONS IN THE RADIO CME

Line of Sight	α	$R_\odot$	ϕ (deg)	n_{th} (cm^{-3})	B (G)	ν_{RT} (MHz)
1	1.81	1.45	234	2.5×10^7	1.47	330
2	0.54	2.05	218.5	1.35×10^7	1.03	265
3	0.03	2.4	219.5	6.5×10^6	0.69	190
4	−1.07	2.8	221	5×10^5	0.33	30

Bastian + 2001

15 April 2001

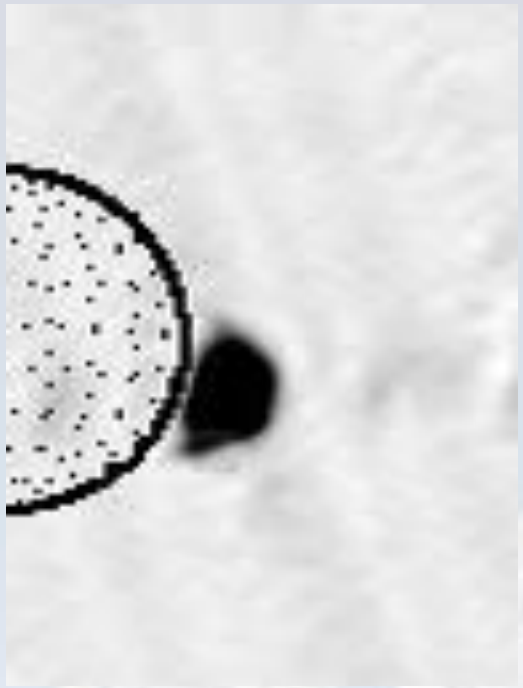

Nancay RH 421 MHz

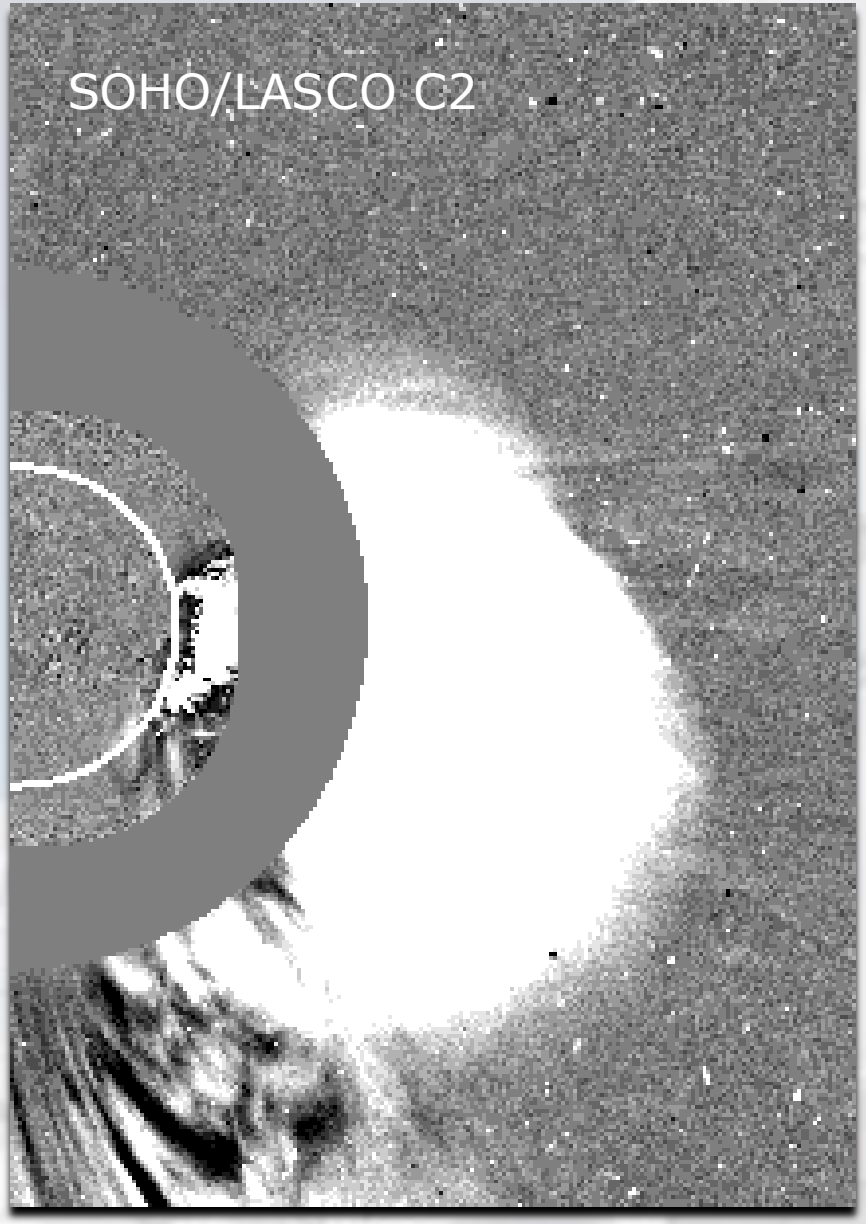

- X14.4 flare
- partial halo CME >1200 km/s
- major SEP event

Detection of synchrotron radiation from MeV electrons interacting with magnetic field entrained by fast CME (Maia + 2004)

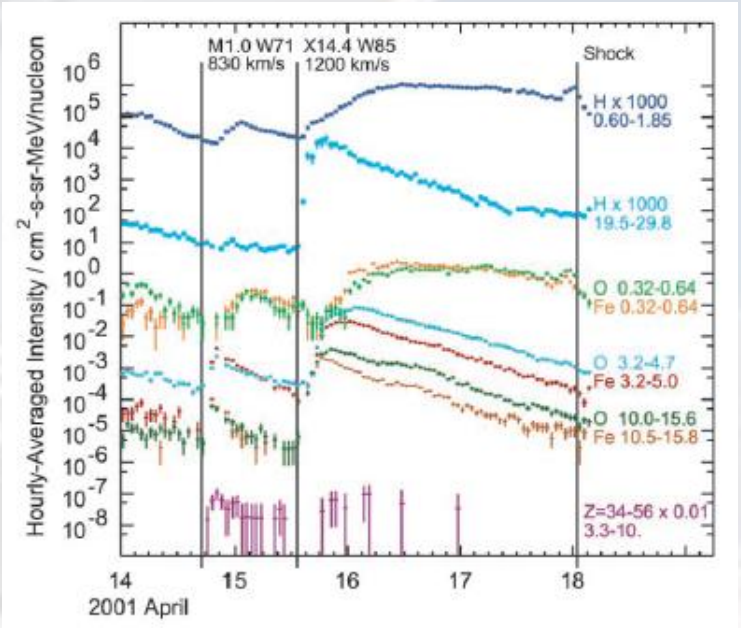

Tylka et al. (2002)

More recently

Additional case studies by Tun + 2013 and Carley + 2017

The availabililty of low-frequency telescopes like the Murchison Widefield Array (70-300 MHz) and the OVRO Long Wavelength Array (15-85 MHz) has led to renewed interest in radio CMEs.

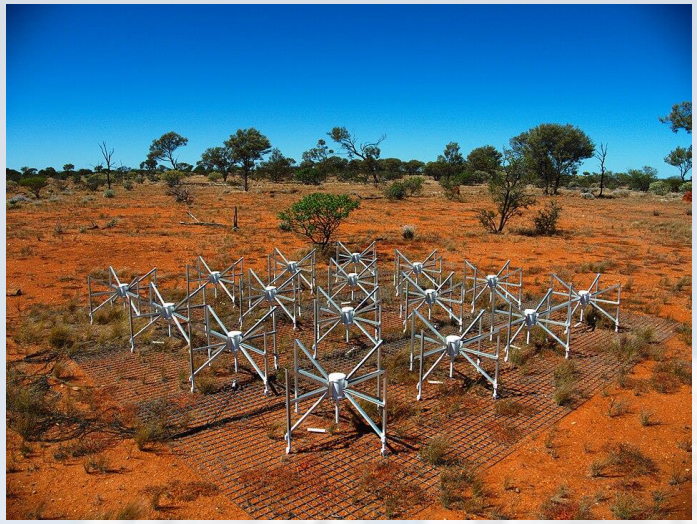

Murchison Widefield Array

OVRO Long Wavelength Array

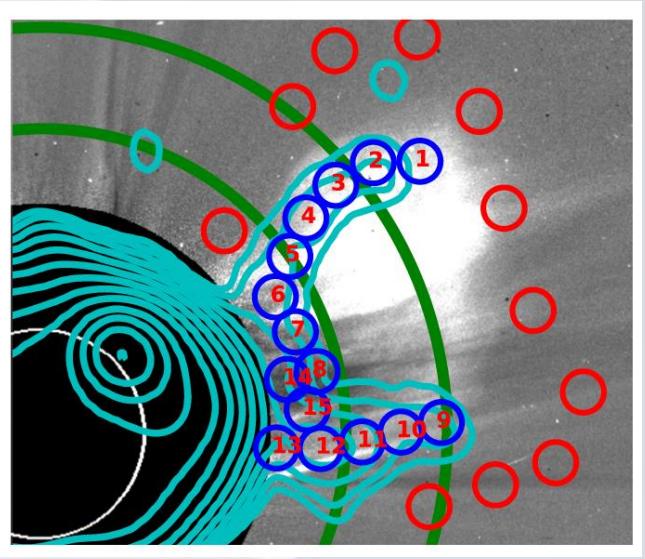

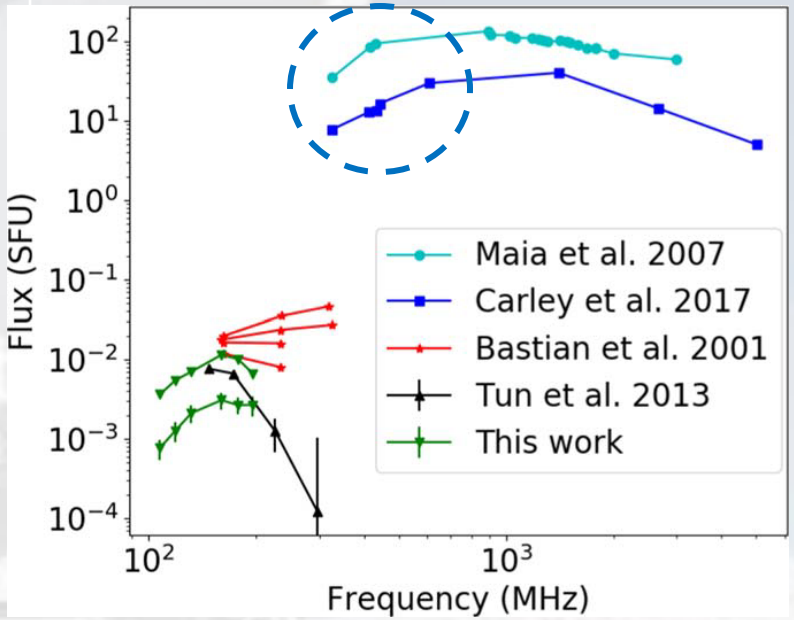

Mondal + 2020

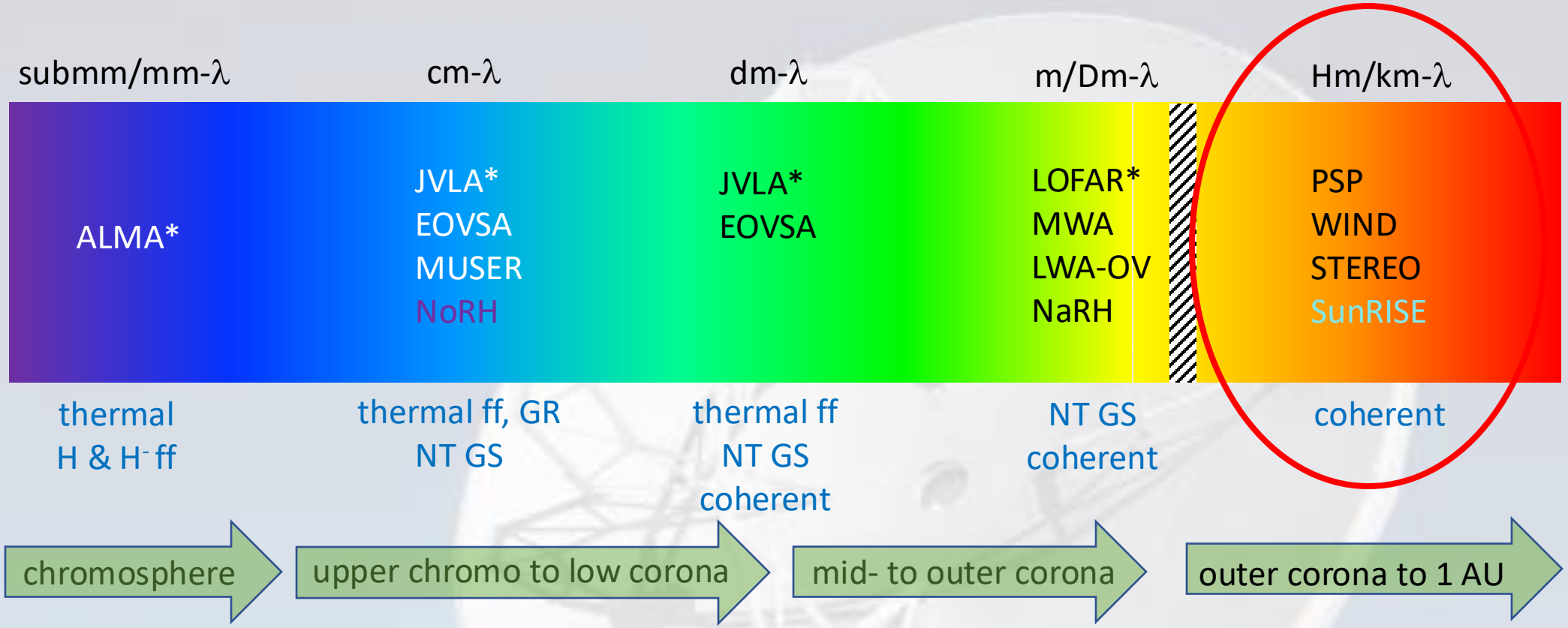
submm/mm-λ
cm-λ
dm-λ
m/Dm-λ
Hm/km-λ
ALMA*
JVLA*
EOVSA
MUSER
NoRH
JVLA*
EOVSA
LOFAR*
MWA
LWA-OV
NaRH
PSP
WIND
STEREO
SunRISE
thermal
H & H- ff
thermal ff, GR
NT GS
thermal ff
NT GS
coherent
NT GS
coherent
coherent
chromosphere
upper chromo to low corona
mid- to outer corona
outer corona to 1 AU

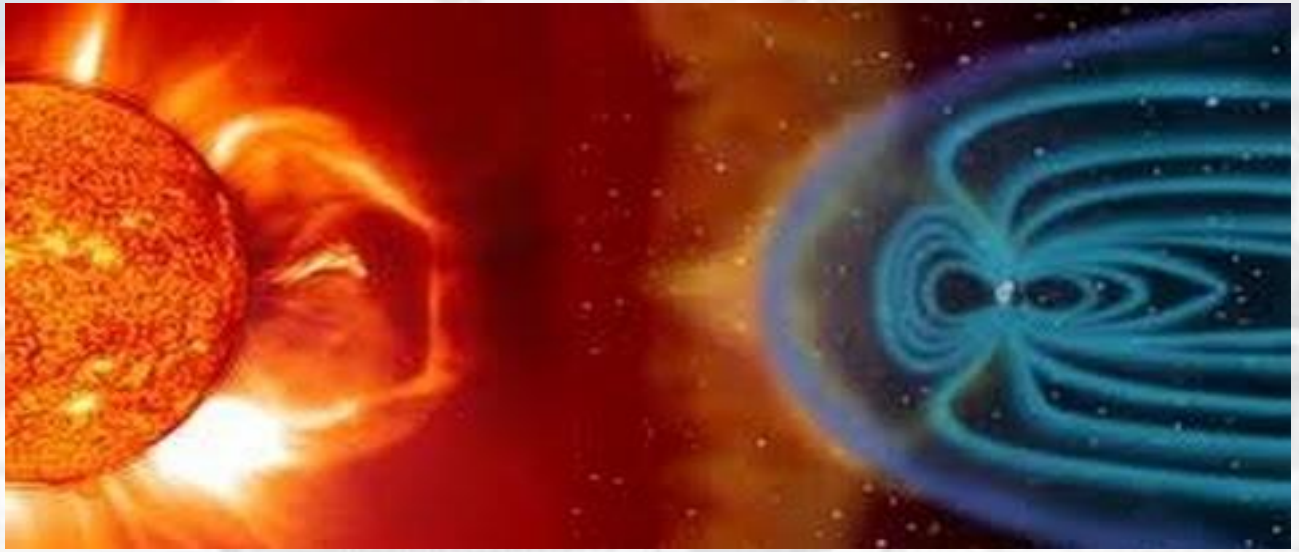

Radio Dynamic Spectroscopy from Space

Radio bursts of type II and type III propagate outward in the corona. Since they emit at $\nu \approx \nu_e \propto n_e^{1/2}$ and n_e declines rapidly with their frequency declines rapidly to the ionospheric cutoff (5-10 MHz) at ~2 $R_\odot$. To be able to observe radio bursts in the outer corona and into the IPM requires space-based instrumentation.

Space-based spectrocopy dates back to the 1970s with, e.g., the Voyagers and ISEE-3, followed by WIND/WAVES, Ulysses/URAP, STEREO/WAVES, PSP/FIELDS-RFS, and SolO/RPW. These are capable of not only observing solar radio bursts, but planetary radio emissions (notably Earth and Jupiter), and the galactic background.

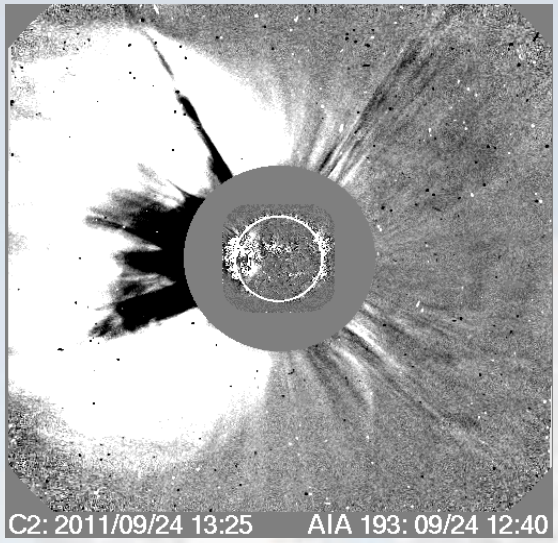

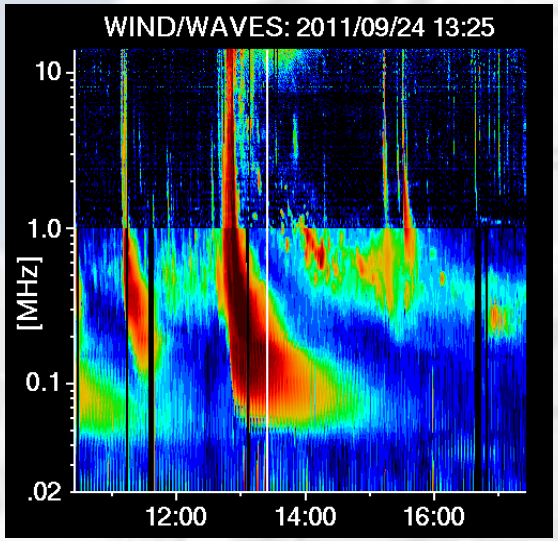

Gopalswamy + 2019
https://cdaw.gsfc.nasa.gov/CME_list/radio/waves_type2.html

In recent years, with multiple missions active and new ground-based observations possible, observations of radio bursts from the ground to space and from multiple vantage points in space have become possible.

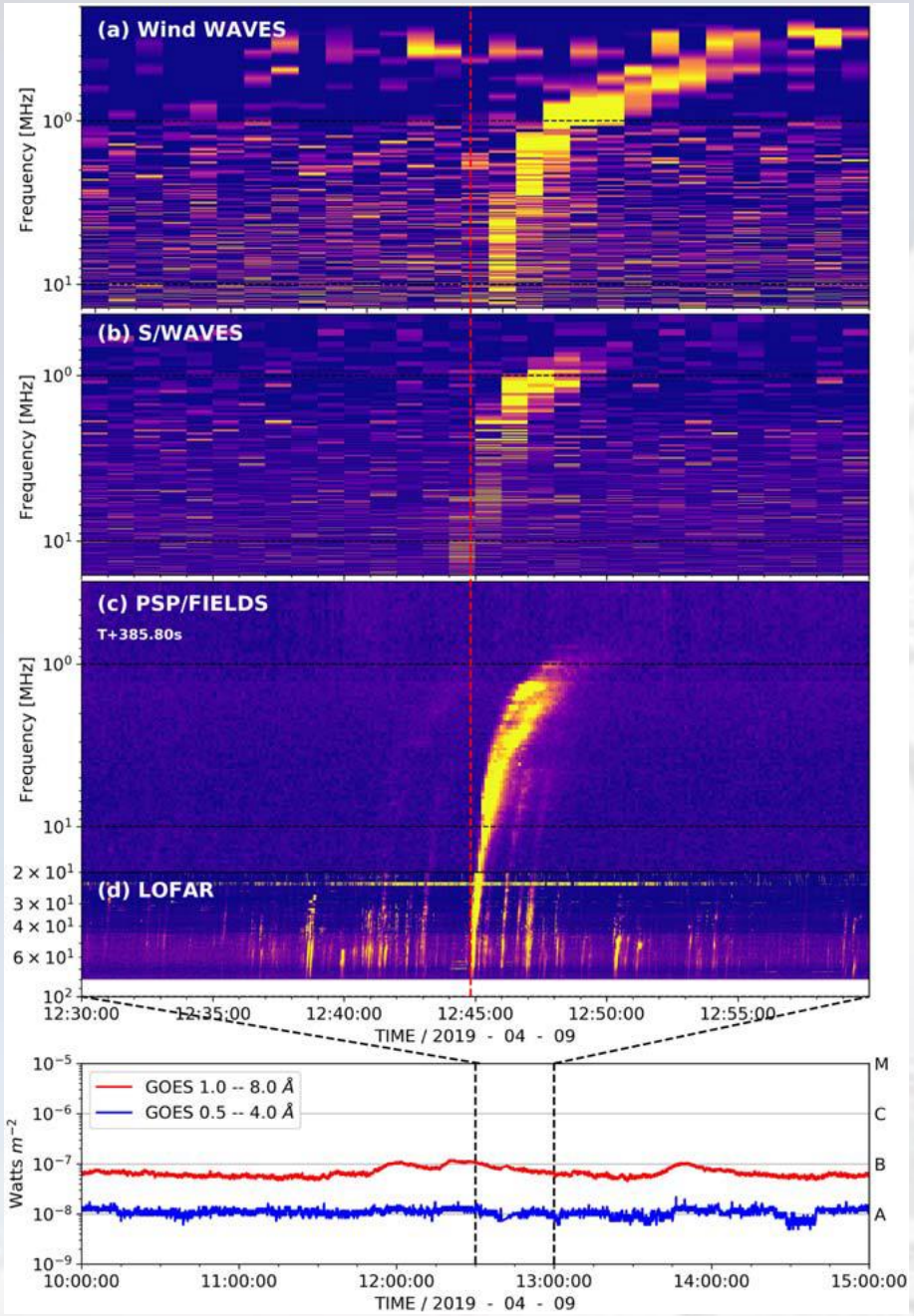
(a) Wind WAVES
(b) S/WAVES
(c) PSP/FIELDS
T+385.80s
(d) LOFAR
Frequency [MHz]
TIME / 2019 - 04 - 09
GOES 1.0 -- 8.0 Å
GOES 0.5 -- 4.0 Å
Watts m⁻²
M
C
B
A

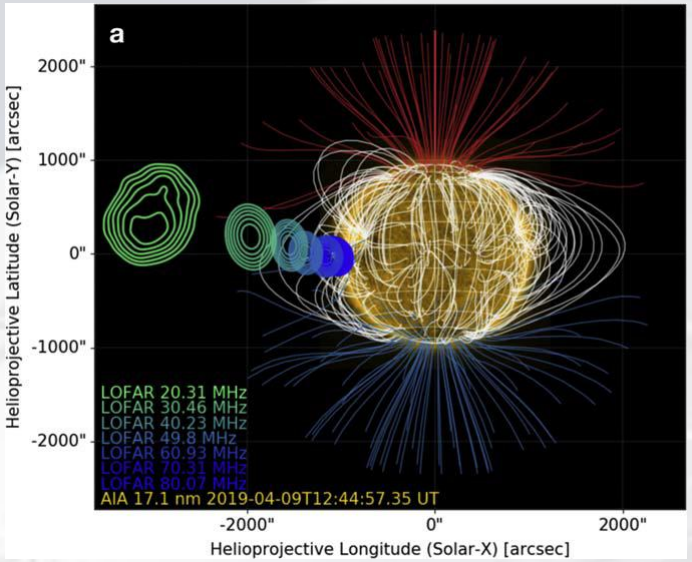
a
LOFAR 20.31 MHz
LOFAR 30.46 MHz
LOFAR 40.23 MHz
LOFAR 49.8 MHz
LOFAR 60.93 MHz
LOFAR 70.31 MHz
LOFAR 80.07 MHz
AIA 17.1 nm 2019-04-09T12:44:57.35 UT
Helioprojective Latitude (Solar-Y) [arcsec]
Helioprojective Longitude (Solar-X) [arcsec]

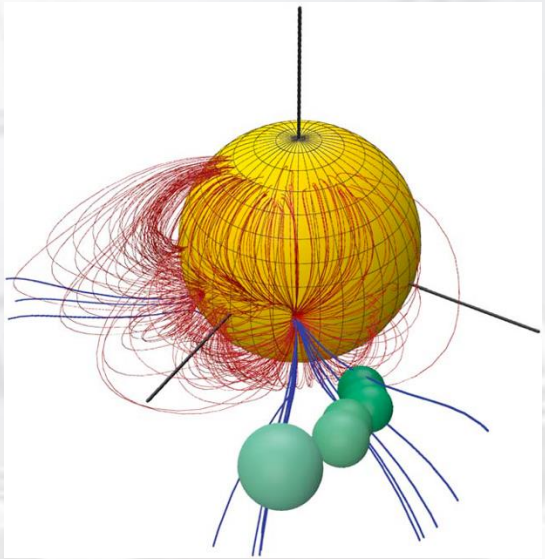

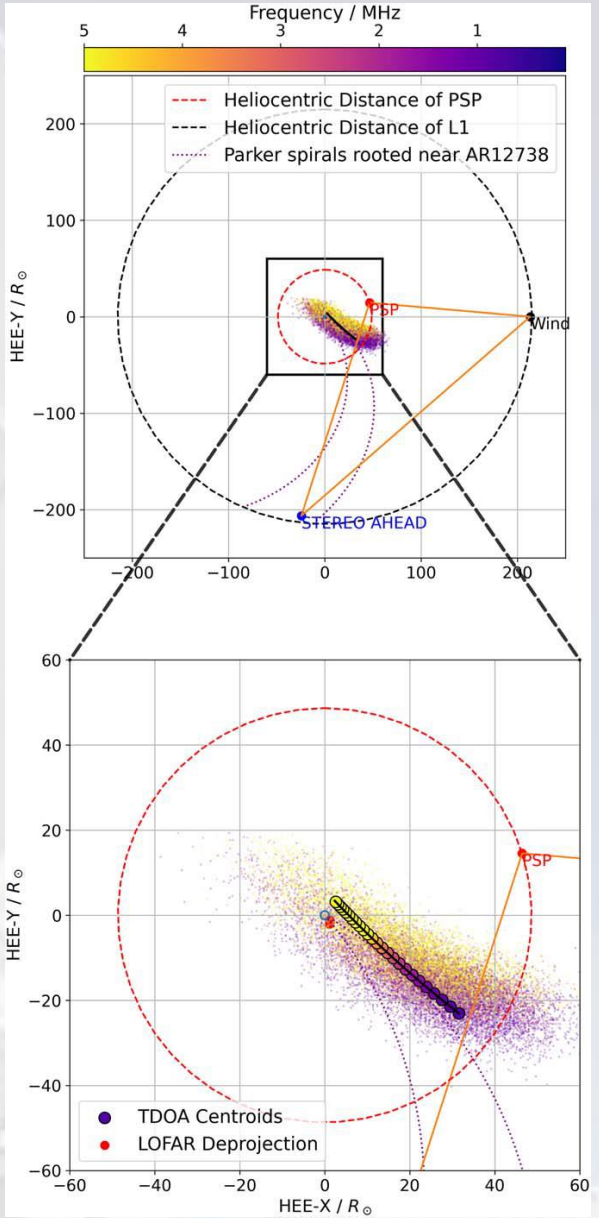
Frequency / MHz
Heliocentric Distance of PSP
Heliocentric Distance of L1
Parker spirals rooted near AR12738
PSP
Wind
STEREO AHEAD
HEE-Y / R⊙
HEE-X / R⊙
TDOA Centroids
LOFAR Deprojection

Badman + 2022

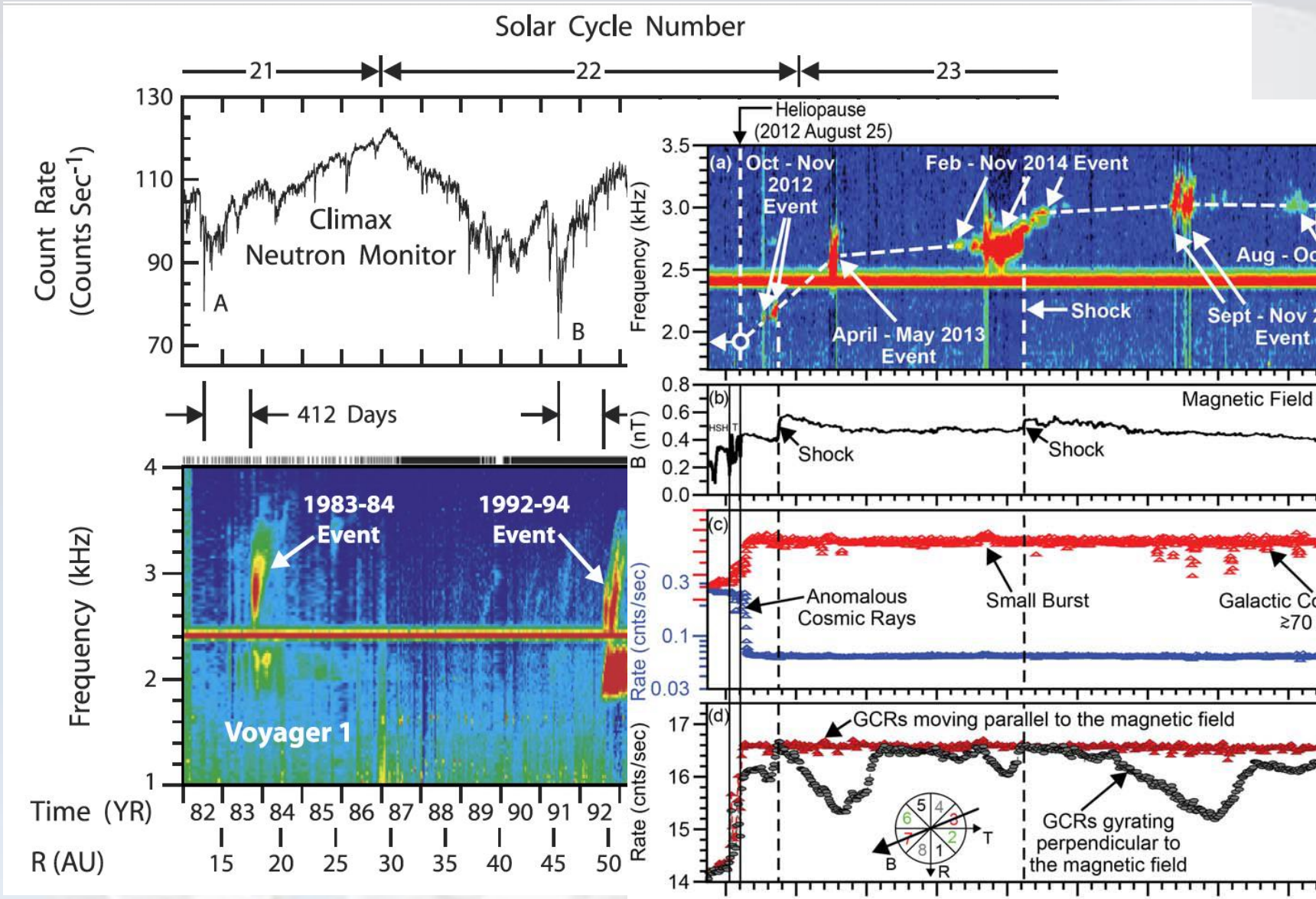

Gurnett + 2003

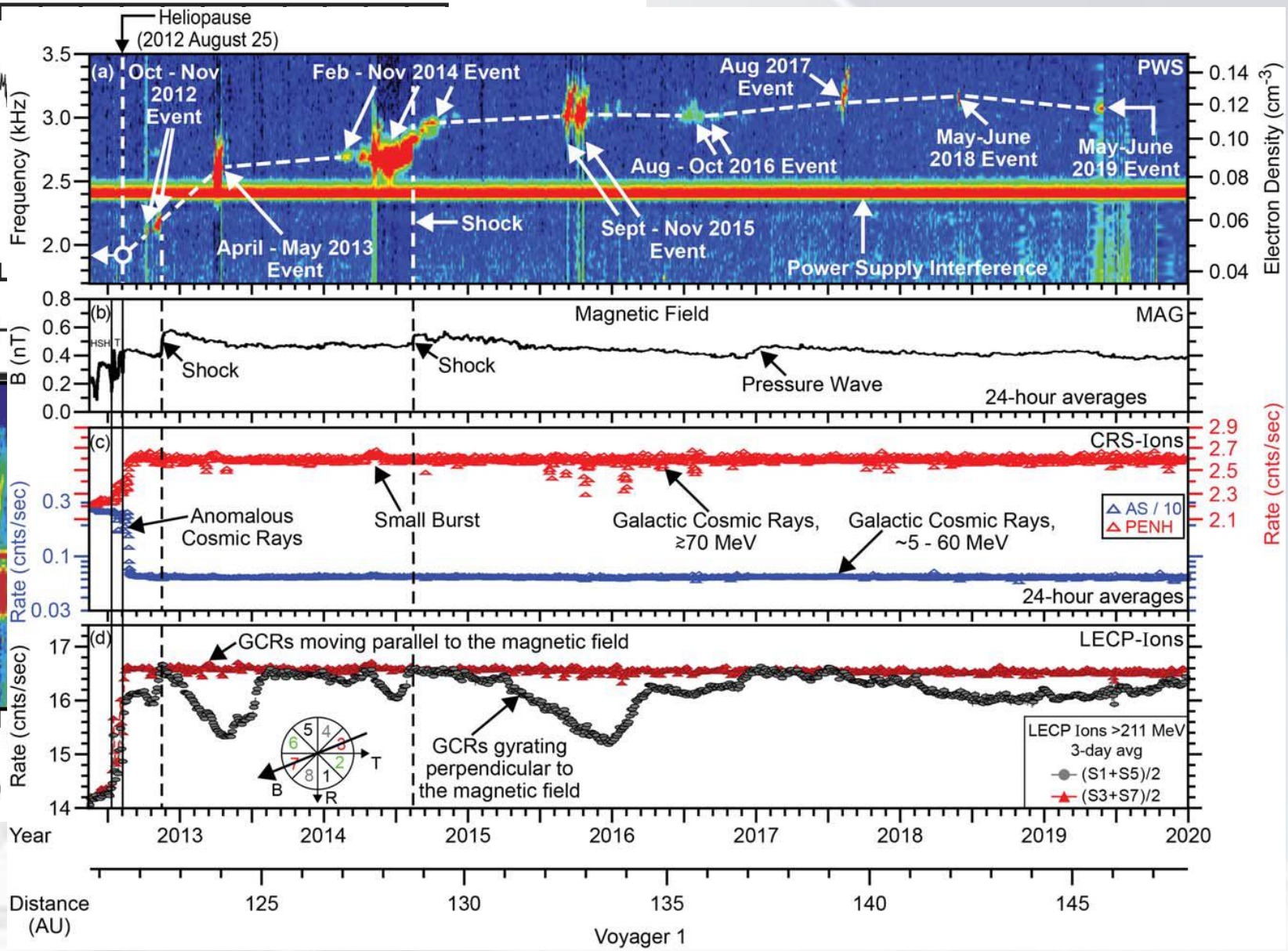

Gurnett + 2021

Sun Radio Imaging Experiment (SunRISE)

PI: Susan Lepri (U Mich)
Proj. Sci: Joe Lazio (JPL)

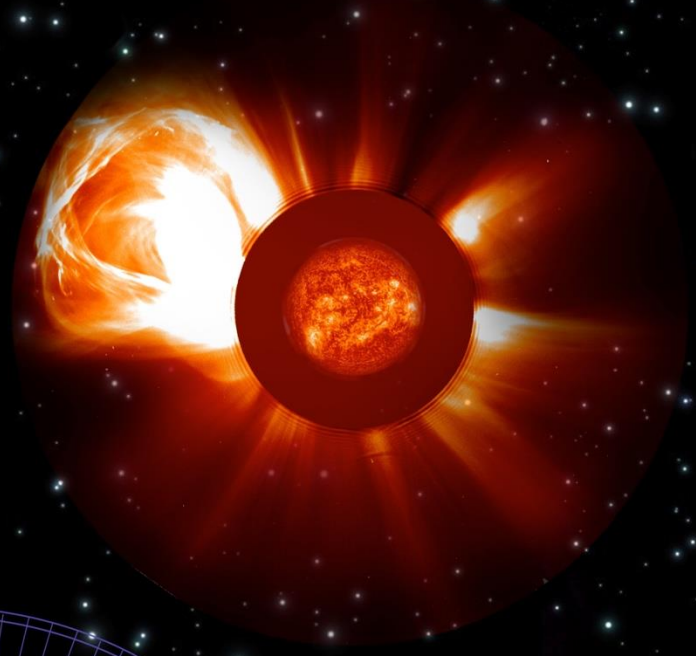

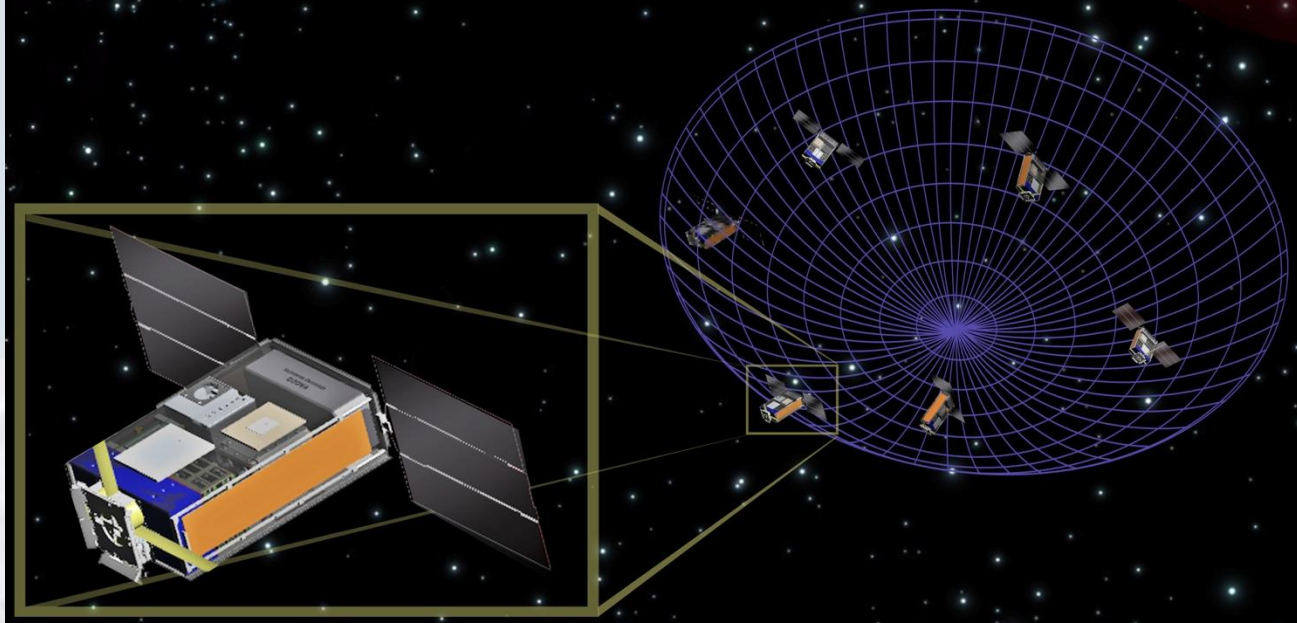

Mission of Opportunity
Systems have been assembled, integrated, and tested.
Launch imminent

Jet Propulsion Laboratory
California Institute of Technology

Observational Heliophysics II:

Radio Propagation Studies

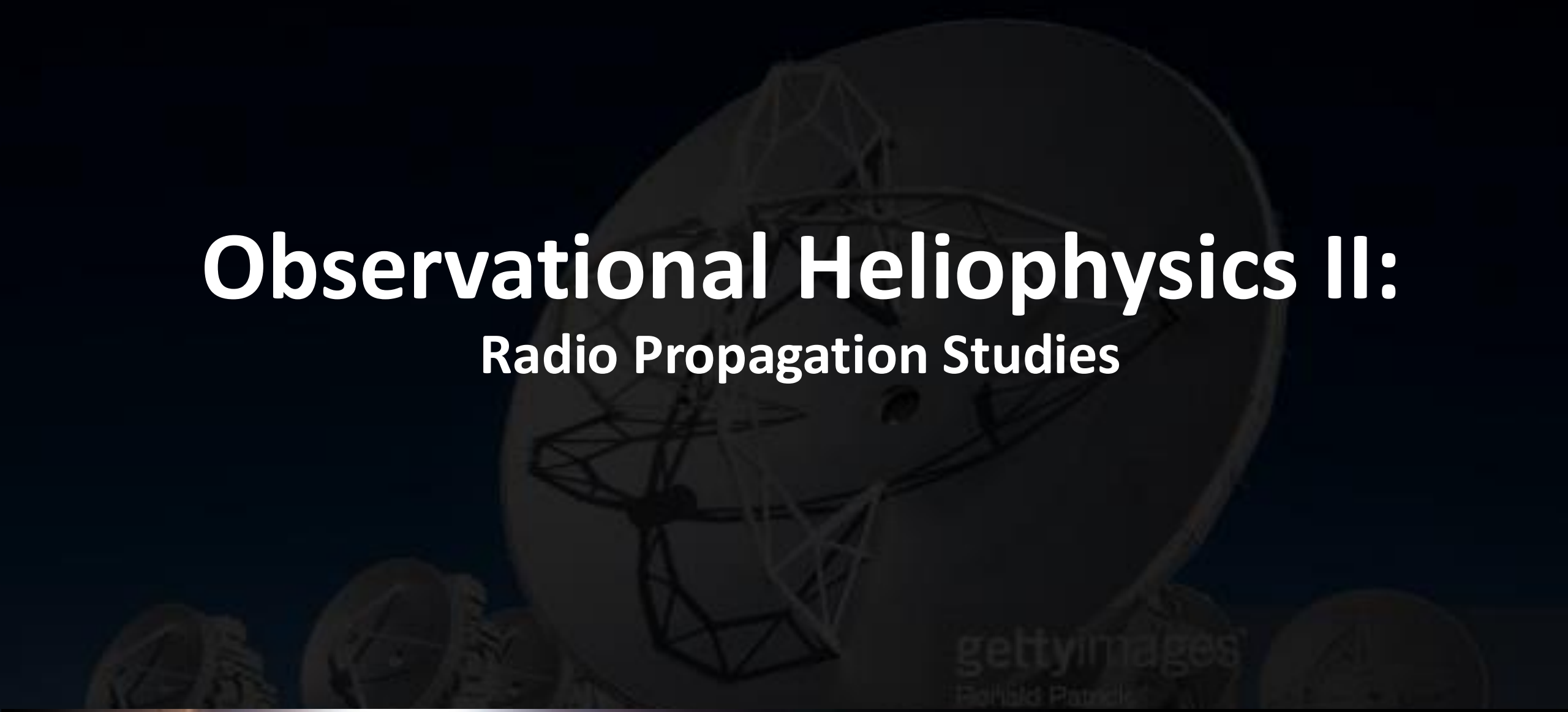

ADVANCING THE SCIENCE OF HELIOPHYSICS

A partnership between NASA UCAR COMMUNITY PROGRAMS | CPAESS

Radio Propagation Studies

Let's now turn things around. Instead of considering the diagnostic utility of radio emission from the Sun and heliosphere, we now consider what can we learn about **the medium** through which the radio waves propagate?

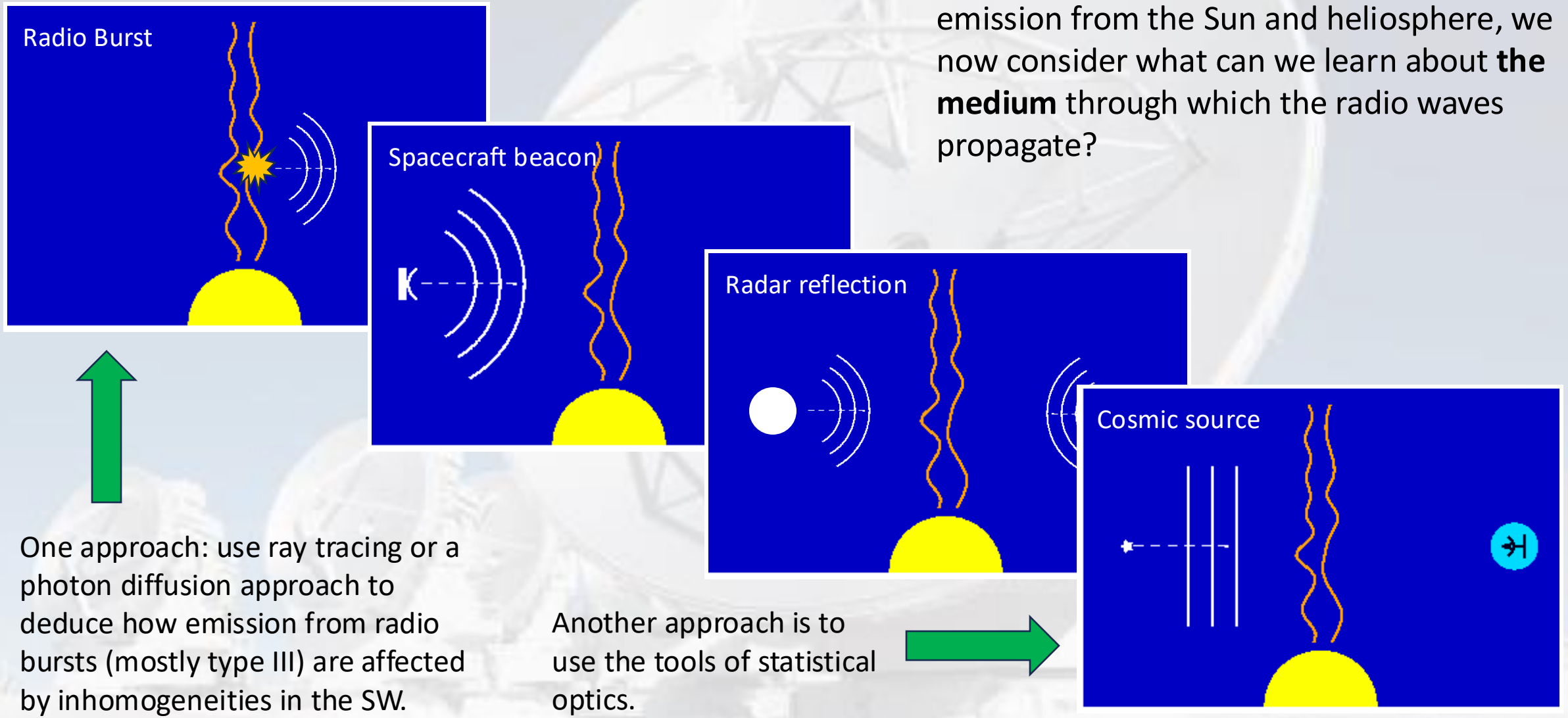

One approach: use ray tracing or a photon diffusion approach to deduce how emission from radio bursts (mostly type III) are affected by inhomogeneities in the SW.

Another approach is to use the tools of statistical optics.

Preliminaries

Consider an EM wave propagating in a fully ionized, unmagnetized plasma. The dispersion relation is $\omega^2 = k^2c^2 + \omega_e^2$. Its group velocity is $v_{gr} = \partial\omega/\partial k = \mu c < c$ where $\mu = (1 - \omega^2 / \omega_e^2)^{1/2}$ is the refractive index; $\omega_e = (4\pi q^2 n_e/m)^{1/2} = 2\pi\nu_e$. If $\mu = \mu_o + \delta\mu$ and $n_e = n_o + \delta n_e$ it follows that

$$\delta\mu = \frac{1}{2\mu_o}\frac{\nu_e^2}{\nu^2}\frac{\delta n_e}{n_o} = \frac{1}{2\pi}\frac{\lambda^2 r_e}{\mu_o}\delta n_e; \qquad r_e = q^2 / mc^2$$

Classical electron radius

We can write two-point correlation functions for fluctuations in μ and n_e

$$B_\mu(r_1, r_2) = \langle\delta\mu(r_1)\delta\mu(r_2)\rangle = \frac{1}{4\mu_o^2}\frac{\nu_e^4}{\nu^4}\frac{\langle\delta n_e(r_1)\delta n_e(r_2)\rangle}{n_o^2} = \frac{1}{4\mu_o^2}\frac{\nu_e^4}{\nu^4}\frac{1}{n_o^2}B_n(r_1, r_2)$$

For a statistically homogeneous, isotropic medium the two-point correlation functions only depend on $\mathrm{r} = |r_1 - r_2|$. The 3D Fourier transform of the correlation functions yield the corresponding spatial spectrum of the fluctuating quantity:

$$B_\mu(r) \overset{\text{FT}}{\rightarrow} \Phi_\mu(q)$$

$$B_n(r\,) \overset{\text{FT}}{\rightarrow} \Phi_n(q)$$

Radio Bursts

Early calculations (Fokker 1968, Steinberg + 1971) assumed that density fluctuations in the corona and SW could be described in terms of a Gaussian correlation function with a single scale h:

$$B_\mu(r_1, r_2) = \langle \delta\mu^2 \rangle exp\left[-\frac{|r_1 - r_2|^2}{h^2}\right] = B_\mu(r\,)$$

Going way back to Chandrasekhar (1952) the mean-square scattering angle $\langle \Delta\Psi \rangle^2$ of a ray along path s is then given by (Gaussian correlation function)

$$\langle \Delta\Psi \rangle^2 \; = 2\pi^{1/2} \int_{ray} \frac{\langle \delta\mu^2 \rangle}{\mu_o^2 h}\, ds$$

In practice, Monte Carlo techniques were used for many years to step a given ray by Δs and for each step

$$\langle \Delta\Psi \rangle^2 \; = 2\pi^{1/2} \frac{\langle \delta\mu^2 \rangle}{\mu_o^2 h} \Delta s \propto \frac{1}{\mu_o^4} \frac{n_o^2}{\nu^4} \frac{\epsilon^2}{h} \Delta s \;\; ; \quad \epsilon = \frac{\delta n_e}{n_o}$$

Note strong dependence on μ_o. Since μ_o can be small for radio bursts the effect can be large. Note, too, that the properties of the medium are embodied in $\epsilon^2 \,/\, h$

Radio Bursts

Type III radio bursts observed from space-based platforms (PSP, SO, STEREO, WIND) have received a lot of attention in recent years. Multiple vantage points!

The ray-tracing approach has been recast in terms of a stochastic Fokker-Planck equation (e.g., Arzner & Magun 1999; Kontar + 2019).

It is now known that the correlation functions and corresponding spectra are **non-Gaussian**: e.g., Φ_n is often parameterized as a power-law inner and outer scales q_i, q_o and a quantity analogous to ϵ^2/h given by $\bar{q}\epsilon^2$, where

$$\bar{q} = \frac{1}{\epsilon^2}\int_{q_o}^{q_i} q\Phi_n dq; \qquad \epsilon^2 = \frac{\delta {n_e}^2}{{n_o}^2} = \int_{q_o}^{q_i} \Phi_n dq$$

If the spectrum is taken to be Kolmogorov-like $\bar{q} = 2q_o^{2/3}q_i^{1/3}$.

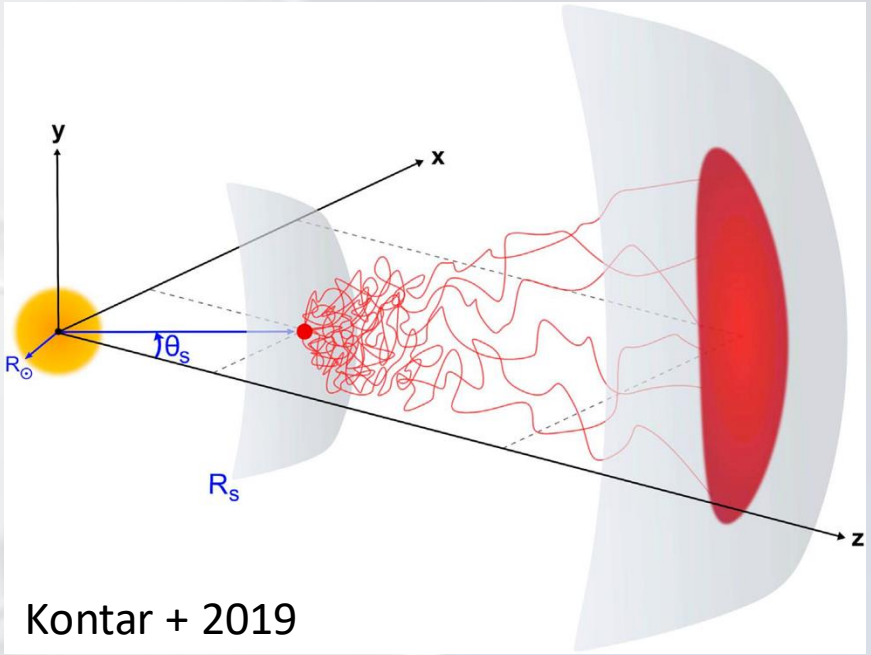

Kontar + 2019

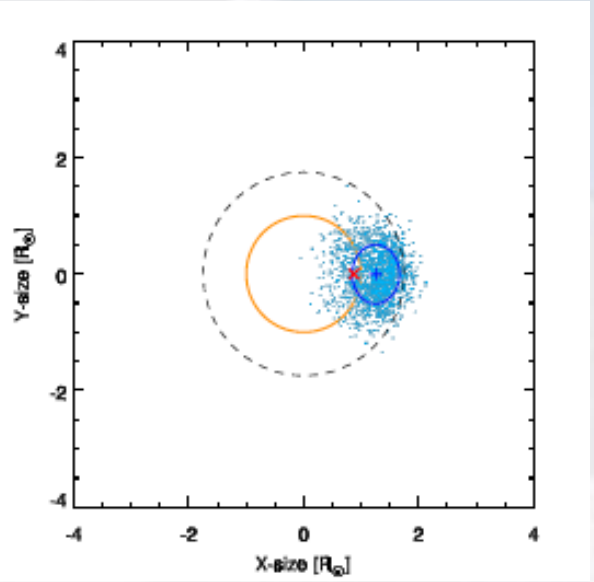

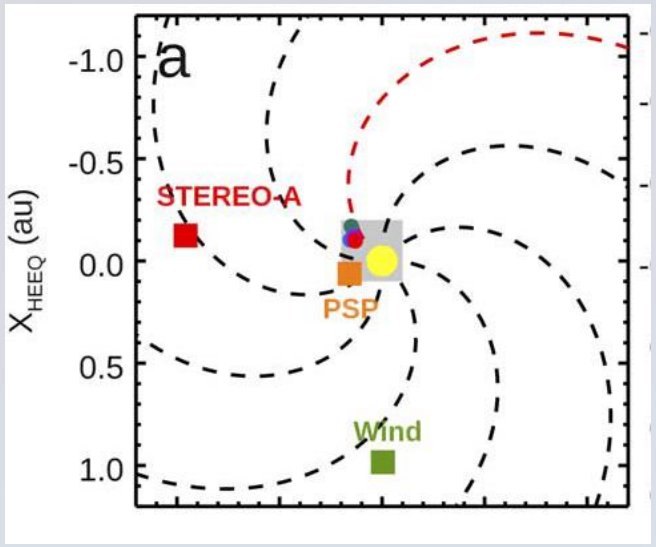

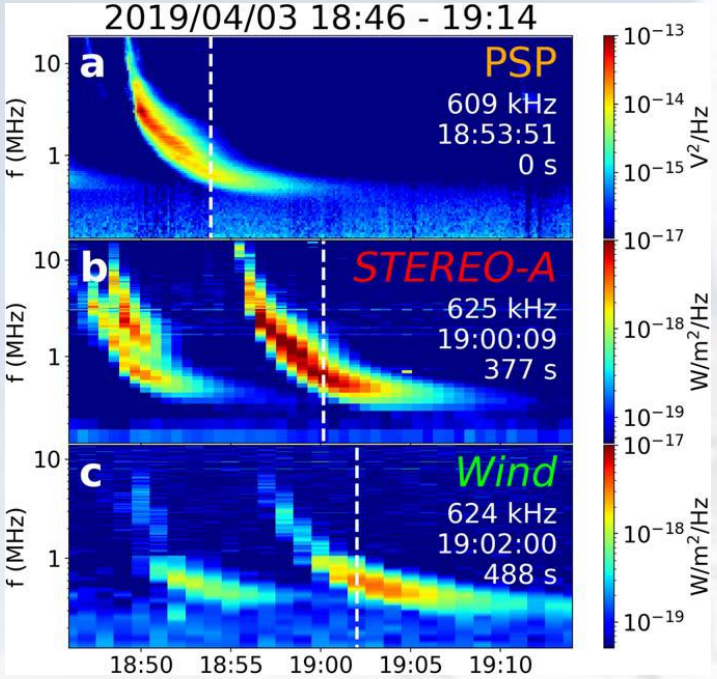

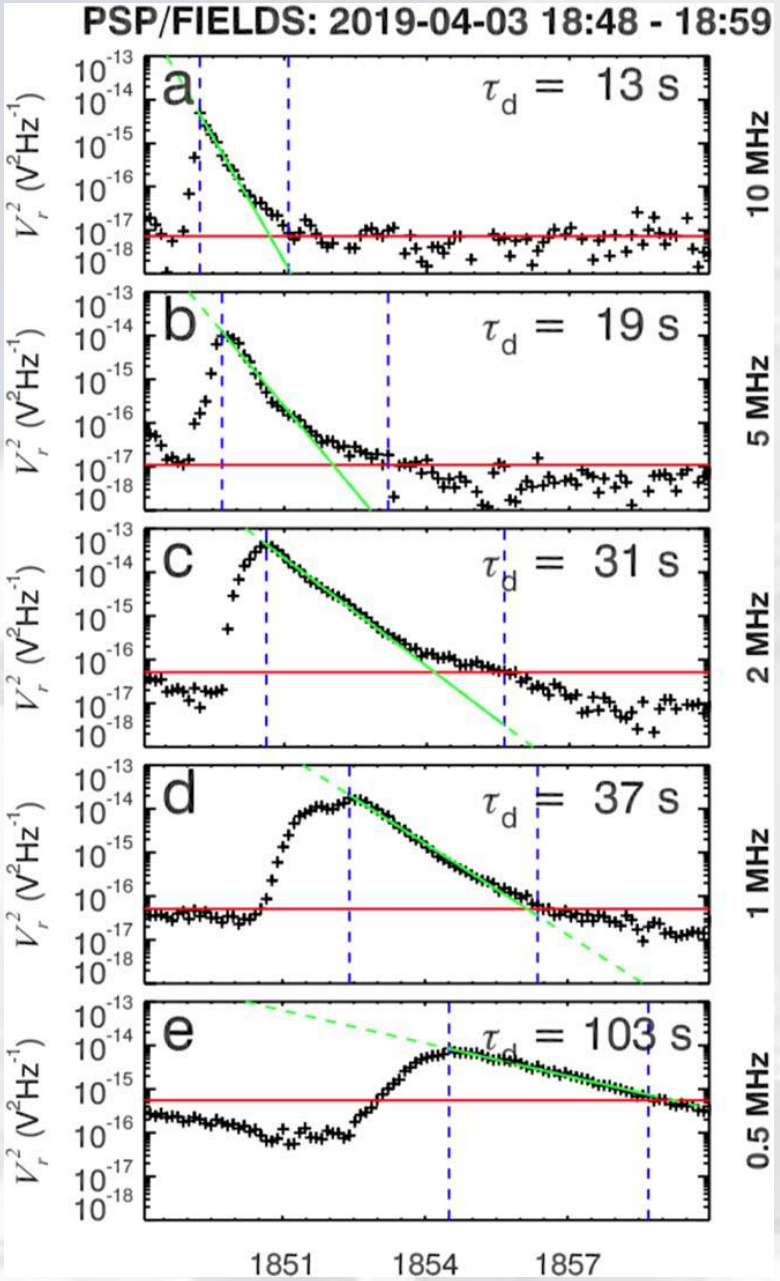

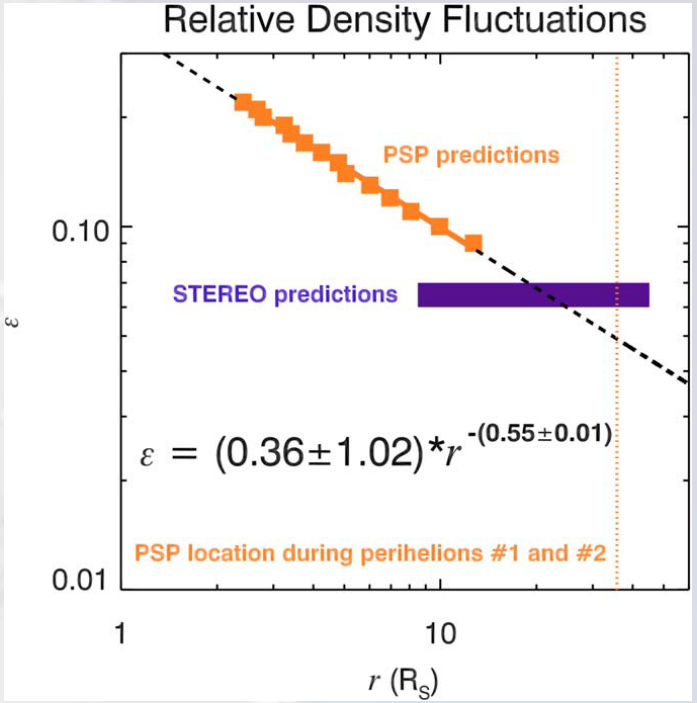

Krupar + 2020

Preliminary PSP results indicate relatively high density fluctuations of 10-20% for r<10 $R_\odot$

More Preliminaries

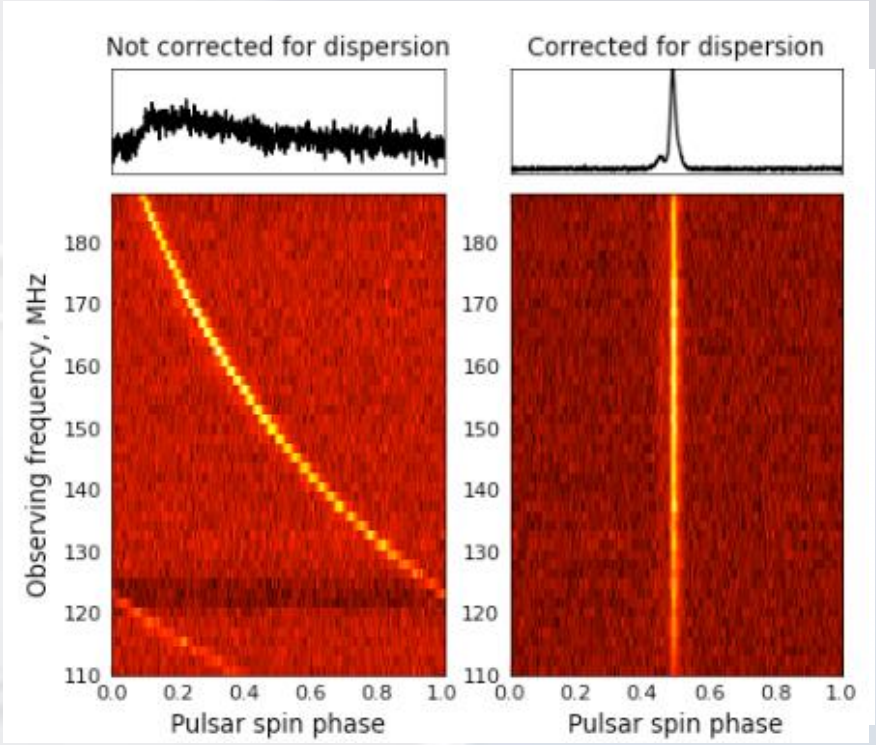

As noted, the group velocity of a wave propagating in a plasma is $v_{gr} = \partial\omega/\partial k = \mu c < c$. The difference in time for a wave to propagate across a plasma slab of thickness Δz and the same distance *in vacuo* is the **group delay:** $t_{gr} = \Delta z\left(v_{gr}^{-1} - c^{-1}\right)$ or, more generally, when $\nu \gg \nu_e$

$$t_{gr} = \frac{\lambda^2 r_e}{2\pi c}\int n_e dz = \frac{\lambda^2 r_e}{2\pi c} DM$$

There is also a change in the **phase** of the wave incident on a plasma slab. The number of wavelengths across the slab in *vacuo is* $\Delta z\ /\ \lambda$ and for the plasma slab it's $\Delta z\mu\ /\ \lambda$ and so the change in phase across the slab is

$$\delta\phi = \frac{2\pi\Delta z}{\lambda}(1-\mu) = k\Delta z\delta\mu = \lambda r_e \Delta z \delta n_e$$

A useful statistic is the **wave structure function**

$$D(s) = \langle|\phi(r) - \phi(s+r)|^2\rangle = 2[B_\phi(0) - B_\phi(s)]$$

Note that $B_\phi(r) = r_e^2\lambda^2 B_n(r)$, so through measurements of the statistics of phase fluctuations we have access to Φ_n!

Angular Broadening

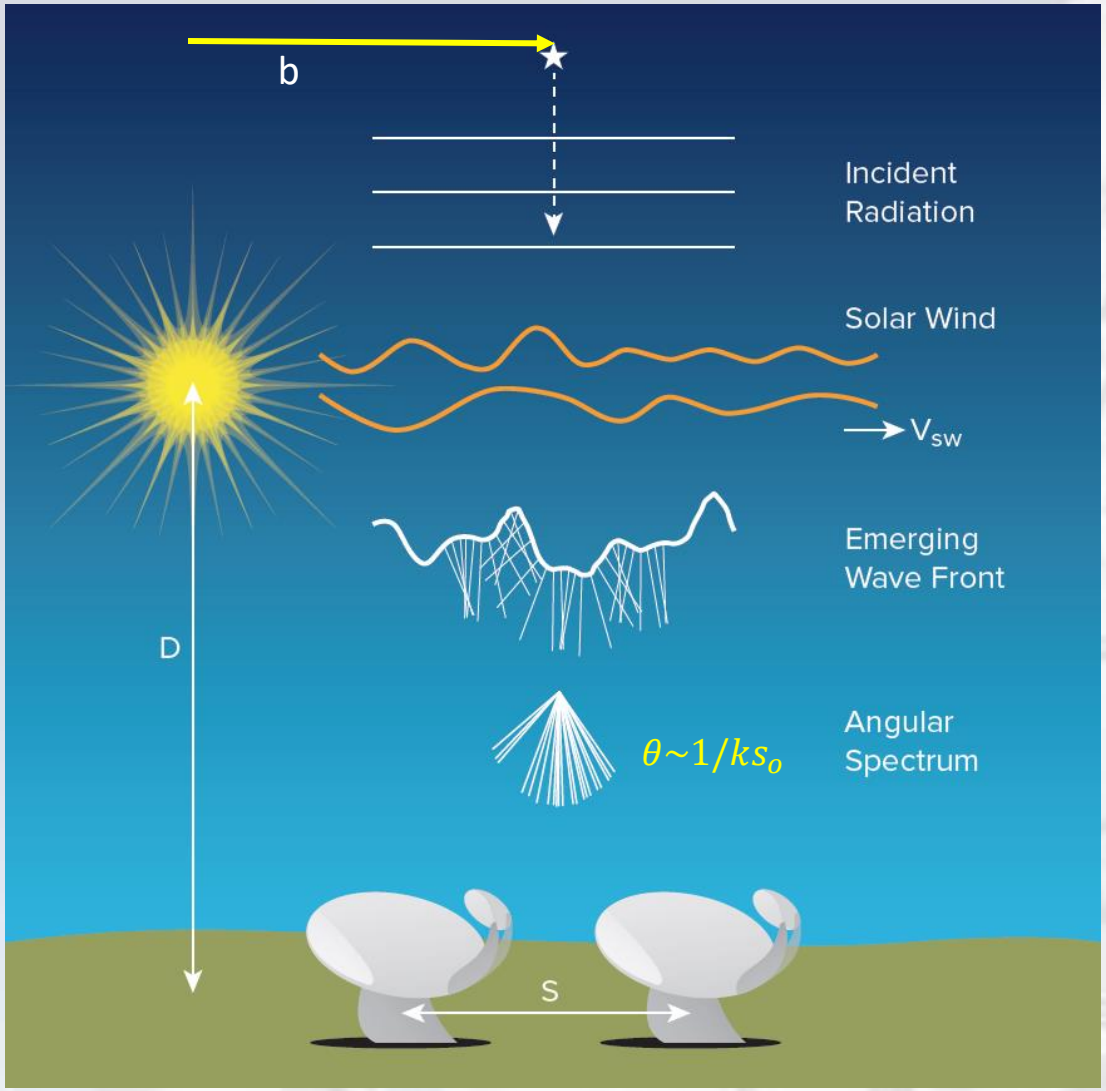

It is useful to treat the plasma medium as a thin, non-absorbing, phase-changing screen ($\Delta z \ll D$). Consider a distant point-like radio source viewed at impact parameter b.

Plane waves are incident on the turbulent screen. The medium perturbs the phase front and the emergent corrugated wave front can be decomposed into a spectrum of planes waves: **angular broadening**.

A radio interferometer measures the spatial coherence of the electric field $E(r)$,

$$\Gamma(s) = \langle E(r)E^*(r+s)\rangle \,/\, \langle E^2\rangle$$

A point source observed in the absence of an intervening turbulent medium has $\Gamma(s) = V(s) \,/\, V(0) = 1$. When a medium is present

$$\Gamma(s) = \frac{V(s)}{V(0)} e^{-[D(s)/2]} \rightarrow D(s) = -2\log\left[\frac{V(s)}{V(0)}\right]$$

Radio interferometers can be used as machines for measuring $D(s)$.

Angular Broadening

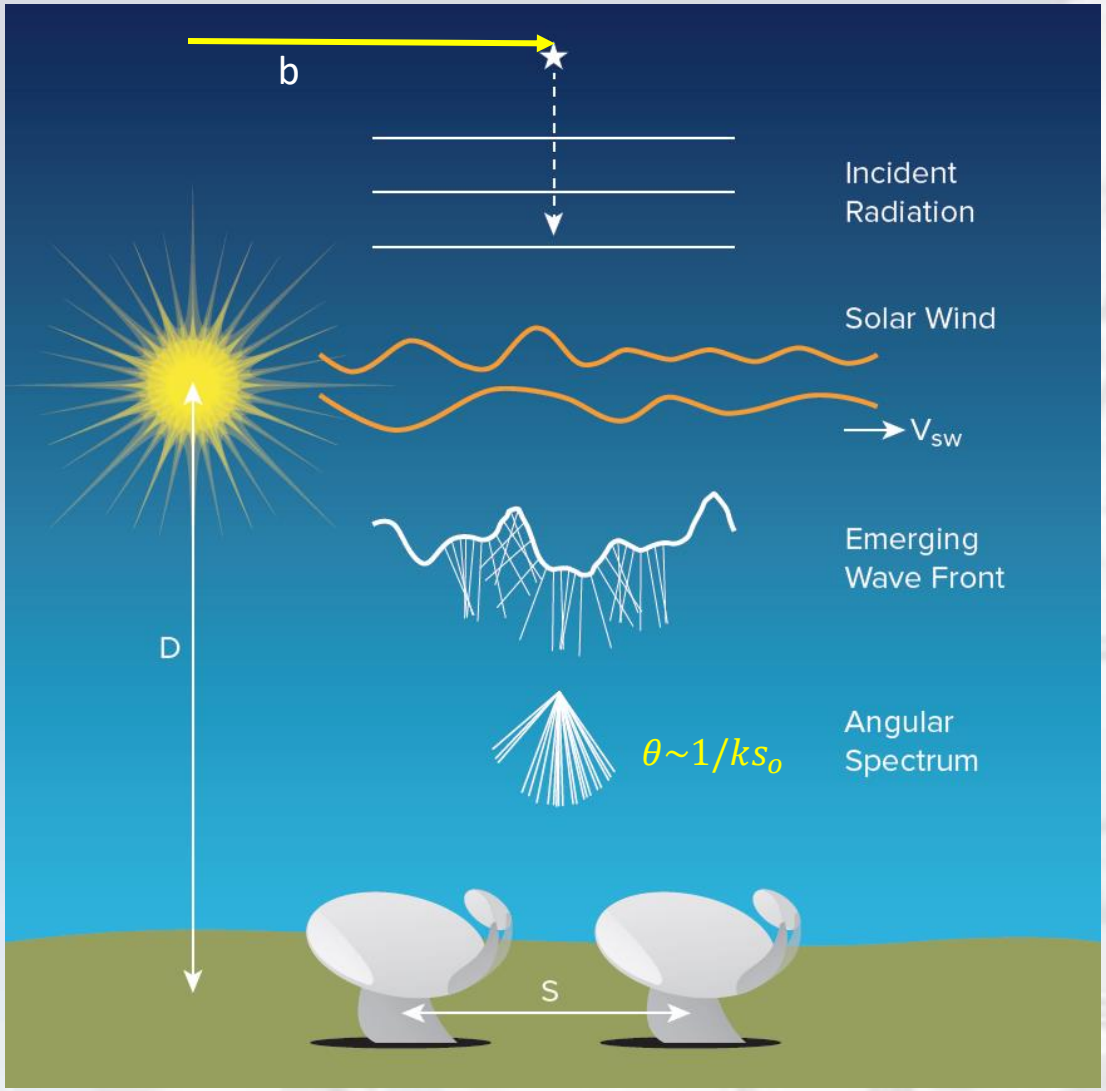

The coherence scale is the transverse scale s_o on which $D(s) = 1$ and the angular width of the source is $\theta = 1/ks_o$.

Since the source is broadened into θ, we now have multi-path propagation from the source with

$$\tau \sim D\theta^2/2c$$: **temporal broadening**

And because the random screen is carried outward by the solar wind with speed v_{SW} a monochromatic source at frequency ν will be broadened as the result of Doppler shifts along the LOS

$$\Delta\nu \,/\, \nu \sim 2v_{\parallel} \,/\, c \sim 2V_{SW}\theta/c$$: **spectral broadening**

Each of these contain information on fluctuations in SW plasma.

Intensity Scintillations

A plane wave incident on an inhomogeneity of dimension d is diffracted into a cone of angular width $\sim \lambda/d$. The solar wind is filled with density inhomogeneities over a broad range of spatial scales.

The diffractive cones emerging from the random phase screen propagate to observer where they constructively and destructively interfere, producing intensity variations (scintillations). The scintillations on the observer's plane sweep by at v_{SW}.

Scintillation is described in terms of two regimes: *weak scattering* ($m = \sigma_I / \langle I \rangle \ll 1$) and *strong scattering* ($m \sim 1$). In the weak scattering regime one can use the power spectrum of a time series of intensity measurements to infer v_{SW} and properties of $\Phi_n(q)$.

One can also see that by simply cross-correlating time series of flux density measurements between telescopes with their spacing aligned with the solar wind outflow, v_{SW} can be also be constrained (e.g., the 3-station STEL system in Japan @ 327 MHz).

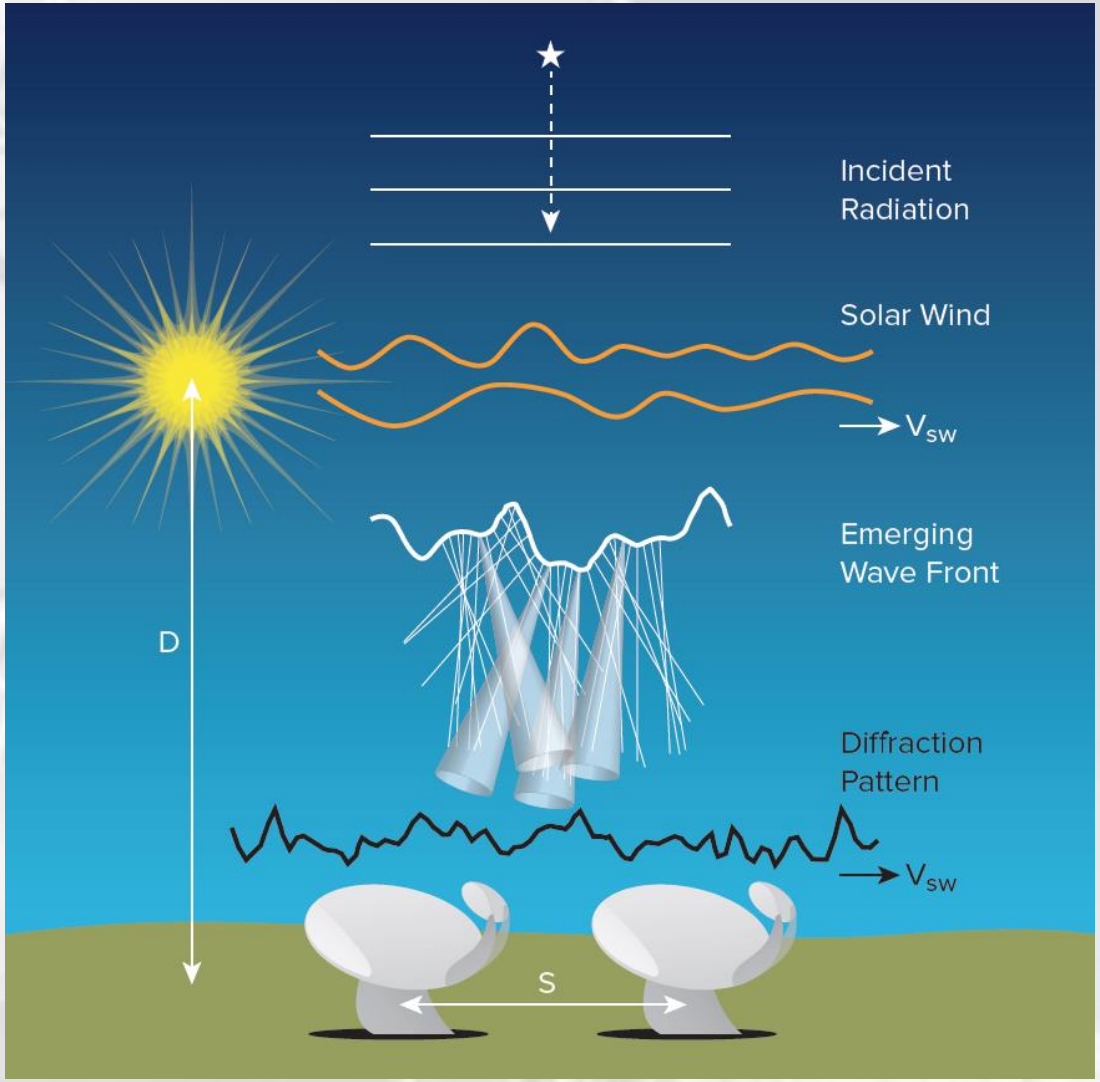

One other effect: Faraday Rotation

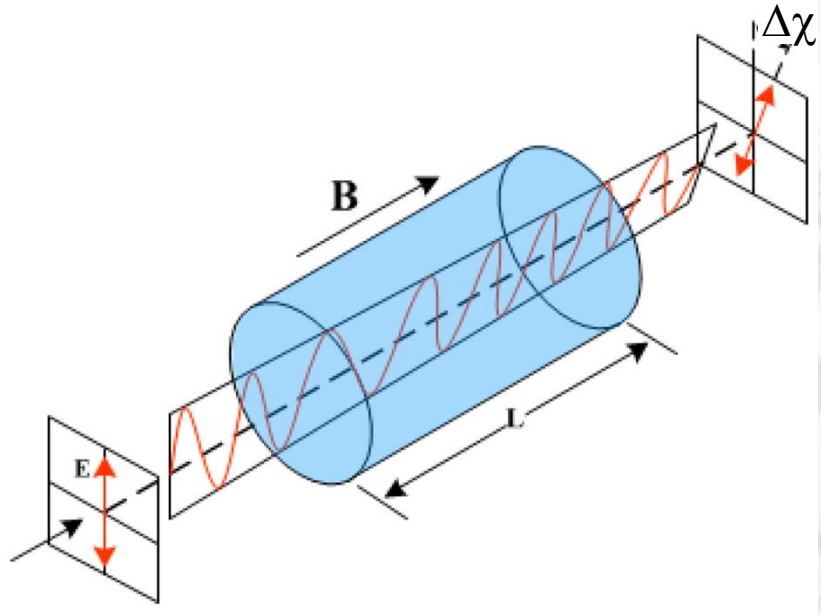

$$\Delta\chi = \frac{r_e^2 \lambda^2}{2\pi e} \int n_e \mathrm{B} \cdot dz \propto \lambda^2 RM$$

Consider a plasma that is is permeated by a weak magnetic field **B**.

Observe a **linearly polarized** source at a large elongation from the Sun to establish $\Delta\chi_o$ (due to the medium between the source and the solar system).

One can then observe the source through the solar wind at various elongations to measure $\Delta\chi$ due to the corona, SW – or even transient phenomenst an ICME.

Fluctuations in FR $\delta\chi$ can also be explored.

The integral, referred to as the **rotation measure,** embodies the net LOS component of the magnetic field and the electron number density.

Remote Sensing at Radio Wavelengths

Observation/Technique	Plasma Property
Group delay	Mean electron number density n_e (DM)
Refraction	Electron density gradient ∇n_e
Angular broadening	Index α of Φ_n on scales of km to 100s of km Inner scale l_o, degree of anisotropy, B orientation
Spectral broadening	Index α of Φ_n on scales of km to 100s of km Inner scale l_{in}
Phase scintillations	Index α of Φ_n on scales of 100s to 1000s of km Outer scale l_{out}
Intensity scintillations	Index α of Φ_n on scales of km to 100s of km Solar wind velocity v_{sw}, δv
Faraday rotation	$B_{\|\|}$, n_e (RM)
Faraday fluctuations	Magnetic field fluctuations δB

The utility of propagation obs: two examples

Radio propagation (“scattering”) experiments are used to constrain properties of the medium through traversed by a given signal (cosmic, spacecraft, radar reflection, radio burst) – often the solar corona and SW and CME/ICMEs, but also planetary atmospheres.

- Angular broadening and solar wind “turbulence”
- Faraday rotation as a probe of CMEs

Solar Wind Spectrum

Unlike the spectrum of B-field fluctuations, $\Phi_n(q)$ is complex, showing a **Kolmogorov-like form** on large spatial scales but showing a **flatter spectrum** (power excess) on smaller spatial scales before "breaking down" at an inner scale.

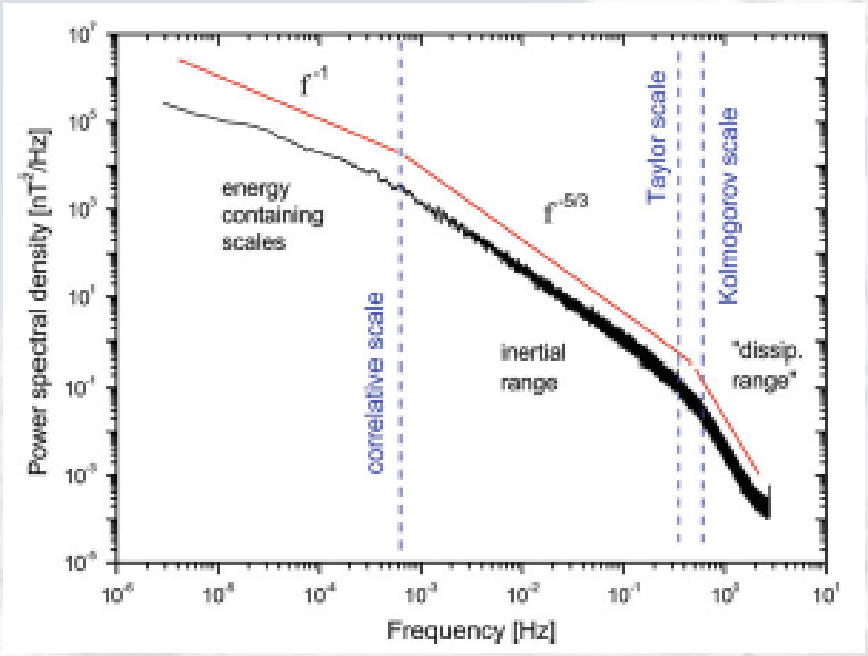

Lepping et al 1995

Coles & Harmon 1989

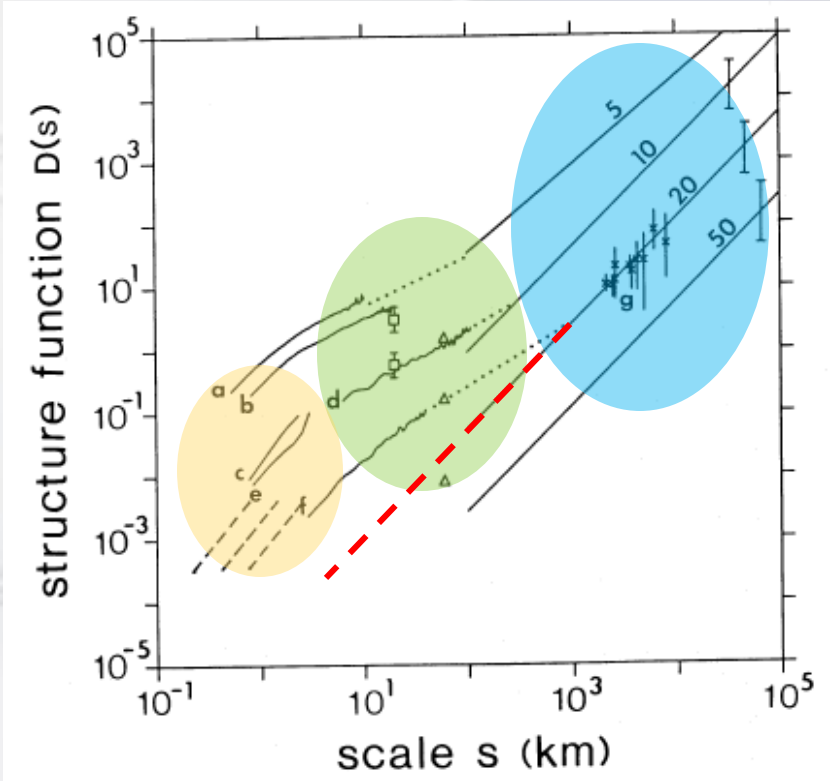

Evolution of the spectrum with radius, latitude, and wind type as a function of time is not well established. For example,

- What is responsible for the spectral flattening?
- What is responsible for the break at small scales?

Const

Use **angula** density
inhomoger

For a statistic re function
is related to

We assume g. Coles + 1987:

totic limits

for which th

$$D(s) = \frac{8\pi^2}{\alpha}\Gamma$$

$^2 s^\alpha \qquad s \gg l_o$

$^2 l_o^{\alpha-2} s^2 \qquad s \ll l_o$

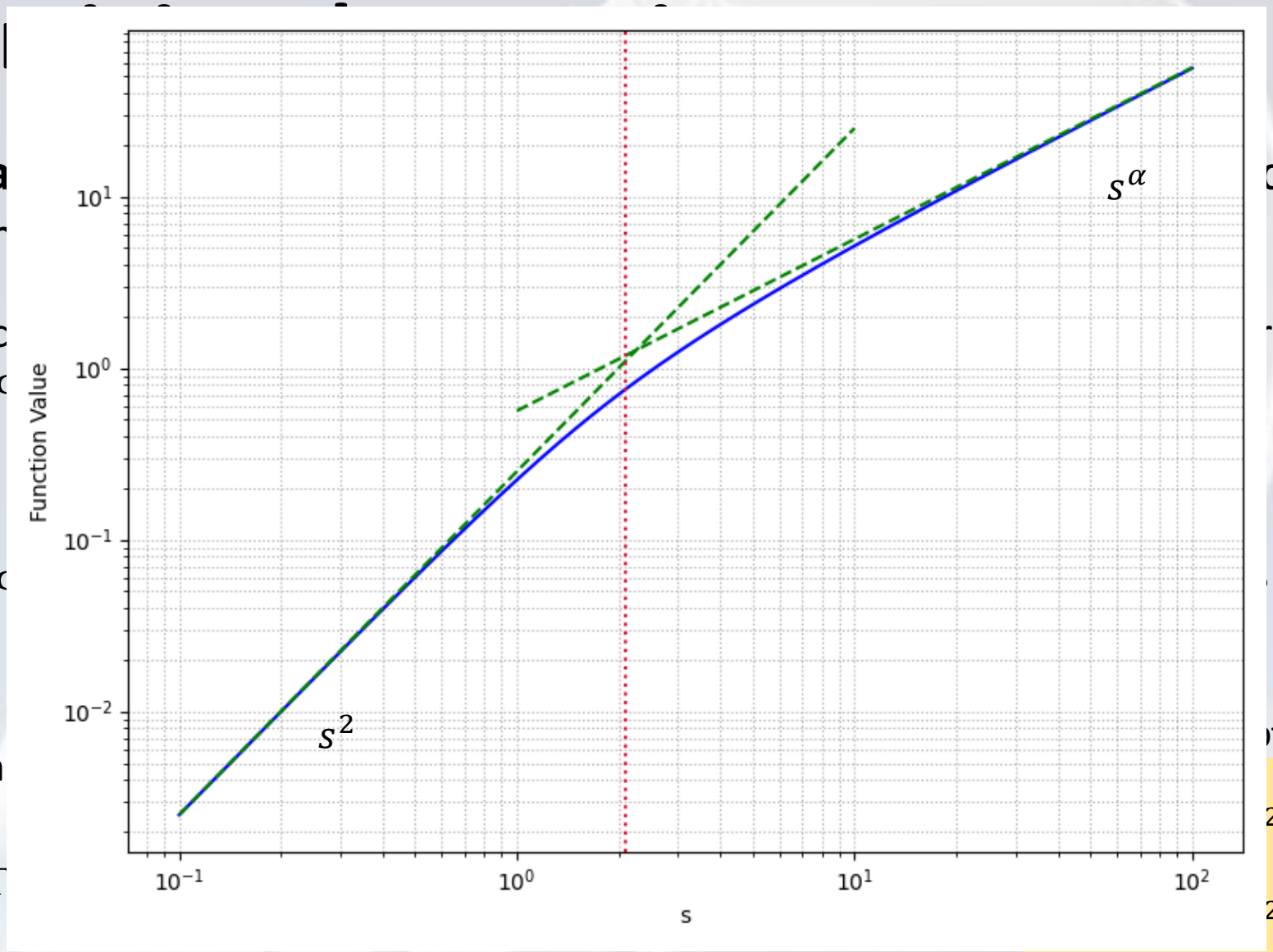

PSP Perihelion 3

2019 September 1

A near-minimum corona

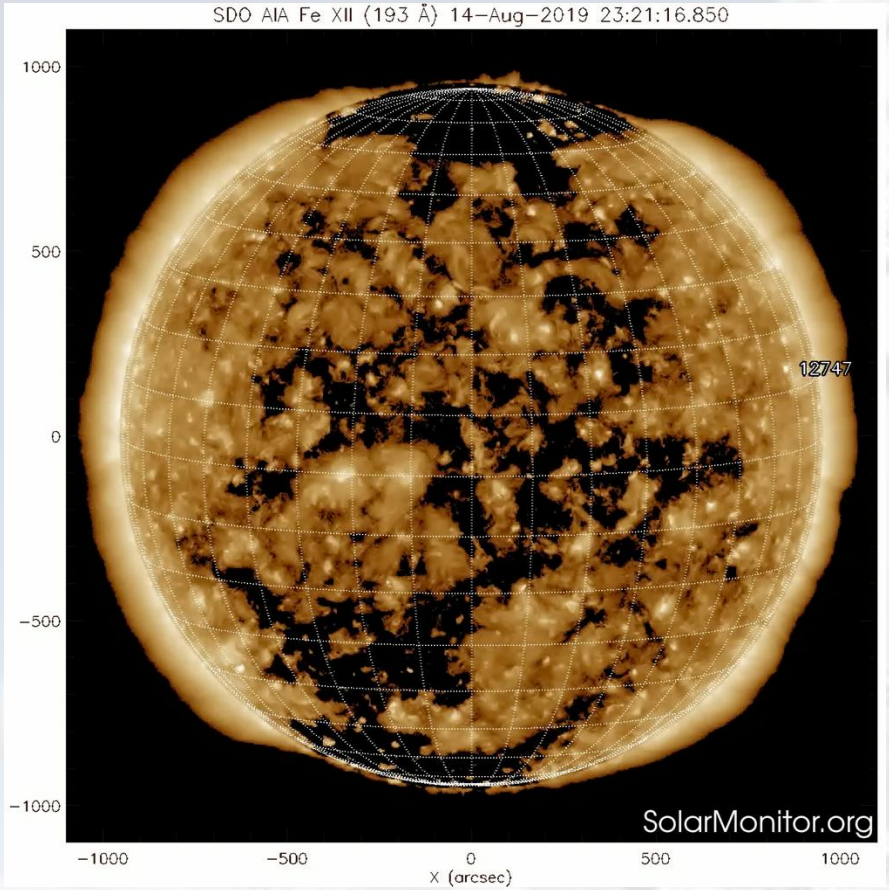

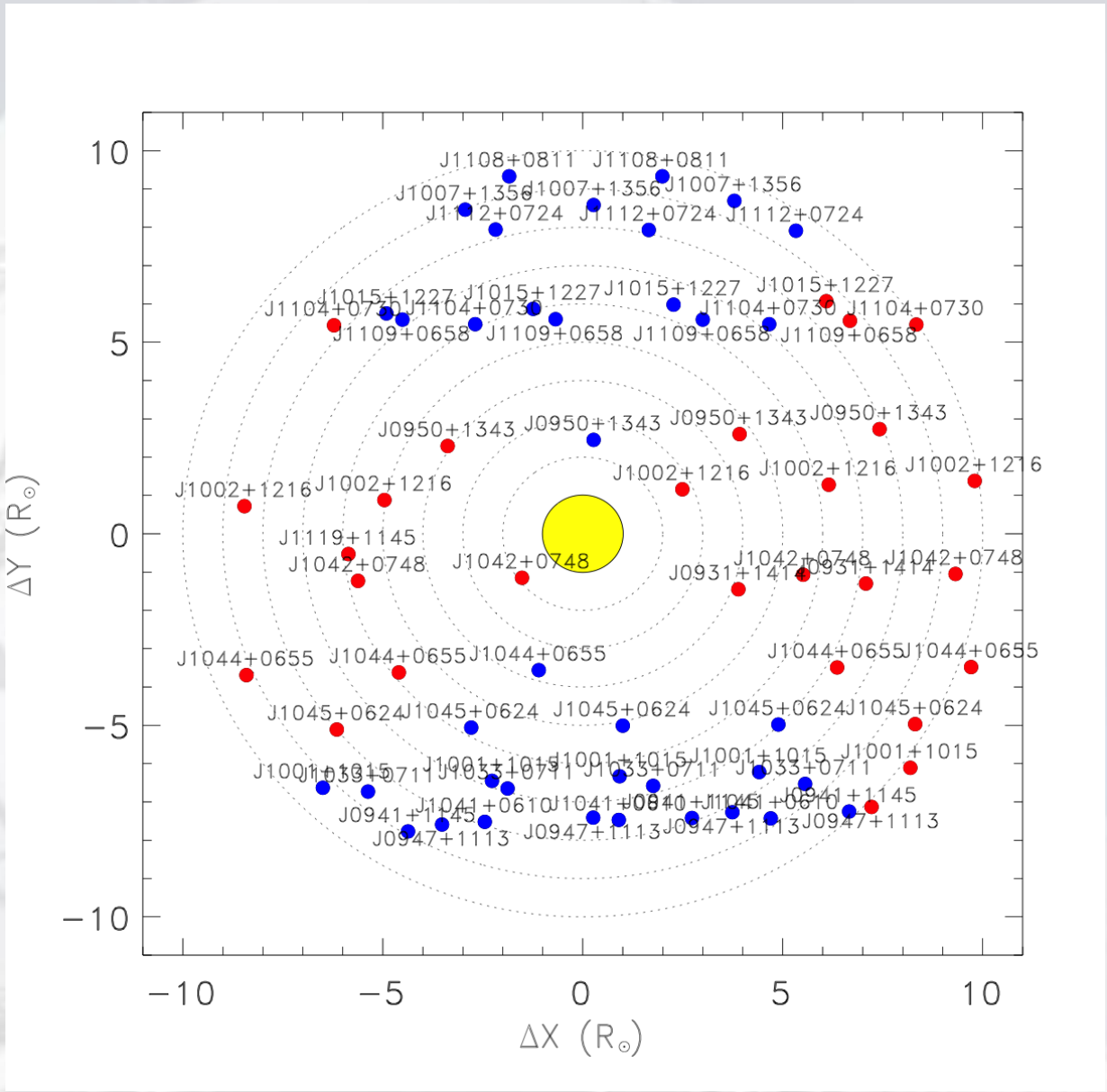

PSP Perihelion 3

The VLA was used from mid-Aug to mid-Sep 2019 to observe a number of point-like background sources.

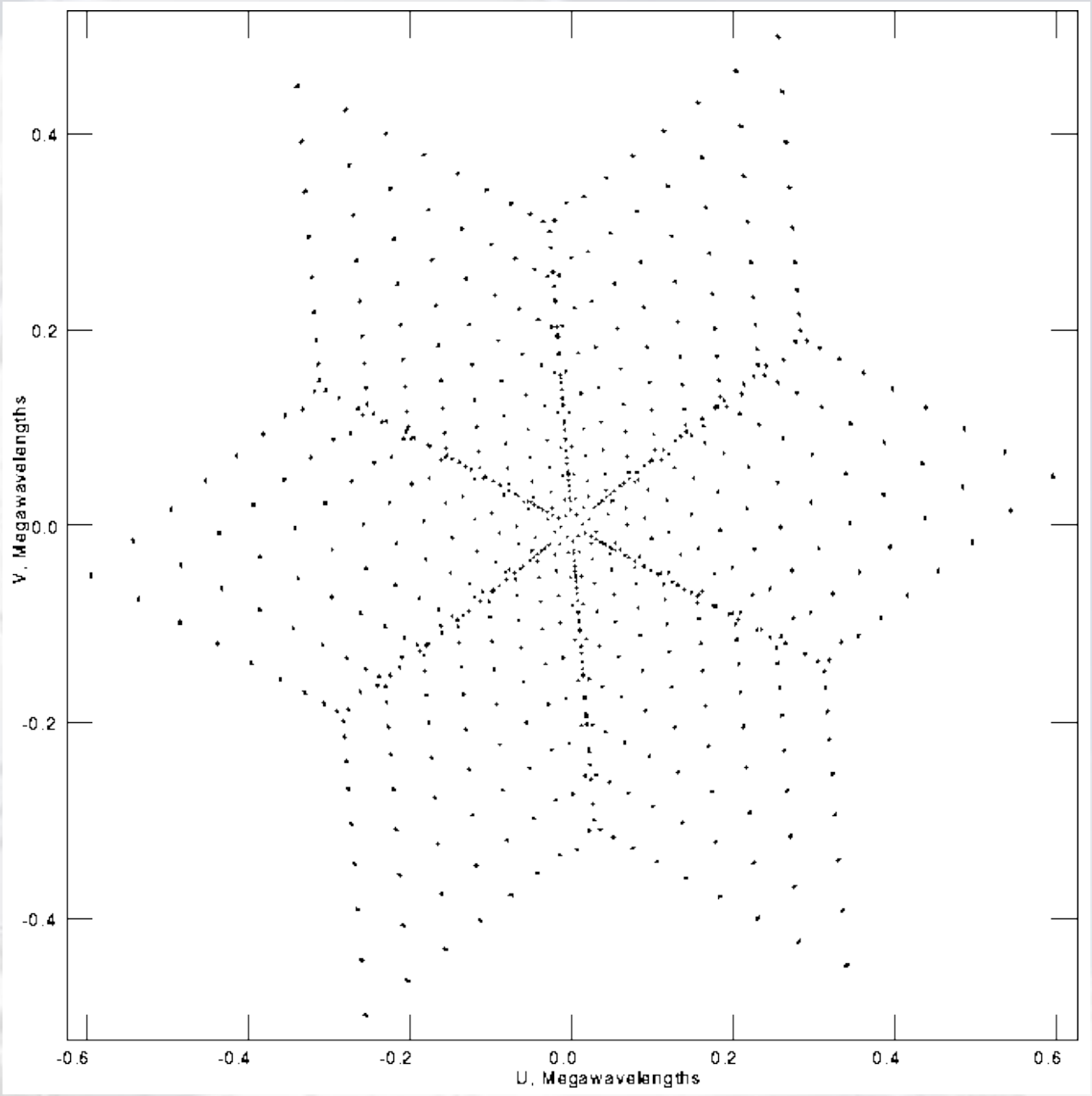

Analysis

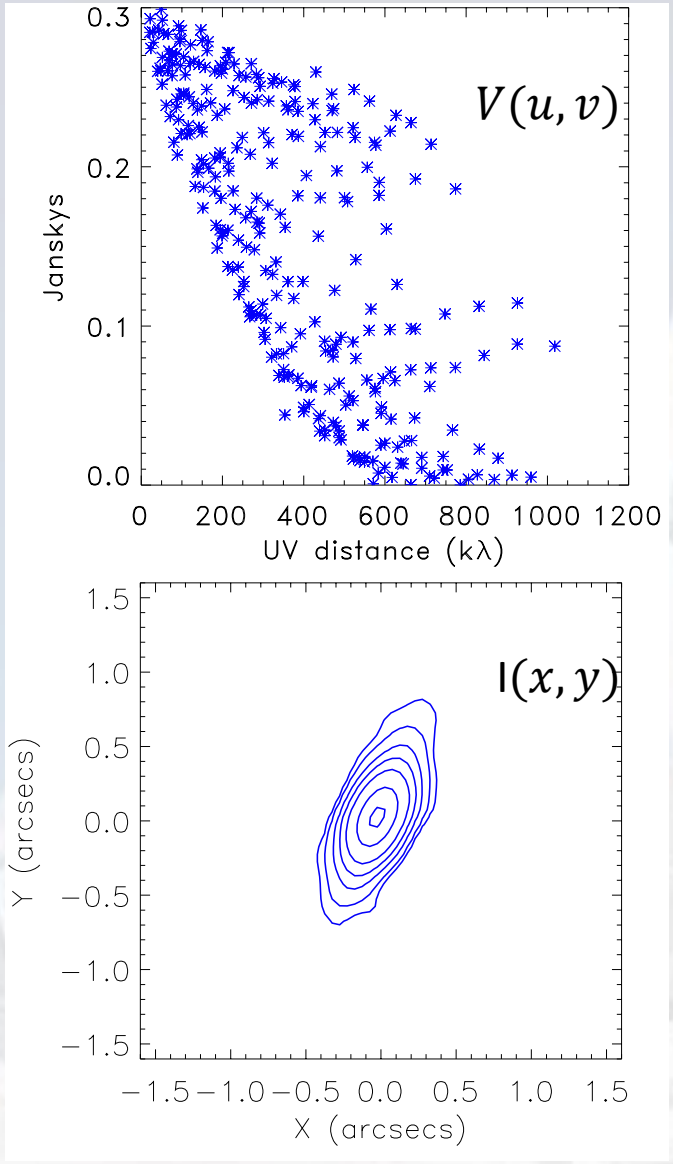

The source is anisotropic, which introduces minor complicaitions. Before we can estimate $D(s)$ we must, in effect, circularlize the structure function. Therefore, we first fit the data to

$$V(u,v) = V(0)exp\left[-\left(\frac{u_t^2}{a^2}+\frac{v_t^2}{b^2}\right)^{1/2}\right]$$

$$u_t = u\cos\phi + v\sin\phi$$
$$v_t = -u\sin\phi + \mathrm{v}\cos\phi$$

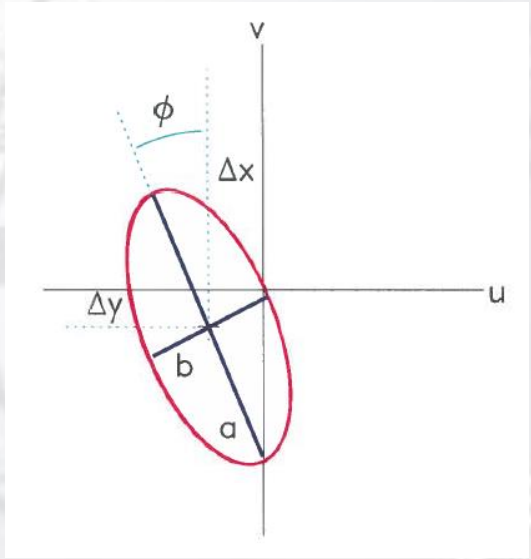

D(s)=1 on an ellipse with major and minor axes a and b; deg of anisotropy η = a/b

$D(s)$ normalized to a, b, ϕ

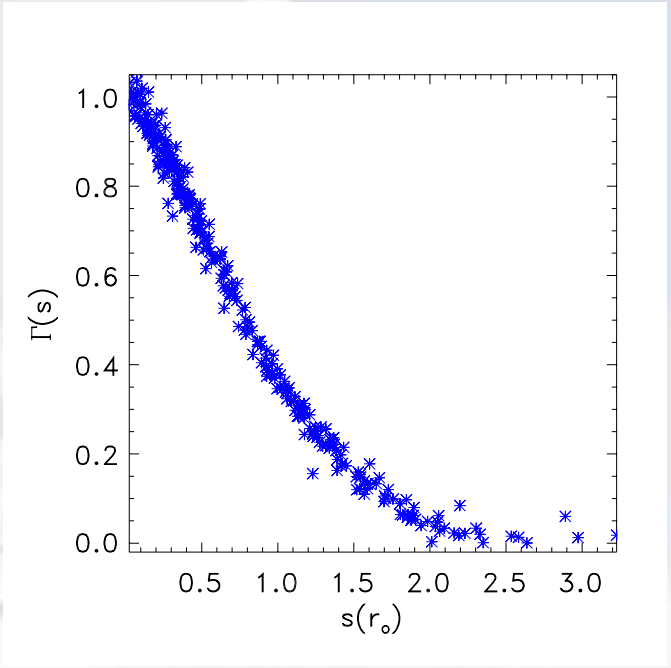

Analysis

The normalized data are then fit for the structure function $D(s)$. As a result of these machinations we have estimates, of η, ϕ, α, and l_i. By integrating over the spatial spectrum $\Phi_n(q)$ we can also estimate $\epsilon = \delta n \, / \, n$.

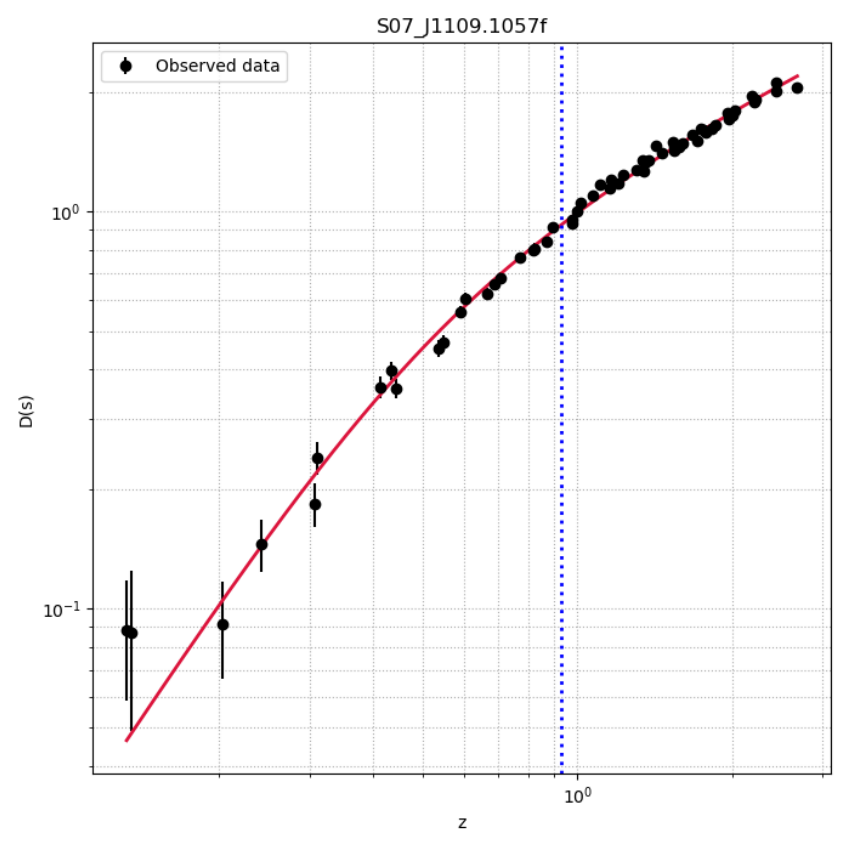

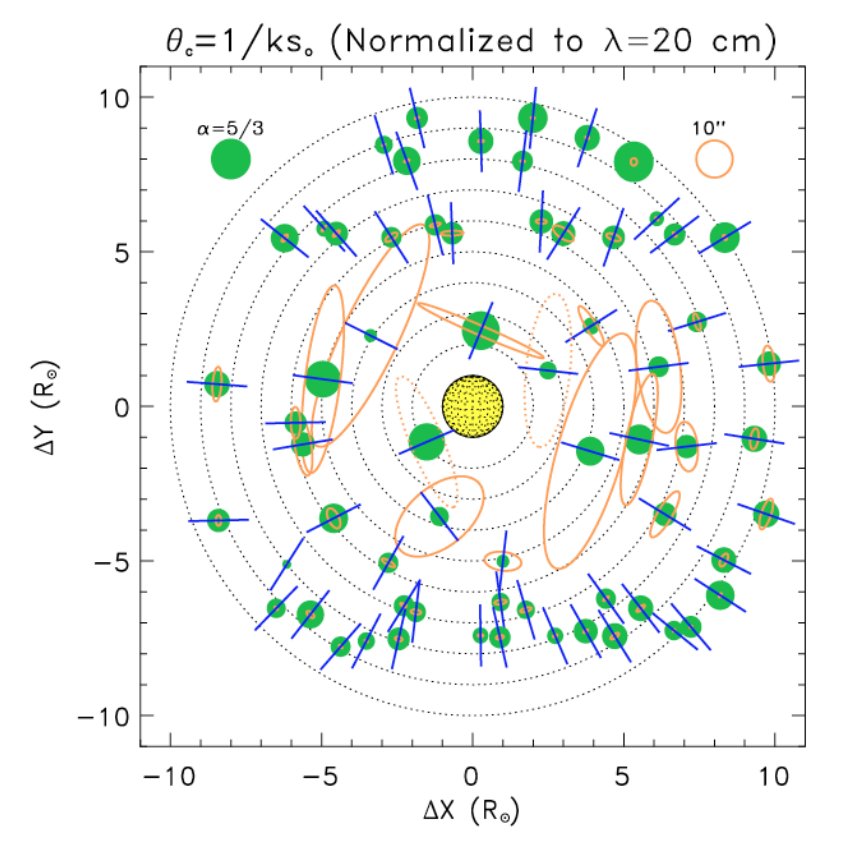

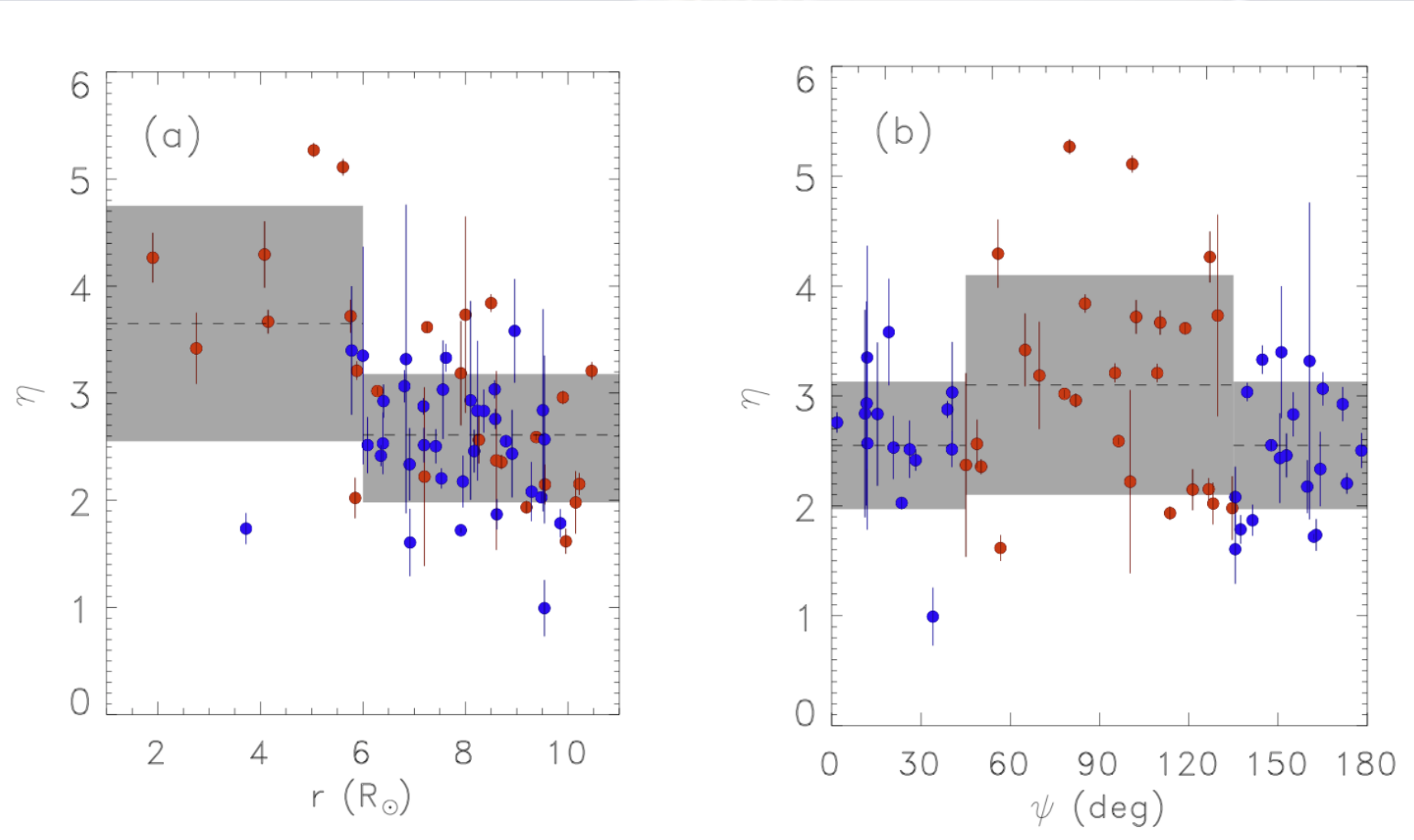
(a)
(b)
η
r (R⊙)
ψ (deg)
0
1
2
3
4
5
6
2
4
6
8
10
0
30
60
90
120
150
180

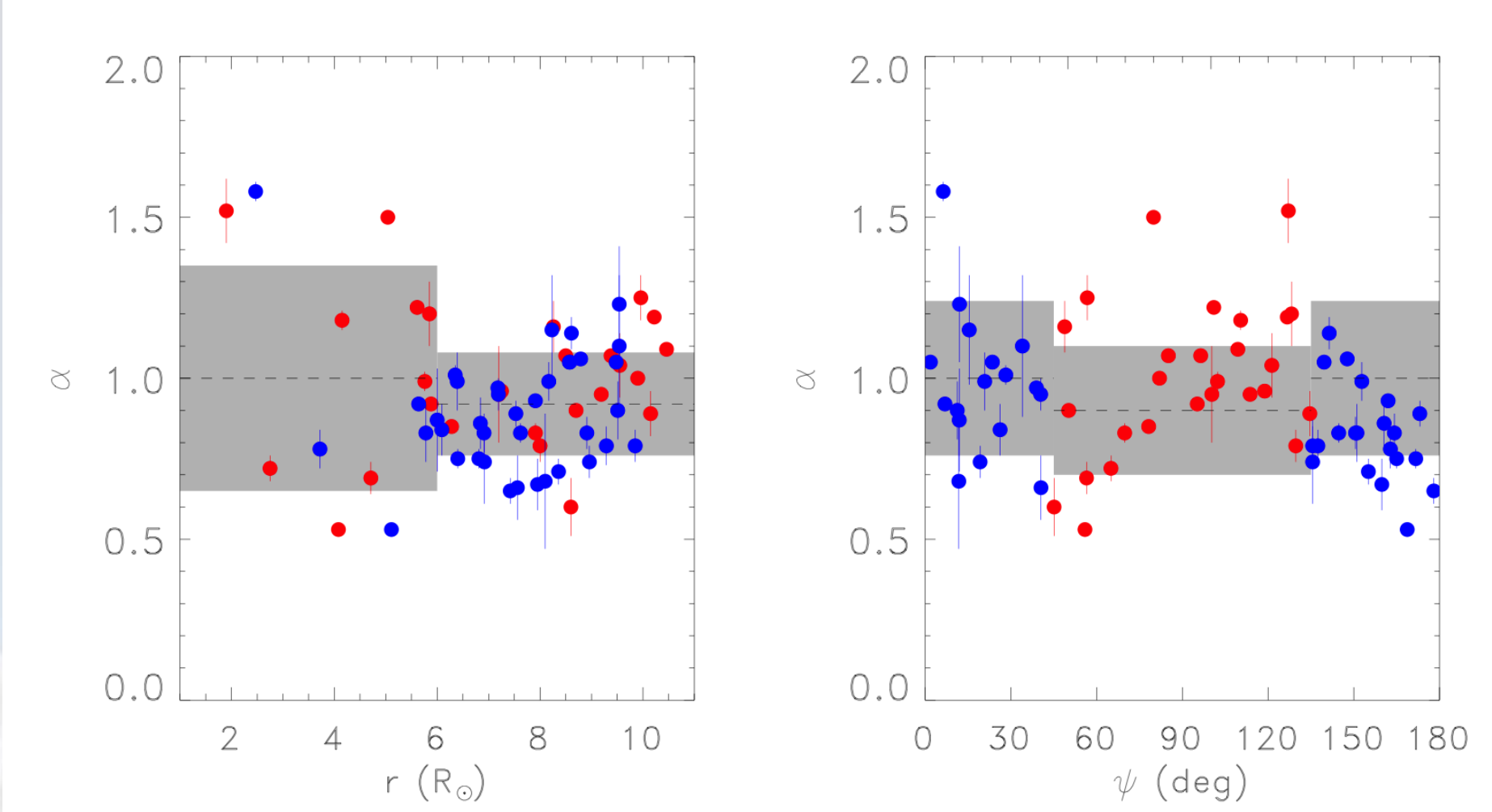
2.0
1.5
1.0
0.5
0.0
α
2
4
6
8
10
r (R⊙)
0
30
60
90
120
150
180
ψ (deg)

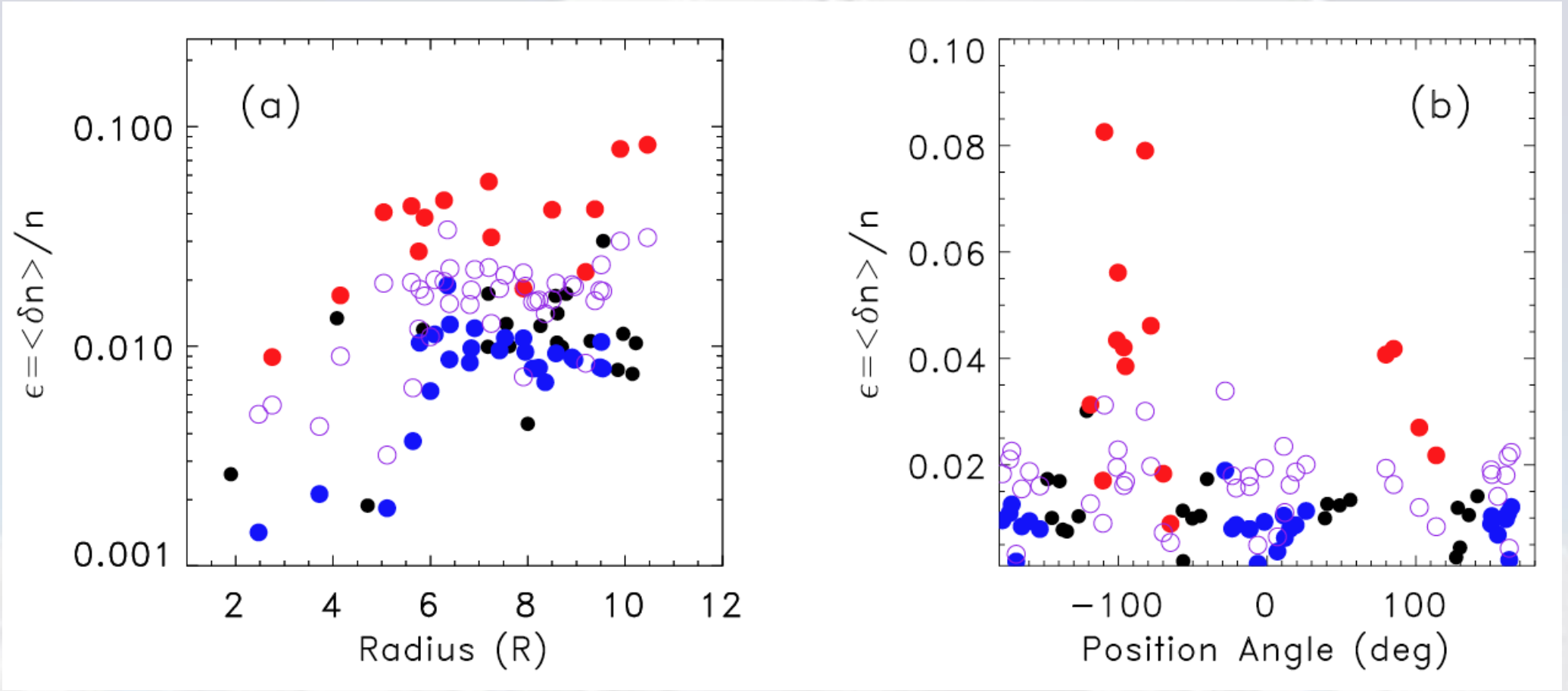
(a)
0.100
0.010
0.001
ϵ=<δn>/n
2
4
6
8
10
12
Radius (R)
(b)
0.10
0.08
0.06
0.04
0.02
ϵ=<δn>/n
−100
0
100
Position Angle (deg)

Faraday Rotation

Observations of Faraday rotation through the quiet solar corona with *Helios*

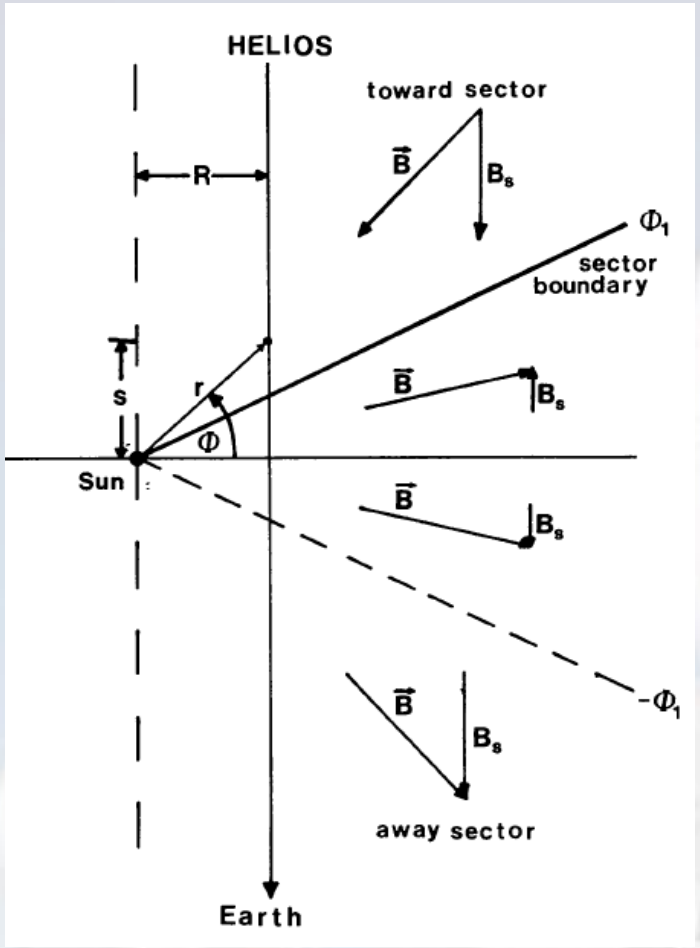

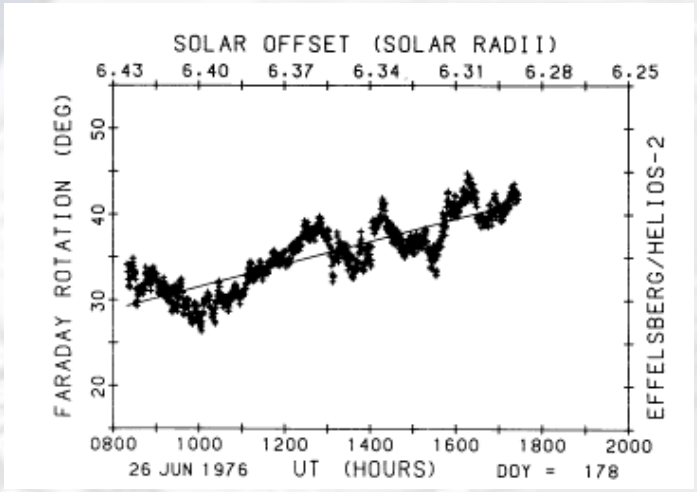

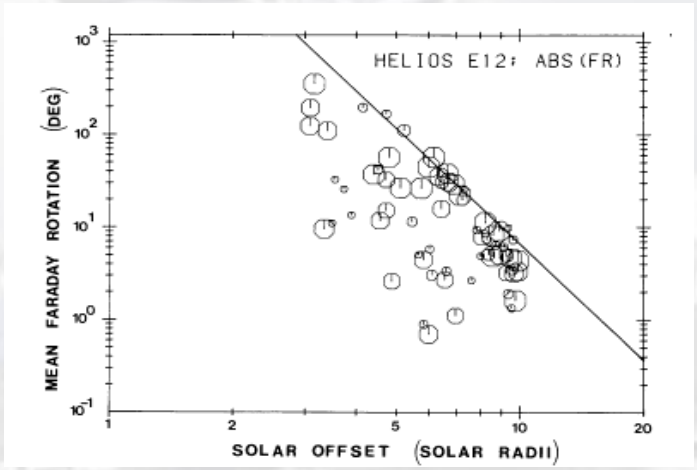

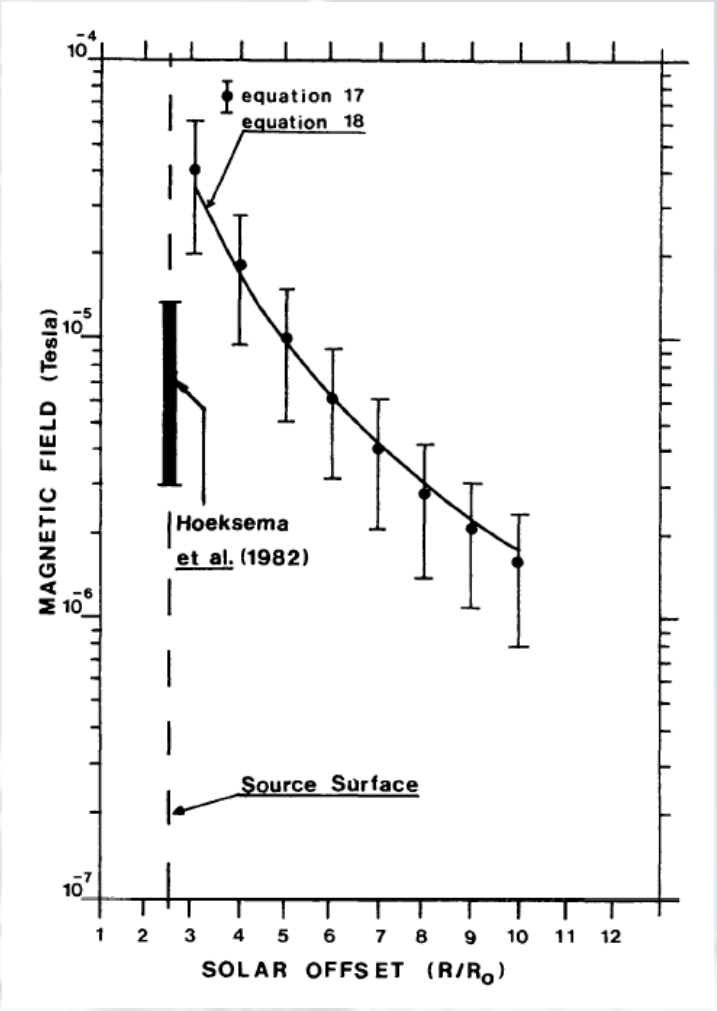

Patzöld et al. (1987)

FR Observations of MFRs

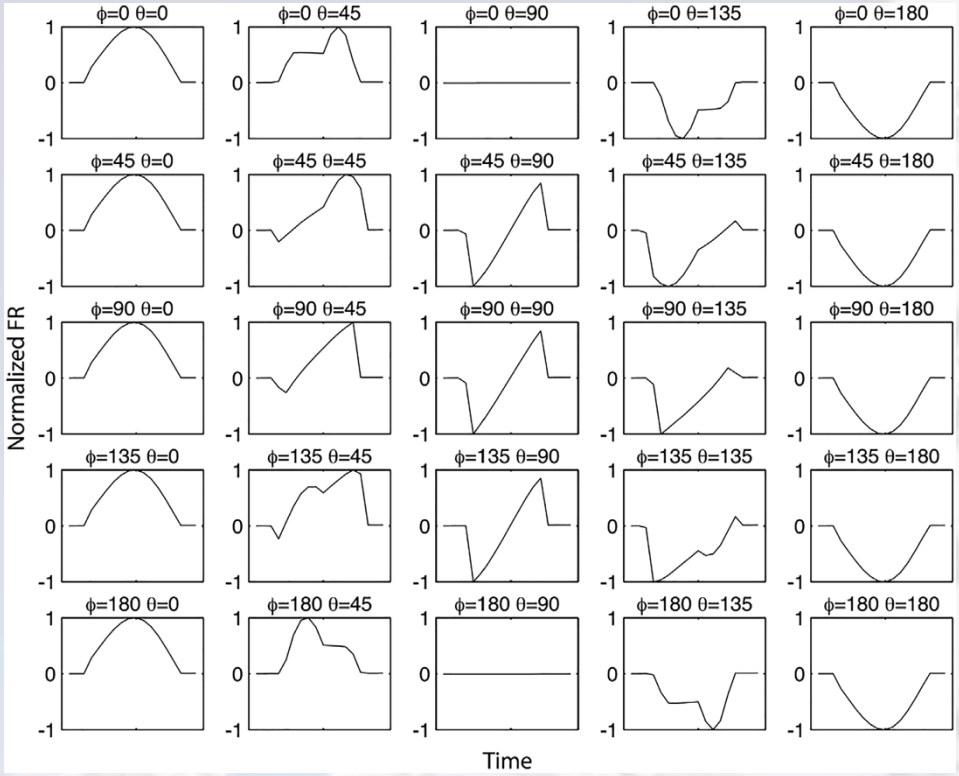

- FR measurements of magnetic flux ropes using polarized spacecraft beacon (Messenger) pioneered by Jensen, Russell, and others.
- Those using polarized background sources (e.g., radio galaxies) were developed by Spangler and students (Ingleby, Kooi).

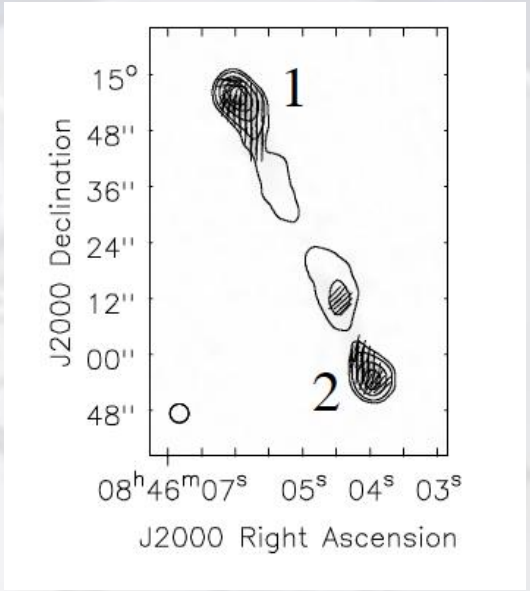

Kooi 2016

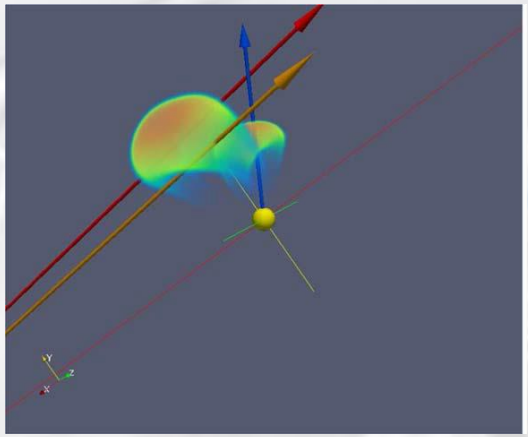

Wood + 2020

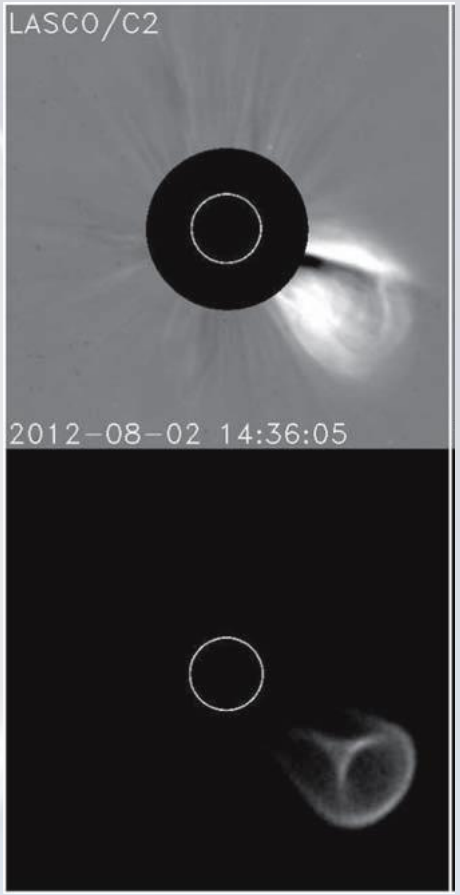

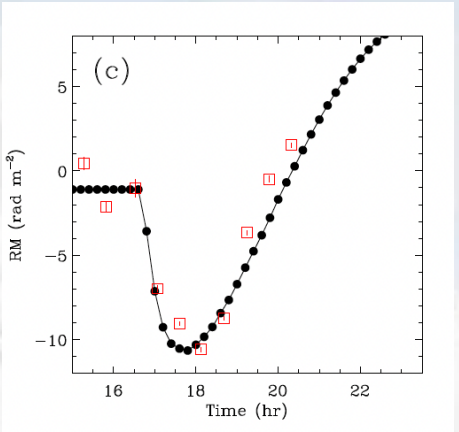


gettyimages

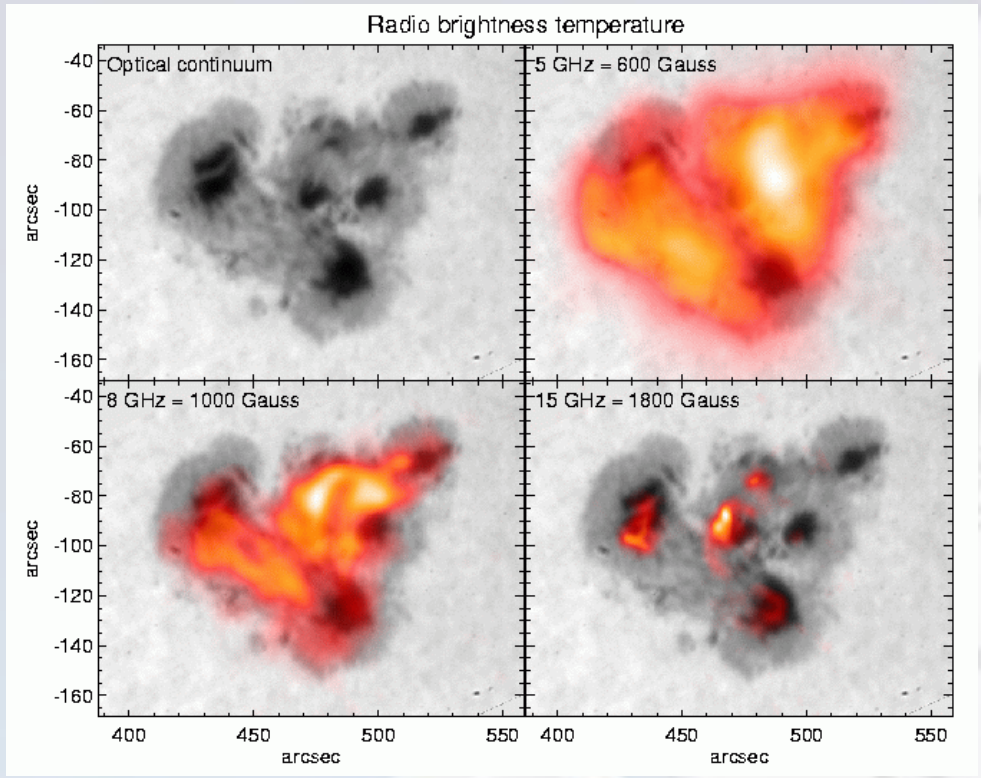
Radio brightness temperature
Optical continuum
5 GHz = 600 Gauss
8 GHz = 1000 Gauss
15 GHz = 1800 Gauss
arcsec
-40
-60
-80
-100
-120
-140
-160
400
450
500
550

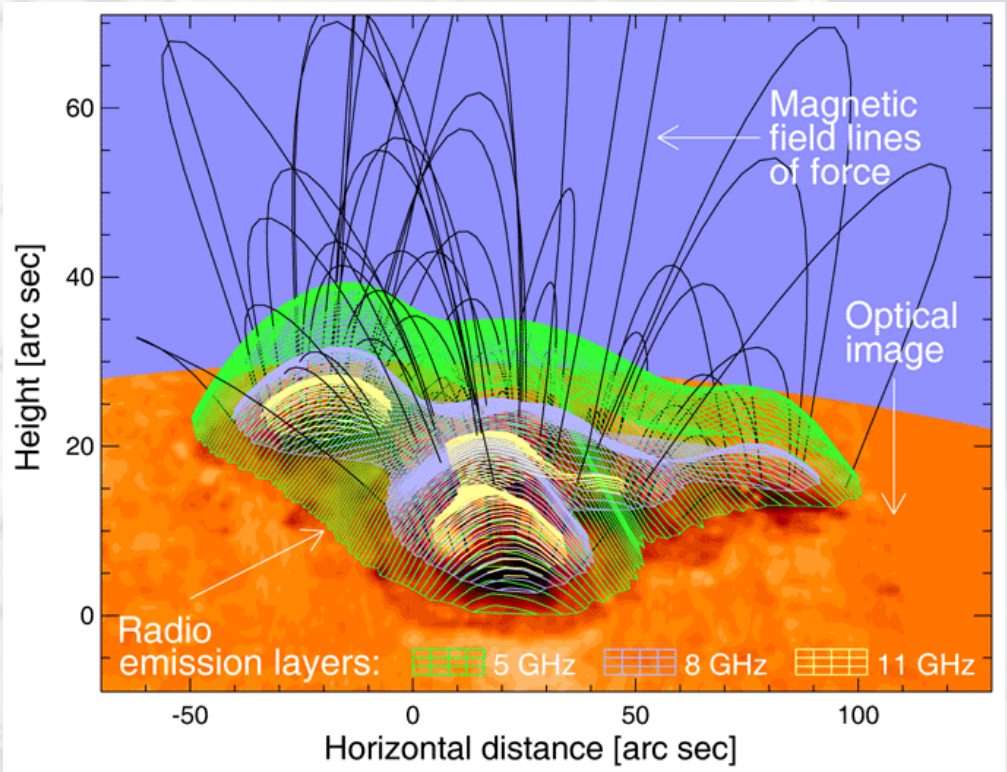
Magnetic field lines of force
Optical image
Radio emission layers:
5 GHz
8 GHz
11 GHz
Height [arc sec]
Horizontal distance [arc sec]
60
40
20
0
-50
0
50
100